UNIVERSITY OF CALIFORNIA

Santa Barbara

Assessment of decarbonizing rapidly-growing technological systems with a life-cycle perspective

A dissertation submitted in partial satisfaction of the

requirements for the degree Doctor of Philosophy

in Environmental Science and Management

by

Jiajia Zheng

Committee in charge:

Professor Ranjit Deshmukh, Chair

Professor Eric Masanet

Professor Mahnoosh Alizadeh

June 2021

The dissertation of Jiajia Zheng is approved.

Mahnoosh Alizadeh

Eric Masanet

Ranjit Deshmukh, Committee Chair

June 2021

Assessment of decarbonizing rapidly-growing technological systems with a life-cycle perspective

Jiajia Zheng

ACKNOWLEDGEMENTS

It has been quite a journey since I started my PhD program. I was very fortunate to have had the help from many people along the way. Firstly, I am grateful to my faculty advisor Prof. Sangwon Suh, who has always been an inspiration and the best resource for my academic work. He encouraged me to aim high and think big, to take on tough problems and to be resilient as a researcher. This dissertation would not have been possible without his guidance. I would like to thank my committee members, Prof. Ranjit Deshmukh, Prof. Eric Masanet, and Prof. Mahnoosh Alizadeh, for providing constructive feedback on my projects with their profound knowledge and deep expertise. My gratitude also goes to Prof. Andrew Chien and other collaborators, who helped me tremendously with my research.

I am grateful to my lab mates at the Suhstainability Lab. Mengya Tao, Yuwei Qin, Runsheng Song and Jessica Vieira offered help and encouragement to me in both my academic work and professional career. I thank Yang Qiu, Haozhe Yang and Qian Gao for keeping me company and bringing me joy. My gratitude also extends to the faculty, staff and fellow PhD students at the Bren School, who maintain such an inclusive and welcoming environment in which I have always felt comfortable and confident.

Lastly, I would like to thank my parents for their tremendous understanding and support all these years. They provided me with the best educational resources they could find for me to thrive. I also thank my fiancée, Dr. John Matsubu, and our dog Short-leg Shultz, who always cheer me up and help me get through hardships with unwavering love and support.

This dissertation is dedicated to my grandmother, Yuexiu Shen. She had little education and dedicated her life to caring for the family and raising kids including me. I am forever indebted to her.

VITA OF JIAJIA ZHENG
May 2021

EDUCATION

- Ph.D., Environmental Science & Management — Jun 2021
  University of California, Santa Barbara *(GPA: 3.95/4.0)*
- M.E. with Honors, Environmental Engineering — Jun 2015
  Fudan University
- B.E. with Honors, Environmental Engineering & B.A. in Economics — Jun 2013
  Wuhan University

RESEARCH EXPERIENCE

Graduate Student Researcher — Oct 2017 - Current
Bren School of Environmental Science & Management — ***UC Santa Barbara***

Graduate Student Researcher — Sep 2013 - Jun 2015
Fudan Tyndall Center for Climate Change Research — ***Fudan University***

PUBLICATIONS

- **Zheng, J.,** & Suh, S. (2019). Strategies to Reduce the Global Carbon Footprint of Plastics. ***Nature Climate Change****, 9*(5), 374-378.
- **Zheng, J.,** Chien, A. A. & Suh, S. (2020). Mitigating Curtailment and Carbon Emissions through Load Migration between Data Centers. ***Joule****, 4*(10), 2208-2222.
- Chamas, A., Moon, H., **Zheng, J.,** Qiu, Y., Tabassum, T., Jang, J. H., ... & Suh, S. (2020). Degradation Rates of Plastics in the Environment. ***ACS Sustainable Chemistry & Engineering****, 8*(9), 3494-3511.
- **Zheng, J.,** Jiang, P., Qiao, W., Zhu, Y., & Kennedy, E. (2016). Analysis of Air Pollution Reduction and Climate Change Mitigation in the Industry Sector of Yangtze River Delta in China. ***Journal of Cleaner Production****, 114,* 314-322.

PROFESSIONAL EMPLOYMENT

Global Environmental Sustainability Intern — Jun - Sep 2019
Illumina, Inc. — ***San Diego, CA***

Sales Advisor/Technical Help Desk Engineer — Aug 2015 - Jun 2017
ExxonMobil (China) Investment Co. Ltd. — ***Shanghai/Guangzhou, China***

Environment, Health and Safety (EHS) Leadership Program Intern — Jul - Dec 2014
General Electric (China) Co. Ltd. — ***Shanghai, China***

FIELDS OF STUDY

Industrial Ecology, Life Cycle Assessment, Climate Change Mitigation

Faculty Advisor: Prof. Sangwon Suh

HONORS & AWARDS

- First Place and Public Choice (Short Talks), Bren PhD Symposium, UCSB Feb 2020
- Bren School Graduate Fellowship, UCSB 2019-2021
- Technology Management Program Young Innovator Fellowship, UCSB Jan 2019
- Mellichamp Sustainability Fellowship, UCSB Jun 2018
- Outstanding Graduate of Shanghai City, Shanghai Higher Education Office May 2015
- Outstanding Graduate of Wuhan University, Wuhan University May 2013
- Outstanding Student Award, three consecutive years, Wuhan University 2009-2012
- First-Tier Fellowship (twice) & Second-Tier Fellowship, Wuhan University 2009-2012

TALKS & SEMINARS

- Talk, Lawrence Berkeley National Laboratory, California, USA, 04/19/2021
- Long Talk, Bren PhD Student Symposium, California, USA, 02/26/2021
- Invited Talk, UCSB Graduate Student Lunch & Learn, California, USA, 07/28/2020
- Short Talk, Bren PhD Student Symposium, California, USA, 02/28/2020
- Talk, UCSB Clean Energy Transition Lab, California, USA, 02/21/2020
- Poster Presentation, American Center for Life Cycle Assessment Conference, Arizona, USA, 09/25/2019
- Poster Presentation, International Society for Industrial Ecology Conference, Beijing, China, 07/09/2019
- Three-min Talk, UCSB GradSlam, California, USA, 04/08/2019 & 04/15/2019
- Short Talk, Bren PhD Student Symposium, California, USA, 03/01/2019
- Oral Presentation, American Center for Life Cycle Assessment Conference, Colorado, USA, 09/25/2018
- Poster Presentation, Gordon Research Conference - Industrial Ecology, Les Diablerets, Switzerland, 05/21/2018

ABSTRACT

Assessment of decarbonizing rapidly-growing technological systems with a life-cycle perspective

by

Jiajia Zheng

Climate change is one of the crucial challenges facing mankind. It is imperative to transition to a low-carbon economy and rapidly reduce anthropogenic greenhouse gas (GHG) emissions. Some technologies that have been growing exponentially in recent decades can be climate-friendly if managed well, but the sheer volume, rapid growth and mismanagement of them could pose great threats to climate change mitigation efforts. In this dissertation, I evaluate the opportunities to decarbonize three rapidly-growing technological systems, namely plastics, data centers and residential solar-plus-storage systems.

Current research is often fragmented in scope and there is a lack of systematic, life-cycle and prospective approaches in assessing the climate impacts of rapidly-growing technologies. By integrating life-cycle GHG emissions accounting and scenario analysis, I assess the GHG emissions mitigation potential of different strategies and interventions to decarbonize these technological systems. I also incorporate cost analysis and optimization methods into my models to assess the economic feasibility and mitigation potential of various decarbonization strategies.

In Chapter II, I quantify the global carbon footprint of plastics to be 1.7 Gigaton (Gt) CO_2 equivalent (CO_2e) in 2015. A low-carbon plastics economy requires demand reduction, adoption of renewable energy, renewable feedstocks and recycling. By combining these strategies, we can keep the global carbon footprint of plastics below the 2015 level in future decades. Among the strategies, renewable energy has the most potential, but sources such as solar and wind are variable in space and time. To successfully integrate them, data centers can play an important role in providing demand response by migrating workloads across regions. In Chapter III, I show that by using load migration, existing data centers in California could have reduced up to 62% yearly renewable curtailment in 2019 and 239 $ktCO_2e$ of GHG emissions with negative abatement cost, and additional data centers could reduce them further with the emissions from non-operational phases taken into account. Energy storage is another key solution for renewable energy integration. In Chapter IV, I assess the life-cycle GHG emissions and cost implications of residential solar-plus-storage systems in California. While PV reduces both emissions and cost, adding battery storage to a PV system increases life-cycle costs with mixed impact on emissions, depending on tariff structure and marginal emission factors. Emissions reduction from residential solar-plus-storage would decrease as the grid increasingly decarbonizes, but there could potentially be cost savings as storage cost declines. A marginal emissions-aligned tariff design, rapid reduction of the capital cost and embodied emissions of battery storage are critical.

This dissertation is a significant contribution to the systematic sustainability assessment of technological systems using a life-cycle approach. It serves as a solid scientific reference for policy-makers in deploying and managing rapidly-growing technologies in a way to minimize system-level GHG emissions and contribute to global decarbonization efforts.

TABLE OF CONTENTS

I. Introduction

A. Background

Over the last few decades, climate change has caused adverse impacts on natural systems and human health across continents, such as extreme weather events and rising sea levels[1]. To avoid further damages from climate change, the total amount of future greenhouse gas (GHG) emissions has to be kept below a certain level, which is referred to as "carbon budget". The remaining carbon budget from 2018 onwards globally has a central estimate of around 600 gigaton (Gt) and 1,500 Gt CO_2 for a 1.5 °C and a 2.0 °C goal of temperature rise, respectively[2]. The required cuts of GHG emissions from 2020 are now more than 7% per year on average to keep the global temperature rise below 1.5 °C, and close to 3% per year for a goal of 2 °C limit[3]. Therefore, a rapid transition towards a low-carbon economy is urgently needed worldwide.

Some technologies and products that have emerged in recent decades have brought convenience, efficiency and productivity to the modern economy, and can play a positive role in reducing global GHG emissions if well managed. For example, plastics, the large-scale production of which dates back to the 1950s, have significantly lower carbon footprints than their substitutes such as paper and glass in packaging applications on a per unit basis[4]. The fast development of digitalization technologies such as Cyber-Physical Systems and artificial intelligence can help accelerate the low-carbon transition of energy systems and achieve the Sustainable Development Goals in many categories[5,6]. Battery storage is believed to be one key solution to overcome the inherent variability of solar and

wind energy, improve their economic values, expedite the clean energy transition and contribute to climate change mitigation[7,8].

Nevertheless, the sheer volume and rapid growth of these technologies are becoming an increasing concern facing the global decarbonization efforts. The massive production and consumption of them often translates to high demands for energy and materials inputs and thus more GHG emissions throughout their life cycles. Plastics and data represent the most fundamental and ubiquitous material in society, in physical and non-physical form, respectively, that have grown exponentially in the last few decades[9,10], but their climate change impacts have only recently been brought to attention. It is projected that plastics' share of global oil consumption would go up to 20% and their share of carbon budget would increase to 15% by 2050[11]. Some researchers have raised concerns about the amount of electricity consumed by rapidly-growing data center capacities[12]. Battery storage, due to its round-trip efficiency loss, as well as the tendency to induce fossil fuel generation through cost arbitrage, can often lead to higher energy consumption and GHG emissions[13,14]. Strategies therefore must be identified and evaluated to decarbonize these technologies as they continue to expand in the future, and make sure that they serve the economy and society in a way that poses minimal impacts on the climate.

Large-scale adoption of low-carbon energy resources is a pivotal strategy for decarbonizing end-use sectors. Electricity and heat production represents the largest portion of global total GHG emissions (25%), most of which is to serve the industrial and residential sectors[15]. Other GHG mitigation measures include improving energy efficiency, emissions efficiency, material efficiency and demand-side management. This dissertation starts with an assessment of a combination of different mitigation strategies to reduce the global carbon

footprint of plastics and concludes that large-scale uptake of renewable energy is the most effective strategy along with demand reduction. But there is an intermittency challenge facing renewable energy, and the dissertation then moves on to evaluate the potential of workloads migration between data centers and residential solar-plus-storage systems in integrating renewable energy and reducing GHG emissions.

A life-cycle approach is used throughout this dissertation, combined with scenario analysis. Life cycle assessment (LCA) is a scientific method used to quantify the environmental impacts of a product, service or technology across its life cycle[16]. Using a life-cycle perspective, a full picture covering the entire life cycle of the technology from material extraction, production, use and end-of-life management can be captured. In assessing the decarbonization opportunities of rapidly-growing technological systems, it is critical to use a holistic approach to avoid overlooking potential impacts and thus develop effective policy recommendations. In this dissertation, I use life-cycle GHG emissions accounting, considering the life cycles of the technological systems, covering both the embodied GHG emissions due to upstream production and the emissions generated during the use or operation phase, as well as emissions from end-of-life phase when data is available. Scenario analysis is often employed in prospective LCA studies to explore the environmental impacts of industrial or technological systems. Different technical and market assumptions are made in a range of future or counterfactual scenarios[17,18], which can provide useful insights for evaluating and developing mitigation strategies prior to large-scale deployment of technologies.

B. Objectives and significance

The main objective of this PhD dissertation is to identify and assess the decarbonization opportunities for the rapidly-growing technological systems aforementioned, using a life-cycle approach. To achieve the objective, the following chapters address below research questions: (1) what is the magnitude of global carbon footprint of plastics, what major mitigation strategies are available and how much potential does each strategy have? (2) how to utilize excess renewable energy production and reduce GHG emissions through load migration between data centers, how much potential does it provide and at what cost? (3) what are the life-cycle costs and GHG emissions implications of residential solar-plus-storage systems in California currently and in a more decarbonized future, and what strategies are critical to minimize them? Throughout the dissertation, I use life cycle GHG emissions accounting under multiple scenarios designed to explore the mitigation potential of different strategies or different configurations of the technological systems.

In Chapter II, I conducted a global assessment of the life-cycle GHG emissions from plastics and evaluated four mitigation strategies, namely use of renewable energy, demand reduction, use of renewable feedstock and recycling. Plastics are the most-consumed basic materials that the global economy increasingly depends upon[9]. However, the magnitude of the GHG emissions that emanates from the production, manufacturing and disposal of plastics at a global scale has not been quantified, and the mitigation strategies have not been evaluated in a systematical manner. In this chapter, I built a life-cycle GHG emissions accounting model for major plastic types at a global level and explored the potentials of the mitigation strategies in different future scenarios. Among the strategies, large-scale adoption

of renewable energy is identified as the most effective strategy to decarbonize plastics' life cycles along with demand reduction.

In Chapter III, I moved on to examine the potential of using workloads migration between data centers in reducing renewable curtailment and GHG emissions through a case study of two large grid operators in the U.S. As discussed, the inherent variability is a major challenge for renewable energy integration, and there is an increasing amount of curtailed electricity in high-renewable-penetration areas like California. With the digitalization of the world economy, the total amount of data generated and processed is growing at an exponential rate. The global data center industry currently consumes approximately 200 terawatt-hours (TWh) electricity per year[10]. Data centers can be used as flexible resources for demand response to utilize excess renewable electricity. In this chapter, I quantified the potential of load migration between data centers to absorb excess renewable electricity and reduce GHG emissions in a range of counterfactual scenarios, considering the life-cycle emissions of the data centers. The cost of implementing load migration and the resulting net abatement cost per unit of GHG emissions reduction were also evaluated.

In Chapter IV, I examined the life-cycle cost and GHG emissions implications of residential solar-plus-storage systems in California. In recent years, a rapid expansion of rooftop solar photovoltaic (PV) in households has been observed, coupled with increasing battery storage installments[19]. Existing studies which reported that residential battery storage would increase the total system emissions are usually retrospective, used marginal emissions factors that did not include renewables and cover only the operational stage. In comparison, I built an optimization model to simulate the energy dispatching of residential solar-plus-storage systems and calculated the life-cycle costs and GHG emissions in current (2020) and

future (2040) scenarios, respectively, using long-run marginal emissions data that consider all generation technologies and capture the structure changes of grid infrastructure. The roles of Time-of-Use tariffs design, capital cost and embodied emissions of battery storage and carbon price were examined in reducing the life-cycle costs and GHG emissions of residential solar-plus-storage systems.

This dissertation presents an important contribution in the sustainability assessment of energy and technological systems by integrating life-cycle approach, scenario analysis and other quantitative methods such as life-cycle cost analysis and optimization. Specifically, Chapter II fills the gap in the sustainability assessment of plastics by uncovering their carbon footprint at a global level and quantifying the mitigation potentials of four key strategies. Chapter III highlights the over-looked potential of data centers in mitigating the renewable curtailment problem and reducing system-level GHG emissions in a cost-effective manner, through migrating load between different geographical locations. Chapter IV identifies the important factors that determine the life-cycle GHG emissions and costs of residential solar-plus-storage systems under an increasingly decarbonized electric grid and proposed multiple solutions for such systems to effectively reduce the cost and emissions. In each chapter, mitigation strategies, policy recommendations and potential challenges are discussed in detail based on the analysis. This dissertation offers scientific evidence and guidance to policy-makers, industries, general public and other stakeholders with regard to how to produce, deploy and manage rapidly-growing technological systems in a way that minimizes their climate change impacts.

II. Strategies to reduce the global carbon footprint of plastics

Material from:

Zheng, J., Suh, S. Strategies to reduce the global carbon footprint of plastics. *Nat. Clim. Chang*. **9**, 374–378 (2019). https://doi.org/10.1038/s41558-019-0459-z

Abstract. Over the last four decades, global plastics production has quadrupled[9]. Continuing this trend, the greenhouse gas (GHG) emissions from plastics would reach 15% of the global carbon budget by 2050[11]. Strategies to mitigate the life cycle GHG emissions of plastics, however, have not been evaluated on a global scale. Here, I compile a new dataset covering ten conventional and five bio-based plastics and their life cycle GHG emissions under various mitigation strategies. Our results show that the global life cycle GHG emissions of conventional plastics was 1.7 Gt CO_2e in 2015, which would grow to 6.5 Gt CO_2e by 2050 under the current trajectory. However, an aggressive application of renewable energy, recycling, and demand management strategies in concert has the potential to keep the 2050 emissions comparable to the 2015 level. In addition, replacing fossil feedstock by biomass can further reduce the emissions to achieve an absolute reduction from the current level. Our study demonstrates the need for integrating energy, materials, recycling, and demand management strategies to curb the growing life cycle GHG emissions from plastics.

A. Introduction

Global production of plastics grew from 2 Mt to 380 Mt between 1950 and 2015, at a compound annual growth rate (CAGR) of 8.4%[9]. Globally, 58% of plastic waste was

discarded or landfilled, and only 18% was recycled in 2015[9]. It is estimated that 4.8-12.7 Mt plastic waste generated by coastal countries entered the ocean in 2010[20]. Growing along the volume of global production and consumption of plastics are the diverse concerns on their impacts to the ecosystem and human health[21–24]. However, relatively little attention has been paid to their contributions to climate change. While the chemical industry as a whole is responsible for about 15% of global anthropogenic greenhouse gas (GHG) emissions[25], the magnitude of global life-cycle GHG emissions from plastics has yet to be quantified.

Various strategies to reduce GHG emissions from plastics have been discussed in the literature. Replacing fossil-based plastics by bio-based plastics, for example, is one of them[26–28]. Bio-based plastics generally show lower life-cycle GHG emissions compared to fossil-based counterparts[29]. Substituting 65.8% of the world's conventional plastics with bio-based plastics is estimated to avoid 241 to 316 Mt CO_2e per year[30]. Both biodegradable and non-biodegradable forms of bio-based plastics are available in the market[31]. Bio-based non-biodegradable polymers such as Bio-Polyethylene (Bio-PE) and Bio-Polyethylene Terephthalate (Bio-PET), also referred to "drop-in" polymers, offer virtually identical properties with their fossil-based counterparts. While bio-based biodegradable polymers, such as Polylactic Acid (PLA), Polyhydroxyalkanoates (PHAs) and Thermoplastic Starch (TPS) display somewhat different mechanical and chemical properties[29]. Strategies to promote bio-based plastics have been initiated by the European Commission and other countries including Japan, Korea and Thailand[32,33]. In 2017, the total global production of bio-based plastics reached 2.05 Mt, and is projected to grow by 20% over the next five years[34].

Low-carbon energy is another strategy to reduce life-cycle GHG emissions of plastics. Under a 100% renewable energy, the GHG emissions from the United States plastics production could be reduced by 50-75%[35]. Another strategy to reduce GHG emissions of plastics is recycling, which reduces, in part, carbon-intensive virgin polymer production[36] while preventing GHG emissions from some end-of-life (EoL) processes such as incineration[37].

However, the literature to date has focused on a subset of plastic types, mitigation options, or geographical locations in isolation[35,38]. Here, I develop a new dataset that covers GHG emissions from resin production, conversion, and EoL of ten fossil-based and five bio-based plastics. I then integrate the dataset with global plastics demand projections and GHG mitigation strategies. I evaluate the following mitigation strategies and their combinations:

(1) Bio-based plastics: fossil-based plastics are gradually substituted by bio-based plastics until a complete phase-out of fossil-based plastics by 2050. While bio-based plastics can be derived from a variety of feedstock, modelled here are corn and sugarcane given their dominance in current market[28]. **(2) Renewable energy**: the energy mix of plastics supply chain is gradually decarbonized and reaches 100% renewables (i.e., wind power and biogas) by 2050. Emissions under the current energy mix are modelled as comparison. **(3) Recycling**: recycling rates of EoL plastics gradually increase and reach 100% by 2050. In comparison, I also model the emissions under a projected EoL management mix scenario and a 100% incineration/composting scenario. **(4) Reducing demand growth:** the current annual growth rate of global plastics demand, which is 4%, is reduced to 2%.

I examine these strategies as illustrative scenarios, rather than as realistic projections of future trajectories, with the purpose of envisioning their potentials for GHG mitigation. I

acknowledge that achieving 100% recycling or renewable energy may be neither practical nor economically feasible in reality.

B. Methods

Life cycle GHG emissions of plastics were compiled for three feedstock types, considering effects of energy mix transformation, different end-of-life management options, and different growth rates of plastics demand. 2015 was selected as the base year, with GHG emissions modelled until 2050 under different scenarios. GHG emission data were collected for three life cycle stages: (a) resin production stage, which includes all activities from cradle to polymer-production factory gate; (b) conversion stage, covering the manufacturing processes that turn polymers into final plastic products; and (c) EoL stage, which refers to the treatment and disposal processes of plastic waste. The use stage was excluded. To calculate the total GHG emissions of a certain year, the annual plastics production and waste generation volumes are multiplied with the life cycle GHG emissions of each plastic type as shown in equation (1):

$$GHG_{s,t} = \Sigma\, Q_{s,j,t} \times E_{s,i,j,k,t} \quad (1)$$

Where $Q_{s,j,t}$ represents the annual global production or waste generation amount of type j plastic in year t under scenario s, and $E_{s,i,j,k,t}$ represents the per-unit weight emissions of GHG i by plastics type j at its life cycle stage k in year t under scenario s. Index i indicates different GHG types including carbon dioxide, methane and nitrous oxide; j indicates different type of plastics including L/LLDPE, HDPE, PET, PVC, PS, PUR, PP&A for fossil-based plastics, and Bio-PE, Bio-PET, PLA, PHAs, TPS for corn- or sugarcane-based plastics; k indicates the life cycle stage of plastics from resin production, conversion, to end-of-life management; t indicates a year between 2015 and 2050, and s indicates scenarios of

different combinations of feedstock, end-of-life options, energy mix and plastics demand growth.

1. Life cycle GHG emissions of fossil-based plastics

For resin production stage of fossil-based plastics, GHG emissions data from ecoinvent 3.4 database[39], European Life Cycle Database (ELCD)[40] and various literature sources were used. Detailed unit processes of resin production are listed by polymer type; emission data of some polymer types with subtypes were calculated as weighted sums according to their market share information (Supplementary Table 2). There is a large gap in life cycle inventory data of plastics additives[41]. Hence, I chose Di-isononyl phthalate (DINP) as a proxy for plastics additives, which is frequently used as a general, all-purpose plasticizer[42]. For the last group, "Others", average GHG emission values of all plastic types were used.

After resin production, the polymers are transformed into various final products for specific applications. Injection molding, blow molding and extrusion are commonly used conversion technologies[43]. There are limited data on plastic products conversion processes in ecoinvent 3.4 and additional data was compiled from the literature. Ref. [43] and ref. [44] served as main data sources for this stage. Ref. 5 shows average GHG emissions from converting various plastic parts for a typical vehicle, and I used the data for GHG emissions from general conversion processes. For PS conversion process, data was drawn from ref. [45]. For PUR conversion process, due to the scarcity of data, the average emissions from PP and PE conversion processes were used. For PP&A fibers, data from ref. [46] was used and the emission values were weighted based on the market share of polyester, polyamide and acrylic. Due to the complex supply chain of textile industry, I cut off at yarn production and exclude the following conversion processes including fabric production and garment

production. Since the amount of additives added into different types of polymers varies, average emissions data were used for the conversion of all the other types for “Additives” and “Others”.

For landfill and incineration processes, I used the life cycle GHG emissions data of mixed plastics from ecoinvent 3.4. For landfilling process, given that fossil-based plastics hardly degrade, only a small amount of GHG emissions is produced during collection and transportation. Incineration of per kilogram of plastic waste generates 3.92 MJ electricity and 7.66 MJ heat plastic according to ecoinvent 3.4, and these credits were used to calculate GHG emissions for incineration process.

The recycling process includes collection, transportation, sorting, separation and material recovery of the waste. The average emission value from PET and HDPE recycling processes (906 kg CO_2e/ton polymer) was calculated and used[47]. To account for the GHG emissions credits from recycling EoL plastics, a substitution ratio of 80% is applied, meaning that 1 kg of recycled plastics avoid producing 0.8 kg of average market-mix plastics[37]. As recycled content of average market-mix plastics changes over time under some scenarios, GHG credits from displacing them are calculated each year and subtracted from the GHG emissions generated from recycling.

The resulting GHG emissions data of fossil-based plastics at different life cycle stages can be found in Supplementary Table 3.

2. Life cycle GHG emissions of bio-based plastics

The most readily available feedstock for a specific region can be different. For example, Thailand and Brazil have excellent conditions for growing sugarcane, the USA is

predominantly growing corn, while Europe has good farmland for growing sugar beet[48]. In our study, corn and sugarcane are chosen. The emission data of Bio-PE, Bio-PET, PLA, PHAs and TPS production derived from corn and sugarcane were collected separately, with the direct and indirect land use change (LUC) emissions already included or calculated as elaborated later in this section. System expansion method was used to handle co-products such as electricity, heat, and digestate. The biological carbon sequestration credits were subtracted from corresponding life cycle GHG emission values for bio-based plastics (e.g. 3.14 kg CO_2/kg Bio-PE, 1.83 kg CO_2/kg PLA, 2.05 kg CO_2/kg PHB[49] and 1.94 kg CO_2e/kg TPS[50]).

Bio-PE and Bio-PET are two major bio-based non-biodegradable plastics used today[34]. The production processes of Bio-PE including corn or sugarcane cultivation and harvest, ethanol fermentation and distillation, bio-ethylene production through dehydration, and polymerization of bio-ethylene to polyethylene[35,51]. To produce Bio-PET, instead of directly going through polymerization, bio-ethylene is oxidized to ethylene oxide and hydrolyzed to ethylene glycol, which then is polymerized with purified terephthalic acid (PTA) to obtain Bio-PET polymers[52]. For corn-based PE and PET, I averaged Bio-HDPE and Bio-LDPE emission data[35]. For sugarcane-based PE, after adding LUC emissions, the net emissions in 2015 under the baseline scenario ranged from -0.7 to 1.8 kg CO_2e/kg Bio-PE[52] and average value was taken. Average value of emissions data from three geographical locations for Bio-PET resin production was used[52].

Polyhydroxybutyrate (PHB), the most common PHAs polymer, was selected as a representative PHAs type. A typical corn-based PLA/PHB polymer production process covers corn cultivation, corn wet milling, fermentation and polymerization/recovery,

successively. The sugarcane-based production follows similar process with only the difference of sugarcane milling instead of corn milling. The production process of TPS involves corn cultivation, starch production and compounding. The emissions data of resin production for corn-based PLA/PHB and TPS are from ref. [49] and ref. [53], respectively. And the ones for sugarcane-based PLA and PHB are from ref. [54] and ref. [55], respectively.

For corn-based plastics, LUC emissions data of 89 kg CO_2e/ton corn was used[49]. I used ref. 18 for the amounts of corn required for Bio-PE, Bio-PET, PLA, PHB and starch production. For sugarcane-based plastics, LUC emissions range between 0.16-2.38 kg CO_2e/kg for Bio-PE and 0.03-0.4 kg CO_2e/kg for Bio-PET[52]; I used an average value for each plastic type. For sugarcane-based PLA, 63.6 kg CO_2e/ton PLA was used for LUC emissions[56].

Regardless whether the feedstock is fossil fuel or plants, further conversion of ethylene to Bio-PE or Bio-PET polymers remains the same[52]. Therefore, the emission values of Bio-PE/PET conversion process are the same with fossil-based ones. The manufacturing technologies for plastics conversion into final products do not differ much between biodegradable plastics and conventional plastics[49,57]. For example, PLA is usually processed by existing methods such as extrusion, thermoforming, injection molding, blow molding or cast film and sheet[16]. One slight difference is that prior to melting processing of PLA, the polymer must be dried sufficiently to prevent excessive hydrolysis which can compromise the physical properties of the polymer[58]. However, no particular life cycle inventory data could be found for biodegradable plastics processing so far. Therefore, I assumed that the emission values for biodegradable polymers conversion is also the same with conventional polymers.

The EoL treatments of Bio-PE and Bio-PET are no different from their fossil-based counterparts, given that they have identical properties and appearances. Therefore, they follow the same EoL mix of fossil-based plastics including recycling, incineration and landfill. In comparison, EoL management methods for biodegradable plastics can be recycling, incineration, landfill, composting or anaerobic digestion. Credits were given to generation of electricity, heat and digestate during incineration and composting processes. The efficiency of waste plastics to substitute virgin polymers is assumed as 80% for all recycling processes, except 74% for TPS, which will undergo higher quality loss during recycling[50]. Recycled contents are assumed to replace an average market-mix of plastics for that year with 80% substitution rate as explained earlier.

The resulting emission values for bio-based plastics at different life cycle stages can be found in Supplementary Table 4.

3. Life cycle GHG emissions under low carbon energy scenario

Building upon the methodology in ref. [35], I explored the emissions under low carbon energy scenario (i.e. electricity from 100% wind power and biogas). Contribution analysis of the life cycle emissions data was performed wherever possible. By closely examining the references, the amount of electricity and heat used in the production, conversion and EoL treatment processes were parsed out for different plastic types. Then I recalculated the emissions from the electricity and heat from low carbon energy sources in 2050, and assumed a linear increase of low carbon energy in the energy mix from 2015 to 2050 to model a gradual energy decarbonization process. The GHG emissions of each plastic type in 2050 under low carbon energy scenario was calculated by Equation (2):

$$E_{lc2050,j,k} = E_{j,k} - (E_{elec} + E_{heat}) + (E_{elec\_lc} + E_{heat\_lc}) \quad (2)$$

Where $E_{lc2050,j,k}$ is the GHG emissions of plastic type j in its life cycle stage k under low carbon energy scenario in 2050; $E_{j,k}$ is the GHG emissions of plastic type j in its life cycle stage k under current energy mix; E_{elec} and E_{heat} are the emissions produced from the generation of electricity and heat under the current energy mix, respectively; E_{elec_lc} and E_{heat_lc} are the emissions from the generation of electricity and heat under a low carbon energy scenario, respectively. All the emissions values are based on one unit of weight (i.e., one kilogram).

For fossil-based plastics resin production stage, the ratios between the emissions under low carbon energy scenario and that under conventional energy scenario in ref. [49] were applied. For conversion stage, blow molding, injection molding and extrusion processes from ecoinvent 3.4 were selected as representative conversion processes to calculate the average contributions of electricity and heat to GHG emissions (81.3% and 9.5%, respectively). For EoL stage, the electricity and heat generation credits from incineration were calculated using low carbon energy emission values. In addition, I calculated the process emissions from recycling by using the energy profile of recycling depicted in ref. [47]. It is assumed that the diesel used for vehicles in waste collection in recycling process is replaced by electricity from wind. Supplementary Table 5 lists the GHG emission data of energy sources used to calculate our results under low carbon energy scenario.

For corn-based Bio-PE and Bio-PET resin production, emissions data in low carbon scenario were from ref. [35]. For corn-based PLA and PHA resin production, the low carbon emissions data from ref. 22 was used, and the LUC emission data from ref. 12 was applied. For TPS production, the maize starch production process in ecoinvent 3.4 was used as a

proxy process, and the contribution of electricity and heat to the GHG emission are 24% and 17%, respectively. For sugarcane-based Bio-PE, 3.09 kWh electricity and 10.5 MJ diesel are used for per kilogram of Bio-LDPE produced[51], and they served as representative data for Bio-PE and Bio-PET due to unavailability of detailed energy use data on Bio-HDPE/PET production. For sugarcane-based PLA, the emissions from electricity and steam are 600 kg and 675 kg CO_2e/ton polymer, respectively[54]. For sugarcane-based PHB, the electricity and steam production are 1.1 kWh and 14.8 MJ per kilogram of polymer, respectively[55].

Bio-PE and Bio-PET are assumed to produce the same amount of GHG emissions as their fossil-based counterparts during EoL management stage. As for biodegradable plastics, GHG emissions are assumed to stay unchanged for landfilling process; for incineration, composting and digestion, electricity and heat generation data from ref. [59] were used.

The GHG emissions values for fossil-based plastics and bio-based plastics under low carbon energy scenario can be found in Supplementary Table 6 and 7, respectively.

4. Plastics demands

Beginning with the amount of plastics produced in 2015[9], two scenarios are evaluated until 2050, assuming an annual resin production growth rate of 4% (average annual growth rate of 2010-2015) and 2% (a slower growth trend of plastics production). For 100% fossil-based plastics scenario, the market share of each plastic type is assumed to remain unchanged. For corn- and sugarcane-based plastics scenario, the market share of bio-based plastics is assumed to linearly grow from zero in 2015 to 100% in 2050, given that the global market share of bio-based plastics in 2017 was less than one percent[34]. Additionally,

it is assumed that bio-based plastics substitute for conventional plastics on a 1:1 scale by weight.

5. Substitution assumptions

Today, there is a bio-based plastic alternative for almost every conventional plastic and the corresponding application[34]. A report regarding the technical substitution potential of bio-based polymers concludes that 90% of the conventional polymers can be technically replaced worldwide[60]. Considering biopolymer technology advancement, it is assumed that all fossil-based plastics can be replaced by bio-based plastics scenarios by 2050.

In 2017, bio-based non-biodegradable plastics accounted for 56% of the global bioplastics market. These so-called "drop-in" solutions have the same properties, conversion processes and disposal methods with their fossil-based counterparts and therefore serve as perfect substitutes. Bio-PE are assumed to replace the majority of fossil-based PE, PVC and PUR, while Bio-PET to replace PET and PP&A fibers. Other types of bio-based non-biodegradable plastics are not considered in this study since they are not yet available at a commercial scale or there is a lack of data in the literature.

Bio-based biodegradable plastics make up the rest 44% of the bioplastics market, with PLA and PHAs driving the growth[34]. PLA is the most versatile biodegradable plastic type and has wide applications across food packaging, medical devices, agriculture films, among others[61–63]. It has comparable mechanical and thermal properties with PS and PET, and can also replace PE, PP, and PVC in some applications[49]. The use of PLA to replace nylon and PET in the textile industry is also increasing[57]. PHAs have been used in fibers, non-woven materials, disposable products[64], cosmetic and food containers[63]. Commercialized PHAs can frequently replace PE, PP and PS, and may also substitute for PET and PVC[49]. The high

price of PHAs is a major barrier to its large scale commercialization[64]. TPS is used in specialized agricultural applications, as filler in plastic composites, or in single-use items like bags, containers, diapers and tampons[63,65]. Pure TPS has poor mechanical properties and is susceptible to water, which limits its potential product applications[66]. However, it is a common practice to blend starch with other polymers such as PLA, PCL, and PHAs to obtain composites to improve its properties[62].

Based on the technical substitution potential, comparable properties, common application areas and the market growth reviewed above, a substitution plan was developed for bio-based plastics to replace conventional plastics (see Supplementary Table 9).

6. End-of-life management

The projected EoL management mix change of all plastic types (fossil-based and bio-based) between 2015 and 2050 is shown in Supplementary Table 10. The mix in 2050 is determined based on the projections of future EoL change[9], as well as the historical changes of the plastic waste EoL management in Europe and the United States. Linear change of the rate of each EoL method is assumed between 2015 and 2050.

7. Limitations

There are uncertainties and limitations associated with the data and the model employed in this study. I made various assumptions to simplify the processes involved in plastics life cycle. For example, I assumed that the indirect land use change and the GHG emissions from agricultural expansion for bio-based plastics would remain at the current level. I also extracted and combined emissions data from multiple sources. Conventional plastics data are from ecoinvent 3.4, which are originally Eco-profiles of the European plastics industry

(PlasticsEurope). The data contains outdated numbers and uses extrapolation for the regions other than Europe. Therefore, the temporal and geographical representation of the data was identified as a weakness, while no better data sources were identified. The methods to calculate LUC emissions associated with bio-based plastics production vary in the literature and warrant further research.

C. Results

Our analysis shows that conventional plastics (fossil-based) produced in 2015 generated 1.8 Gt CO_2e emissions over their life cycle, excluding any carbon credits from recycling (Fig. 1). The amount corresponds to 3.8% of the 47 Gt CO_2e global emissions that year[67]. Resin production stage generated the majority of the emissions (61%), followed by conversion stage (30%). Of all plastic types, PP&A fibers had the highest GHG emissions at both stages. Polyolefin family (PP, L/LLDPE, and HDPE), which accounts for nearly 50% of the world's plastics consumption, was also a significant contributor. GHG emissions from bio-based plastics are not considered for 2015 given their negligible market share (<1 percent).

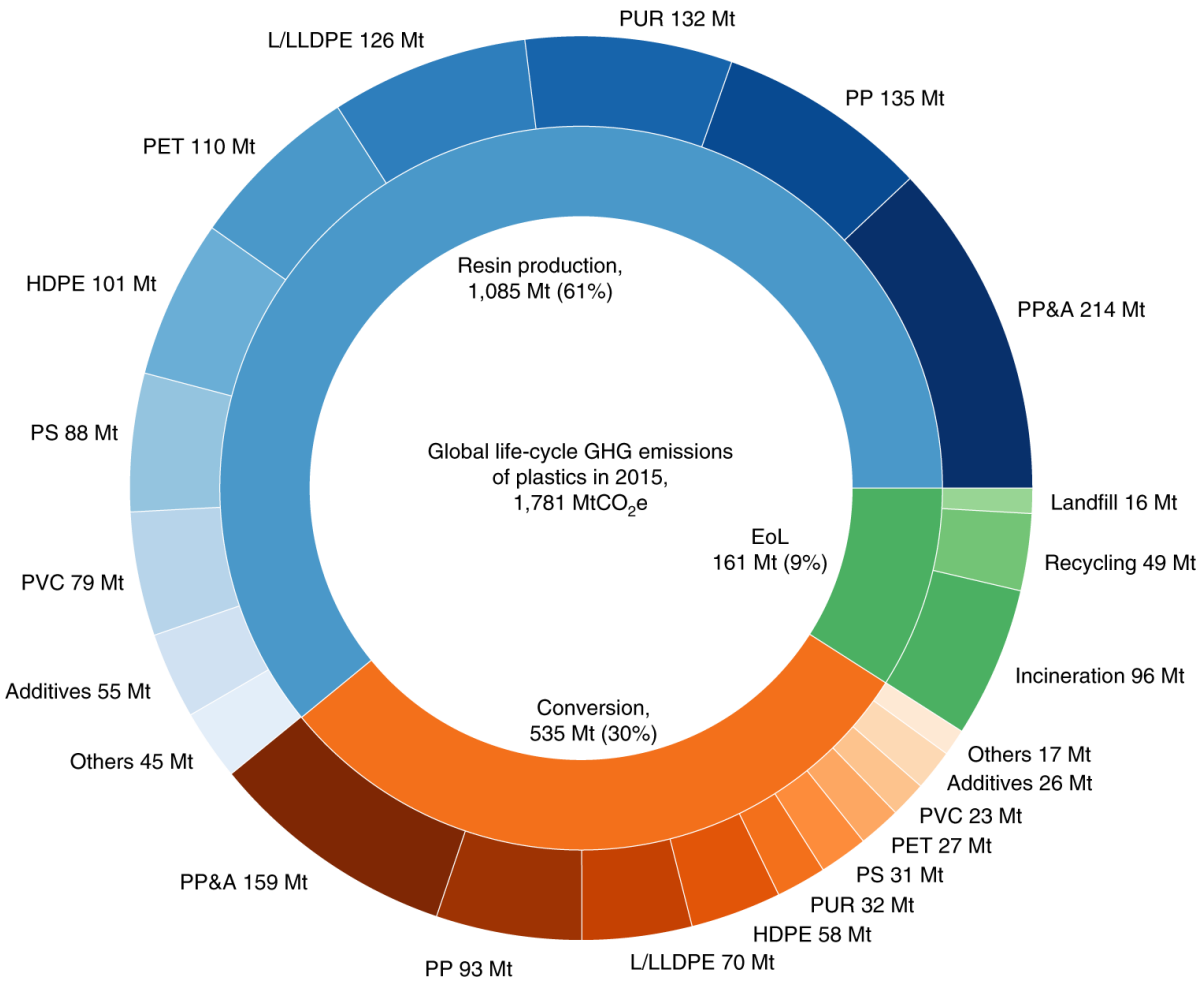

Figure 1. Global life cycle GHG emissions of conventional plastics in 2015 by life cycle stage and plastic type. Carbon credits generated by recycling are not included. Blue, orange, and green represent resin production, conversion, and end-of-life management stage, respectively. The emissions from each stage are broken down by plastic type or end-of-life treatment method, indicated with different shades of the corresponding color. Abbreviations: Polyethylene terephthalate (PET), High density polyethylene (HDPE), Polyvinyl Chloride (PVC), Low-density/linear low-density polyethylene (L/LLDPE), Polypropylene (PP), Polystyrene (PS), Polyurethane (PUR), Polyester, Polyamide and Acrylic fibers (PP&A), Additives, and Others.

The EoL stage accounted for 9% of total life cycle emissions, excluding the carbon credits from recycling. Incineration was the dominant source of GHG emissions among EoL processes. Landfill generated the least GHG emissions although the process handles the

largest share of plastic wastes (58%). The recycling process itself generated 49 Mt CO_2e emissions. However, if the displacement of carbon-intensive virgin polymer production by recyclates is considered, the GHG emissions of recycling would go down to -67 Mt, and the total emissions from EoL stage would be reduced from 161 Mt to 45 Mt CO_2e. In this case, the total global life cycle GHG emissions of plastics become 1.7 Gt CO_2e, or 3.5% of the global annual GHG emissions in 2015.

Under the current trajectory, the global life cycle GHG emissions from plastics are poised to grow rapidly (Fig. 2a). The global economy produced 407 Mt plastics in 2015, with an average annual growth rate of 4% between 2010-2015[9]. Following this trend, annual plastics production is expected to grow to 1,606 Mt by 2050, and the life cycle GHG emissions are expected to grow from 1.7 Gt CO_2e in 2015 to 6.5 Gt CO_2e in 2050, using the projected EoL management mix change[9], and maintaining current energy mix (baseline: red solid line in Fig. 2a). If all plastic waste are incinerated by 2050, total annual emissions will reach 8.0 Gt CO_2e (a 22% increase from the baseline). Recycling all plastic waste, however, would reduce the emissions to 4.9 Gt by 2050 (a 25% reduction from the baseline).

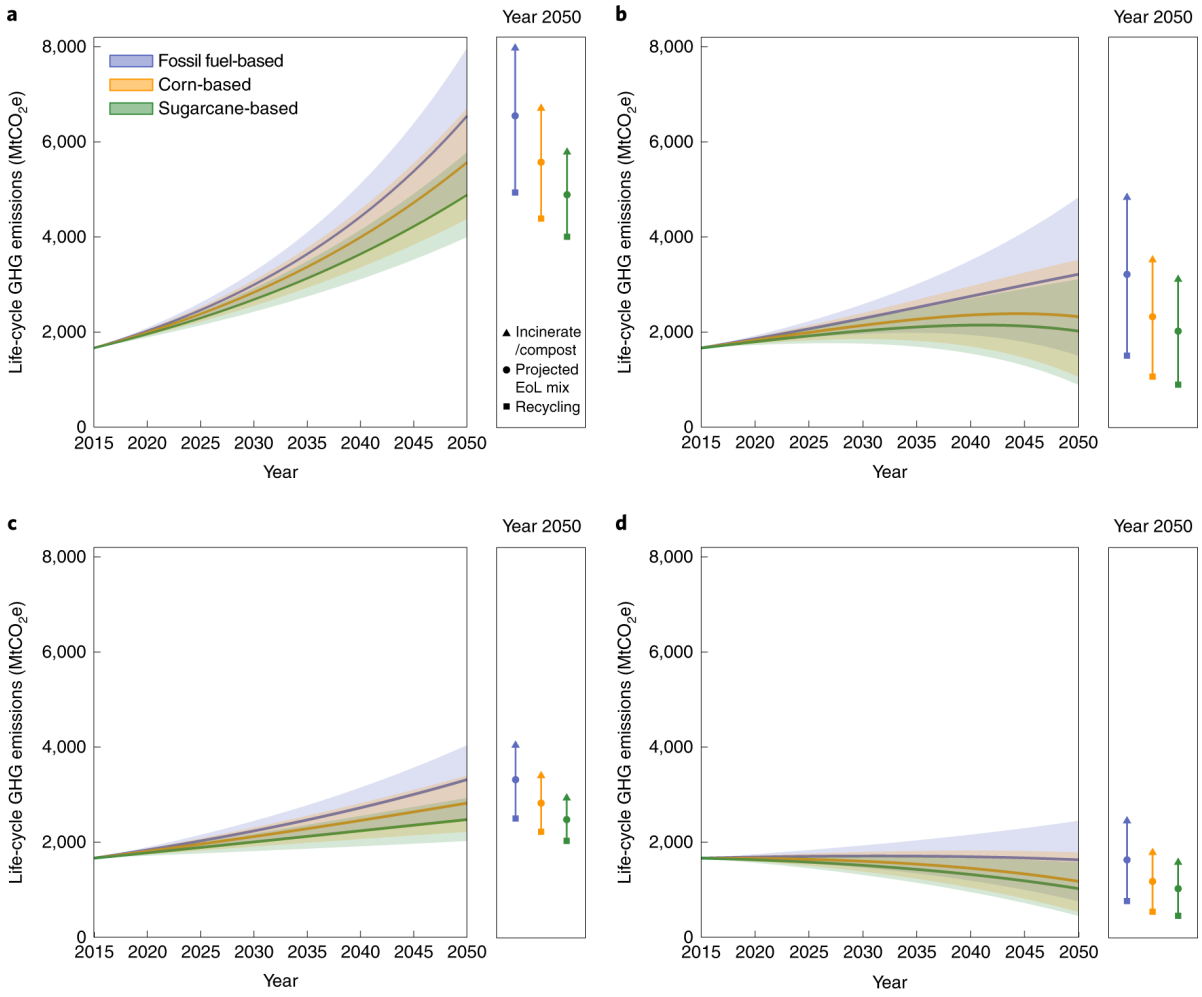

Figure 2. Global life cycle GHG emissions of plastics under scenarios of different feedstock sources, energy mix, end-of-life management and plastics demand growth, 2015-2050. Solid lines: projected end-of-life management mix (Supplementary Table 10); shaded areas: ranges due to EoL options; right-side bar of each panel: ranges due to different EoL options in 2050. **a,** plastics demand grows at 4% year^{-1} under current energy mix. **b,** plastics demand grows at 4% year^{-1}, and energy mix decarbonizes until 2050. **c,** plastics demand grows at 2% year^{-1} under current energy mix. **d,** plastics demand grows at 2% year^{-1}, and energy mix decarbonizes until 2050.

With a plastics demand growth rate of 4% year^{-1}, a complete replacement of fossil-based plastics by corn-based plastics is estimated to reduce global life cycle GHG emissions of plastics to 5.6 Gt CO_2e by 2050 under current energy mix and the projected EoL mix, which

is 1.0 Gt or 15% less than the baseline (Fig. 2a). If all EoL "drop-ins" are incinerated and all EoL biodegradable plastics are composted, global life cycle GHG emissions of corn-based plastics would increase to 6.7 Gt CO_2e. Recycling all EoL bio-based plastics, however, would reduce the emissions to 4.4 Gt CO_2e. Sugarcane-based plastics can further reduce global life cycle GHG emissions of plastics to 4.9 Gt CO_2e, which is 1.7 Gt or 25% less than the baseline, with a range between 5.8 Gt (100% incineration/composting) and 4.0 Gt (100% recycling). Our model shows that fossil-based plastics under 100% recycling scenario achieves similar or even lower emissions compared to bio-based plastics with the projected EoL mix (Fig. 2a and 2b, sidebars). This implies that the recycling of conventional plastics may be as beneficial as using renewable feedstock.

Decarbonising energy shows a significant potential to reduce GHG emissions (Fig. 2b and Fig. 2d). On average, switching to 100% renewable energy reduces life cycle GHG emissions from plastics by 62% in 2050, assuming 4% year^{-1} demand growth. Even if fossil sources (petroleum, natural gas and coal) serve as the sole feedstock for future plastics production, using 100% renewable energy can achieve 51% reduction (projected EoL mix) compared to the baseline, although the absolute total emissions would double the 2015 level by 2050. However, recycling all EoL plastics under 100% renewable energy allows 77%, 84% and 86% reductions in life cycle GHG emissions from fossil, corn and sugarcane-based plastics, respectively. This result shows that absolute reduction of emissions can only be achieved by combining aggressive deployment of renewable energy and extensive recycling of plastics.

Reducing plastics demand growth rate from 4% to 2% year^{-1} achieves 56% (under the current energy mix) to 81% (under low carbon energy) reduction from the baseline in 2050

(Fig. 2c and 2d). Using 100% renewable energy keeps the emissions flat at 2015 level for fossil-based plastics with projected EoL mix, and replacing them with bio-based ones brings the emission levels down further. Among all the scenarios tested, the global life cycle GHG emissions of plastics were the lowest under the 100% sugarcane-based plastics with 100% renewable energy combined with 100% recycling and reduced demand growth, which achieved 0.5 Gt CO_2e/year, or 93% reduction from the baseline. This demonstrates that a drastic reduction in global life cycle GHG emissions of plastics would be possible in a technical sense, but it would require implementing all of the four strategies examined at an unprecedented scale and pace.

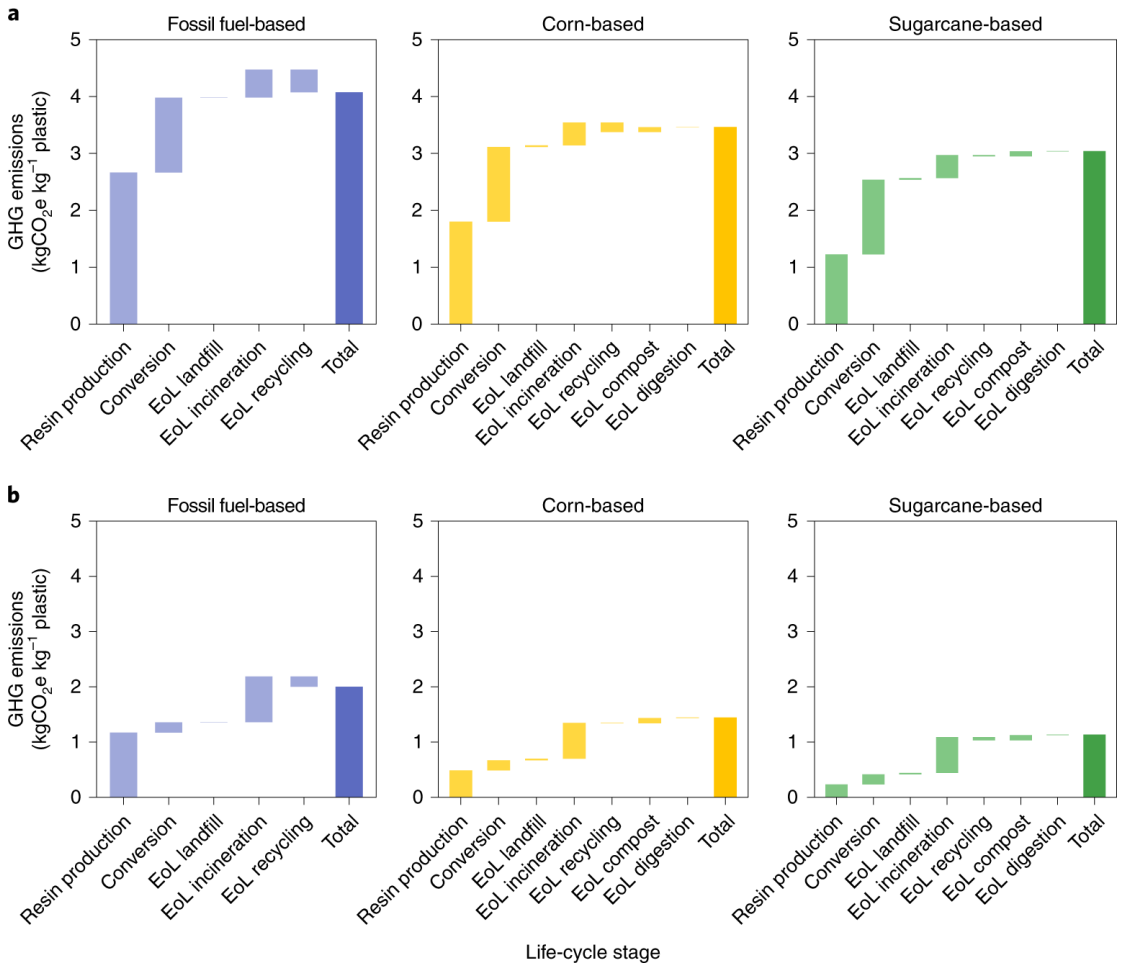

Figure 3. GHG emissions breakdown by life cycle stage of plastics derived from different feedstock types under two energy mix scenarios in 2050. a, GHG emissions per kilogram of plastics under the current energy mix scenario in 2050. **b,** GHG emissions per kilogram of plastics under a 100% renewable energy scenario in 2050. Emissions results are based on the scenario of 4% annual plastic demand growth rate and the projected end-of-life management mix (Supplementary Table 10). Carbon credits of recycling are considered.

Figure 3 shows the breakdown of GHG emissions by life cycle stage, normalised to per kilogram of plastics derived from different feedstock types. The total life cycle GHG emissions for fossil-based, corn-based and sugarcane-based plastics are on average 4.1, 3.5 and 3.0 kg CO_2e/kg plastic in 2050, respectively, under current energy mix (Fig. 3a). Under a 100% renewable energy scenario, however, the average life cycle emissions will be

reduced to 2.0, 1.4 and 1.3 kg CO_2e/kg plastic, respectively (Fig. 3b). Plastics derived from renewable feedstock (assuming projected EoL mix) generate less GHG emissions over the whole life cycle compared to their fossil-based counterparts regardless of the energy system used.

Resin production and conversion stages are major contributors to the life cycle GHG emissions of all feedstock types under current energy mix (Fig. 3a). However, under the 100% renewable energy scenario, incineration becomes the largest contributor to the total emissions for bio-based plastics (Fig. 3b). Under the 100% renewable energy scenario, recycling generates fewer carbon credits, as the low GHG emissions of renewable energy undercuts the carbon benefits of avoided virgin polymer production.

D. Discussion and conclusions

In sum, our results show that none of the four strategies, namely bio-based plastics, renewable energy, recycling, and demand management, can achieve sufficient GHG mitigation for absolute reduction below the current level on its own; only when implemented in concert, these strategies can achieve the much-needed absolute reduction. Among them, decarbonization of the energy system, which is an economically more favorable option for GHG mitigation as compared to the use of bio-based plastics[35], shows the largest potential. Even if fossil feedstock is used as the sole source for plastics production, 100% renewable energy will reduce the average life cycle GHG emissions by half from the baseline emissions. If combined with extensive recycling or demand management, decarbonization of energy can virtually keep the current level of GHG emissions until 2050. Reducing GHG emissions even further to achieve absolute reduction from the current level requires large-

scale adoption of bio-based plastics in addition to implementing all the other three strategies examined.

Going forward, I see both opportunities and challenges in reducing the life cycle GHG emissions of plastics. The current global average plastics recycling rate of 18%[9] certainly presents a significant room for further improvement. The low price of fossil-based plastics, however, is a key barrier to dramatically increasing recycling rates. Together with technological innovations in plastics recycling, fiscal policies, such as carbon pricing and incentivizing recycling infrastructure expansion, should be considered to overcome such barriers[68,69].

Replacing fossil-based plastics with bio-based plastics plays an important role in GHG mitigation. Nevertheless, our results show that the emissions of bio-based plastics are highly dependent on the EoL management method chosen. Composting or incinerating bio-based plastic waste, for example, showed similar or even higher GHG emissions than the case of using 100% fossil-based plastics under projected EoL mix in 2050. Moreover, EoL management of bio-based—especially biodegradable—plastics requires systematic changes such as separate collection and recycling infrastructure, since inclusion of biodegradable plastics in the mix of conventional plastic waste can affect the quality of the recyclates[70]. Furthermore, composting of biodegradable plastics in home composting conditions or natural environments is much less effective than in industrial composting facilities[31]. Lastly, the land use implications of a large-scale shift to bio-based plastics need further research. In 2017, land use for bioplastics was reported to be 0.82 million hectares, or 0.016% of global land area, which would increase to 0.021% in 2022 under the projected market growth[34]. A complete shift of the plastics production of approximately 250 million tones to bio-based

plastics would require as much as 5 percent of all arable land[71], which, depending on where they take place, may undermine the carbon benefits of bio-based plastics. The use of lignocellulosic or waste biomass as feedstock and growing material crops in fallow lands would alleviate the pressure of cropland expansion and associated GHG emissions from land use change.

Our study shows that an aggressive implementation of multi-layered strategies would be needed in order to curb the GHG emissions from plastics. GHG mitigation strategies are often implemented within energy, materials, waste reduction and management policies in isolation. Our results indicate that absolute reduction in life cycle GHG emissions of plastics requires a concerted action among decarbonization of energy infrastructure, improvement of recycling capability, adoption of bio-based plastics, and demand management.

E. Acknowledgements

We acknowledge the financial support of the U.S. Environmental Protection Agencies Science to Achieve Results (STAR) Program under Grant No. 83557907. I also acknowledge UCSB Mellichamp Sustainability Fellowship and TMP Young Innovator Scholarship for financial aids. We thank Yuwei Qin, Elise Wall and Yanan Ren (at UCSB) for their helpful comments.

F. Appendix

Supplementary Table 1. Considered mitigation strategies and description of scenarios

Strategy	Scenario	Description
Feedstock	Fossil fuels	Conventional plastics continue to dominate the plastics market, without the presence of bio-base plastics. Plastic types considered: Polyethylene terephthalate (PET), High density polyethylene (HDPE), Polyvinyl Chloride (PVC), Low-density/linear low-density polyethylene (L/LLDPE), Polypropylene (PP), Polystyrene (PS), Polyurethane (PUR), Polyester, Polyamide and Acrylic fibers (PP&A), Additives, and Others.
	Corn	Bio-based plastics substitute for fossil-based plastics, with their market penetration grows from zero in 2015 to 100% in 2050. Plastic types considered: Bio-Polyethylene (Bio-PE), Bio-Polyethylene Terephthalate (Bio-PET), Polylactic Acid (PLA), Polyhydroxyalkanoates (PHAs) and Thermoplastic Starch (TPS).
	Sugarcane	
Energy mix	Current energy mix	Maintaining current energy structure and the emission data at each life cycle stage of plastics remain unchanged during 2015-2050.
	Low carbon energy	Energy structure decarbonises gradually and reach 100% renewable energy (wind power and biogas) in 2050.
End-of-life management	Projected EoL mix by 2050	Projection of future EoL management change based on literature and government statistics (see Supplementary Table 10 or below). For fossil-based plastics and Bio-PE/PET, recycling, landfill and incineration rates change from 18%, 58% and 24% in 2015 respectively, to 44%, 6% and 50% in 2050 respectively. For bio-based biodegradable plastics, recycling, landfill, incineration, industrial composting and anaerobic digestion rates change from 2%, 58%, 24%, 15% and 1% in 2015 respectively, to 44%, 6%, 30%, 18% and 2% in 2050 respectively.
	100% incineration or composting by 2050	The upper bound of EoL emissions. The higher emission value of incineration or composting is taken. Incineration or composting rate is assumed to grow linearly to 100% in 2050, with the rates of other EoL options decrease linearly.
	100% recycling by 2050	The lower bound of EoL emissions. Recycling rate is assumed to grow linearly to 100% in 2050, with the rates of other EoL options decrease linearly.
Plastics demand growth	4% $year^{-1}$	Plastics production follow the trend of recent years and continue to grow at 4% until 2050.
	2% $year^{-1}$	Plastics production grows a slower rate of 2% each year until 2050.

Supplementary Table 2. GHG emissions data sources of resin production processes for conventional plastics

Plastic type	Subtype	Global market share*	Unit process**
PET	-	-	polyethylene terephthalate production, granulate, bottle grade - RoW
HDPE	-	-	polyethylene production, high density, granulate - RoW
PVC	-	-	polyvinylchloride production, bulk polymerisation - RoW
PP	-	-	polypropylene production, granulate - RoW
L/LLDPE	LDPE	42.9%	polyethylene production, low density, granulate - RoW
	LLDPE	57.1%	polyethylene production, linear low density, granulate - RoW
PS	General Purpose Polystyrene (GPPS)	50%	polystyrene production, general purpose - RoW
	High Impact Polystyrene (GPPS)	50%	polystyrene production, high impact - RoW
PUR	PUR, flexible foam	55.5%	polyurethane production, flexible foam - RoW
	PUR, rigid foam	44.5%	polyurethane production, rigid foam - RoW
PP&A	Polyester	88.5%	polyethylene terephthalate production, granulate, amorphous - RoW
	Polyamide	8%	Nylon 6-6 and Nylon 6 average
	Acrylic	3.5%	Polyacrylonitrile fibres (PAN); from acrylonitrile and methacrylate; production mix, at plant

Note: *For polymers with different subtypes, the emission value of resin production is a weighted sum based on the market share of each subtype. Market share data are from www.statista.com.

**Most unit processes are from ecoinvent 3.4, except PAN production process, which is from ELCD 3.3 and is used as a proxy for acrylic production.

Supplementary Table 3. Emission data of different conventional plastic types at each life cycle stage under current energy mix (kg CO_2e/ton polymer)

Plastic type	Production	Conversion	End-of-life		
			Landfill	Incineration	Recycling*
PET	3,332	805	89	1,324	906
HDPE	1,949	1,123			
PVC	2,066	593			
L/LLDPE	1,962	1,088			
PP	1,983	1,366			
PS	3,517	1,240			
PUR	4,900	1,192			
PP&A fibers	3,625	2,700			
Additives	2,200	1,036			
Others	2,837	1,036			

Note: Please see "Life cycle GHG emissions of fossil-based plastics" section in Methods for detailed references and calculation methods. *The emission value of recycling here does not include credits.

Supplementary Table 4. Emission data of different bio-based plastic types at each life cycle stage under current energy mix (kg CO_2e/ton polymer)

Feedstock	Plastic type	Production	Conversion	End-of-life*				
				Recycling	Incineration	Landfill	Industrial composting	Anaerobic digestion
Corn	Bio-PE	995	1,314	906	1,324	89	-	-
	Bio-PET	2,280			1,324	89	-	-
	PLA	1,820			1,240	44	1,538	670
	PHA	3,385			1,310	3,400	1,771	790
	TPS	1,279			1,260	1,250	1,410	600
Sugarcane	Bio-PE	550		906	1,324	89	-	-
	Bio-PET	2,040			1,324	89	-	-
	PLA	566			1,240	44	1,538	670
	PHA	2,034			1,310	3,400	1,771	790
	TPS	1,279			1,260	1,250	1,410	600

Note: Please see "Life cycle GHG emissions of bio-based plastics" section in Methods for detailed references and calculation methods. *The emission value of recycling here does not include credits. References for EoL emission data of bio-based biodegradable plastics: landfill, ref. [49] and ref. [72]; Incineration/industrial composting/anaerobic digestion, ref. [59].

Supplementary Table 5. Life cycle emissions data of energy sources used under two different energy scenarios

Scenario	Energy source	Life cycle emissions	Unit	Data source
Low carbon energy scenario	Renewable biogas	18	g CO_2e/MJ LHV	Ref. [35]
	Electricity from wind power	12	g CO_2e/kWh	Ref. [35]
Current energy mix scenario	Current electricity mix*	544	g CO_2e/kWh	Calculated based on ref. [73] and ref. [74]
	Natural gas	56	g CO_2e/MJ LHV	Ref. [49]
	Diesel	82	g CO_2e/MJ LHV	Ref. [49]

Note: *World gross electricity production by source (2016): 38.3% coal, 3.7% oil, 23.1% natural gas, 10.4% nuclear, 16.6% hydro, 2.3% biomass, and 5.6% solar/wind/geothermal/others[74]

Supplementary Table 6. Emission data of different conventional plastic types at each life cycle stage in 2050 under low carbon energy scenario (kg CO_2e/ton polymer)

Plastic type	Production	Conversion	End-of-life		
			Landfill	Incineration	Recycling*
PET	1,466	113	89	2,227	372
HDPE	780	158			
PVC	599	83			
L/LLDPE	785	153			
PP	1,091	192			
PS	1,864	174			
PUR	2,107	167			
PP&A fibers	1,595	379			
Additives	946	145			
Others	1,220	145			

Note: Please see "Life cycle GHG emissions under low carbon energy scenario" section in Methods for detailed references and calculation methods. *The emission value of recycling here does not include credits.

Supplementary Table 7. Emission data of different bio-based plastic types at each life cycle stage in 2050 under low carbon energy scenario (kg CO_2e/ton polymer)

Feedstock	Plastic type	Production	Conversion	End-of-life				
				Recycling*	Incineration	Landfill	Industrial composting	Anaerobic digestion
Corn	Bio-PE	-435	184	372	2,227	89	-	-
	Bio-PET	670			2,227	89	-	-
	PLA	252			1,692	44	1,655	1,413
	PHA	1,017			1,928	3,400	1,908	1,641
	TPS	292			1,812	1,250	1,606	1,294
Sugarcane	Bio-PE	-496		372	2,227	89	-	-
	Bio-PET	-61			2,227	89	-	-
	PLA	-416			1,692	44	1,655	1,413
	PHA	958			1,928	3,400	1,908	1,641
	TPS	292			1,812	1,250	1,606	1,294

Note: Please see "Life cycle GHG emissions under low carbon energy scenario" section in Methods for detailed references and calculation methods. *The emission value of recycling here does not include credits.

Supplementary Table 8. Global primary plastics production and waste generation in 2015 by plastic type[75]

Plastic type	Primary resin production in 2015		Primary waste generation in 2015	
	Amount (Mt)	Percentage	Amount (Mt)	Percentage
PP	68	16.7%	55	18.2%
L/LLDPE	64	15.7%	57	18.9%
HDPE	52	12.8%	40	13.2%
PVC	38	9.3%	15	5.0%
PET	33	8.1%	32	10.6%
PS	25	6.1%	17	5.6%
PUR	27	6.6%	16	5.3%
PP&A	59	14.5%	42	13.9%
Additives	25	6.1%	17	5.6%
Others	16	3.9%	11	3.6%
Total	407	100%	302	100%

Supplementary Table 9. Substitution of bio-based plastics for conventional plastics

Plastic type		Bio-based non-biodegradable plastic substitutes		Bio-based biodegradable plastic substitutes		
		Bio-PE	Bio-PET	PLA	PHA	TPS
Conventional plastics	PE	70%	0	10%	10%	10%
	PS	0	0	35%	30%	35%
	PP	0	0	35%	30%	35%
	PET	0	55%	35%	10%	0
	PP&A	0	70%	30%	0	0
	PVC	90%	0	0	10%	0
	PUR	80%	0	0	10%	10%

Note: Please see “Substitution assumptions” section in Methods for detailed references and explanations.

Supplementary Table 10. Projection of global EoL management mix in 2015 and 2050

EoL Method	Fossil-based plastics & Bio-based non-biodegradable plastic		Bio-based biodegradable plastics	
	2015	2050	2015	2050
Recycling	18%	44%	2%	44%
Landfill	58%	6%	58%	6%
Incineration	24%	50%	24%	30%
Industrial composting	-	-	15%	18%
Anaerobic digestion	-	-	1%	2%

Note: The EoL mix estimation of fossil-based and bio-based non-biodegradable plastics are from ref. [75]. The EoL mix estimation of bio-based biodegradable plastics are estimated based on ref. [76], ref. [77], ref. [78] and ref. [75].

Supplementary Table 11. Numeric results of global life cycle GHG emissions (Mt CO_2e) of plastics in 2050 under different scenarios, varying feedstock, end-of-life management method, annual growth rate of plastics demand and energy mix (corresponding to Figure 2 in Main text)

Feedstock	EoL	4% yr-1, current energy mix	4% yr-1, 100% renewable energy	2% yr-1, current energy mix	2% yr-1, 100% renewable energy
Fossil fuel	Predicted*	6544	3214	3316	1629
	Incineration	7969	4831	4039	2448
	Recycling	4930	1504	2499	762
Corn	Predicted*	5569	2323	2822	1177
	Compost/Incineration**	6702	3517	3397	1782
	Recycling	4381	1061	2220	538
Sugarcane	Predicted*	4885	2020	2476	1024
	Compost/Incineration**	5779	3107	2929	1575
	Recycling	4001	892	2028	452

Note: *Projected EoL refers to the end-of-life management mix shown in Supplementary Table 10.
**In 100% composting/incineration scenarios with corn or sugarcane as feedstock, all EoL Bio-PE and Bio-PET are assumed to be incinerated, and all EoL biodegradable plastics are either composted or incinerated, depending on which emission value is higher.

Supplementary Table 12. Numeric results of average GHG emissions of plastics (kg CO_2e/ton plastic) by life cycle stage in 2050 under two energy scenarios and 4% annual demand growth rate (corresponding to Figure 3 in Main text)

Energy mix	Current energy mix			Low carbon energy		
Feedstock/ Life cycle stage	Fossil fuel	Corn	Sugarcane	Fossil fuel	Corn	Sugarcane
Resin production	2665	1800	1225	1172	487	232
Conversion	1314	1314	1314	184	184	184
End-of-life						
Landfill	4	27	27	4	27	27
Incineration	491	404	404	826	648	648
Recycling	-400	-170	-21	-185	-5	61
Industrial Composting	0	87	87	0	95	95
Anaerobic Digestion	0	4	4	0	9	9
Total	4074	3468	3042	2001	1447	1258

III. Mitigating curtailment and carbon emissions through load migration between data centers

Material from:

Zheng, J., Chien, A. A. & Suh, S. Mitigating Curtailment and Carbon Emissions through Load Migration between Data Centers. *Joule* **4**, 2208–2222 (2020).

https://doi.org/10.1016/j.joule.2020.08.001

Abstract. As the share of variable renewable energy (VRE) grows in the electric grid, so does the risk of curtailment. While energy storage and hydrogen production have been proposed as solutions to the curtailment problem, they often pose technological and economic challenges. Here, I analyze the potential of data center load migration for mitigating curtailment and greenhouse gas (GHG) emissions. Using historical hourly electricity generation, curtailment, and typical data center server utilization data, I simulate the effect of migrating data center workloads from fossil fuel-heavy PJM to renewable-heavy CAISO. The results show that load migration within the existing data center capacity during the curtailment hours in CAISO has the potential to reduce 113-239 $KtCO_2e\ yr^{-1}$ of GHG emissions and absorb up to 62% of the total curtailment with negative abatement cost in 2019. Our study demonstrates the overlooked role that data centers can play for VRE integration and GHG emissions mitigation.

A. Introduction

Driven by aggressive public policy and compelling economics, global capacity of Variable Renewable Energy (VRE), such as solar photovoltaics (PV) and wind electricity, is growing rapidly. European Union, for example, has a target to achieve at least 32% share of renewable energy by 2030,[79] and California aims at 60% renewable portfolio standard by 2030.[80]

As the penetration of VRE in the grid grows, so do the concerns of large-scale curtailment[81–83]. Curtailment is the reduction of output of a VRE resource below what it could have otherwise produced. It has been repeatedly reported in different world regions across Europe, America and Asia, significantly decreasing the market value of VRE.[83,84] Near-term reasons for VRE curtailment include minimum generation requirement for non-renewable energy sources and transmission constraints, but long term, fundamental causes drive increasing pressure for curtailment.[83,85] Large-scale energy storage and electricity transmission network expansion can mitigate VRE curtailment, but they are costly. With a system cost between $380 to $895 per kWh,[86] the battery storage capacity deployed globally (12 GWh in 2018)[87] is infinitesimal compared to the amount of global electricity consumption (about 23,000 TWh per year).[88] Long-distance transmission of VRE-generated electricity is possible but the construction of transmission infrastructure and the associated transmission losses are often cost-prohibitive.[89] Pumped hydro can be another storage solution, but it requires certain geographical features and may raise ecological concerns.[90]

Another approach to reduce curtailment is to use excess VRE electricity to produce more easily storable materials or products, such as hydrogen through water electrolysis, which can be shipped upon demand.[91,92] However, the logistics and handling of these materials and

associated costs can pose additional challenge.[93] A potential solution to this logistics and handling problem is to use over-generated electricity to produce something that can be transported at minimal cost and energy: information.

Data centers can provide battery-like demand side management service by powering data processing with excess VRE. The technical and economic potential of zero-carbon cloud data centers which solely run on stranded renewable power has been explored.[94,95] Geographical load balancing has been widely studied to maximize renewable energy use by distributing the workloads among data centers in different locations.[96,97] Data centers are highly automated and monitored with little human interventions. Importantly, they have considerable flexible workloads which can be distributed geographically.[95,98] Provided the requisite data is available, those data centers with access to renewable energy can process the requests routed from other regions and return the results to users while meeting Service Level Agreements (SLAs). Moreover, most data centers operate well below 100% capacity most of the time – over-provisioning for peaks leaves servers and network resources underutilized.[99] Furthermore, the peak loads for data processing often does not coincide with the peak time of VRE over-generation, providing room for data centers to use their excess capacity to process additional workloads with excess VRE.

Compared with building large-scale transmission infrastructure, building fiber optics networks and transmitting data are much cheaper, and takes significantly less time.[89] Therefore, the transmission of data is more economically favorable than the transmission of electricity, i.e. “moving bits, not watts”.[100] Furthermore, the society’s needs for data processing is growing rapidly. Global data centers used 205 TWh electricity in 2018 or 1% of global electricity consumption.[10] In 2014, U.S. data centers consumed 70 TWh electricity,

which was 1.8% of the total annual U.S. electricity consumption.[101] It is estimated that the global datasphere will grow from 33 zettabytes (ZB) in 2018 to 175 ZB in 2025 at an annual growth rate of 27%, implying growing needs for data center infrastructures.[102] The decarbonization of data centers is imperative, and require combined efforts including maximizing IT-device efficiency, adoption of low-carbon electricity and improving infrastructure efficiency.[103] Load migration between data centers can collectively improve IT efficiency and utilization of renewable energy. Nevertheless, the potential for load migration between data centers to utilize excess VRE generation and reduce greenhouse gas (GHG) emissions has not been quantified.

In this chapter, I use two Independent System Operators (ISOs) in the U.S., California ISO (CAISO) and Pennsylvania-New Jersey-Maryland Interconnection (PJM), as a case study to explore the potential of workloads migration between data centers to mitigate curtailment and GHG emissions. PJM is the largest ISO in the U.S., which predominantly relies on thermal energy sources like coal and natural gas, with solar and wind accounted for only 3.2% in 2019.[104,105] The states covered by PJM host a large amount of data centers, with the most noteworthy area being North Virginia. In the second half of 2018, North Virginia absorbed over a third of the world's new data center capacity, with an addition of 270 Megawatts (MW) data center power.[106] As the hub of technology and media companies, California also has many data centers, mostly located in the Bay Area and Southern California.[107] Of all the data center colocation establishments in the U.S., 15% are located in California and about 16% are in PJM region.[108,109]

Based on the historical hourly curtailment data of CAISO and a typical data center energy consumption profile, I evaluate the potential of the existing and additional data

center capacities to absorb excess VRE and reduce GHG emissions by migrating data center workloads from PJM region. In this analysis, I use counterfactual scenarios as an illustration of the potential rather than as a record of historical accounts.

B. Methods

1. Historical curtailment and GHG intensity

I collected the historical solar and wind curtailment data of CAISO at a 5-min interval during 2015-2019.[110] I analyzed and visualized the curtailment data on an hourly basis. To calculate the hourly GHG intensity of the two grids, I first collected the data of electricity supply by energy resource type. I collected the hourly generation data by resource type with breakdown of renewable resources of CAISO during 2015-2019 from CAISO website.[111] For PJM, the generation data was obtained from the Generation by Fuel Type dataset from Data Miner 2 database.[105] The generation data for year 2015 was not available in PJM database so only 2016-2019 data was used. Due to daylight savings time change, the generation data of PJM at 2 a.m. in a certain day in March was missing, and I handled it by filling it with the average value of two adjacent hours; there were duplicate data points at 1 a.m. in a November day, and I only kept the latter one of the two duplicate hours.

To calculate the GHG emissions and intensities, I used the life-cycle GHG emissions data for each energy resource. Life-cycle GHG emissions are the total emissions from all stages of an energy resource's life cycle, covering upstream, operational and downstream processes. These processes include fuel/raw material extraction, transport, infrastructure construction/equipment manufacturing, combustion (for fossil fuels), equipment operation and maintenance and waste treatment. For natural gas, I used the life-cycle GHG emissions

value of natural gas combined cycle in the U.S. reported by National Energy Technology Laboratory.[112] For coal, I used the generation-weighted average life-cycle GHG emissions data based on an investigation of over 300 coal power plants in the U.S.[113] For low-carbon energy resources, the median values of the life-cycle GHG emissions presented in the Fifth Assessment Report by Intergovernmental Panel on Climate Change (IPCC) were applied.[114] The category "thermal" in CAISO generation data was treated as natural gas as the share of coal is negligible. The category "other renewables" in PJM generation data is considered as an equal mix of biomass and biogas. For any unspecified resource type such as "multiple fuels" and "other", an average unspecified emission value was used.[115] Table S1 summarizes the life-cycle GHG emissions values of electricity generation by energy resource that were used in this study. Imports of CAISO were not included when calculating the GHG intensity of generation as the energy mix was not clear. PJM was a net exporter of electricity as I summarized its interchange dataset.[116]

The hourly GHG intensity of electricity supply during 2016-2019 was calculated as the weighted average of the life-cycle GHG emissions of all the energy resources in that hour (equation 1).

$$GHG\_intensity_h = \sum_i (GHG_{LC,i} \times Generation_{i,h}) \div \sum_i Generation_{i,h} \quad (1)$$

In equation (1), h is a certain hour in a year, and i is a certain resource type. $GHG\_intensity_h$ (in $kgCO_2e/MWh$) is the GHG intensity of the grid in hour h, $GHG_{LC,i}$ (in $kgCO_2e/MWh$) is the life-cycle GHG emissions of resource i, $Generation_{i,h}$ (in MWh) is the electricity generated by resource i in hour h and $\sum_i Generation_{i,h}$ (in MWh) is the total electricity generation by all resources in hour h.

2. Reductions in curtailment and GHG emissions

The electricity consumption profile of a real-world data center on an hourly basis is difficult to obtain due to the secretive nature of the industry. Therefore I use the simulated energy consumption profile of a data center which has a critical (IT) power of 10 MW and a typical data center design.[117] I obtained the hourly electricity consumption data of the typical data center in a week and extended the weekly profile to a year. The data center has a total peak power of 21 MW and consumes approximately 114 GWh electricity annually.[117] The detailed technical specifications and the energy consumption data of this typical data center are shown in Table S2. Seasonal variations of the energy consumption are not considered.

Energy consumption of a data center is jointly determined by their IT and non-IT energy efficiency. I made assumptions of two key parameters to model future data center energy use, Dynamic Range (DR) and Power Usage Effectiveness (PUE), considering the energy efficiency improvement of both IT and non-IT components. The yearly values of the parameters assumed for 2016-2019 are shown in Table S3. DR determines the lowest power (idling power) consumption of servers, which serves as the intercept in the linear model between server power usage and server utilization rate. As server power efficiency improves, DR value gets lower. In other words, the power usage of servers while idling would decrease over time as a result of improved energy proportionality.[118] I assume that the average DR value drops from 0.25 to 0.11 from 2012 to 2019 based on the historical DR value changes reported in several literature sources.[118–120] For the energy efficiency improvement of non-IT components in data centers, I simulate the change of PUE value during the examined period. I assume that the average PUE of data centers served by CAISO decreases from 1.59 to 1.30 from 2012 to 2019 based on the PUE trend in the data

center industry surveys conducted by Uptime Institute[121,122] and recent PUE values of California data centers from a colocation website.[123] I also developed a model based on the energy profile from the reference to simulate the linear relationship between hourly non-server energy consumption and server utilization rate ($R^2 = 0.988$). With this model, I calculated the hourly non-server energy consumption given certain annual average PUE value assumed for the year. Both PUE and DR values are assumed to change linearly during the examined period.

Under Migration Scenario, during the hours when there is excess VRE in CAISO, workloads from the data centers served by PJM are assumed to be migrated to the data centers served by CAISO. The time difference between CAISO and PJM regions of three hours is considered. I assume using the remaining capacity of existing data centers to respond to excess VRE generation of CAISO first, and then use additional data center capacity to absorb the rest of the excess generation. The remaining capacity of existing data centers is determined by the allowed maximum server utilization rate during underutilized hours, for which I set different levels between 65% and 90% as explained in the main text. While in theory, servers should be able to run at 100% utilization rate, in practice they are run at significantly lower utilizations to tolerate the burstiness of computations, and fluctuations of loads[118]. Our assumption of 90% as the upper bound of the maximum server UR is a conservative assumption with respect to the benefits of workloads migration. The additional data centers, assumed to be Zero-Carbon Cloud (ZCC) data centers, run at the maximum server utilization rate with the remaining excess VRE that exceeds the existing data centers' capacity. The GHG emissions reduction is then calculated as the difference of total GHG emissions between the Baseline Scenario and the Migration Scenario, i.e., by

multiplying the amount of excess VRE generation absorbed by CAISO data centers and the GHG intensity difference between PJM generation and the excess VRE generation in CAISO.

To ensure a holistic perspective, the embodied GHG emissions of additional data centers are taken into account. They include all the non-operational emissions that come from the manufacturing of IT, electrical, mechanical equipment and building materials, etc. Life cycle assessment (LCA) studies of data centers are scarce in the literature, but I identified one study that has the energy consumption breakdown by data center component. The study shows that non-operational emissions account for 6.5% of the total life-cycle climate change impacts of a data center[124]. I calculated that the yearly non-operational energy consumption of a data center is around 432 MWh electricity per MW of critical (IT) power based on the data from the reference, assuming a 5-year IT refresh rate as the additional data centers run intermittently.[124] According to the Emissions & Generation Resource Integrated Database (eGRID) by U.S. EPA, the average GHG intensity of U.S. grid was 456 and 432 $kgCO_2$/MWh in 2016 and 2018, respectively. I extrapolated the two points linearly and estimated that the average GHG intensity in 2017 and 2019 was 444 and 421 $kgCO_2$/MWh, respectively. The embodied GHG emissions of a U.S. data center therefore amounted to 0.20-0.18 $KtCO_2e$/MW critical power per year during 2016-2019. I validated the number by analyzing the data from another earlier data center LCA study and it yielded similar estimate.[125]

3. Estimation of abatement cost

For the costs of additional data center capacity under the Migration Scenario, I use the cost estimates developed for the ZCC data centers that run solely on stranded renewable

power.[94] They typically co-locate with existing renewable generation facilities and therefore the costs of power transmission and distribution can be reduced. The total abatement cost sums up the changes between the Baseline Scenario and Migration Scenario in facility cost, electricity cost and additional cost for a certain year.

(1) Facility cost. The amortized physical facility cost of ZCC data centers ($0.50 per watt of critical power) is markedly lower than that of traditional data centers ($5.25/W) by using containers and co-locating at renewable generation sites[94]. But ZCC data centers run intermittently depending on the availability of excess VRE generation, and traditional ones run continuously as a comparison. Under the Migration Scenario, the amortized facility cost of ZCC data centers is obtained by simply multiplying $0.50/W with the total IT power, e.g., a 10 MW ZCC data center has an amortized facility cost of $5 million. To capture the facility cost of typical data centers served by PJM under the Baseline Scenario, I divided the amortized facility cost (e.g., $52.5 million for a typical traditional 10 MW data center) by its annual energy consumption, and then multiplied this unit facility cost (in $/MWh) with the amount of excess VRE generation absorbed by additional data centers through workloads migration in that year. In other words, I allocated the facility cost of data centers under the Baseline Scenario based on the amount of load that could be migrated to additional data centers under the Migration Scenario. Supplemental Equation S15-S17 represent the mathematical expressions of calculating facility costs.

(2) Electricity cost. I assume zero cost for the over-generated electricity under the Migration Scenario since excess VRE generation is regarded as “stranded energy” and it would have been curtailed if not utilized. I used the historical average retail electricity prices

for Virginia during 2016-2019 as representative values to calculate the electricity costs of typical data centers powered by PJM under the Baseline Scenario.

(3) Additional cost. Due to the fact that ZCC data centers run on intermittent excess VRE generation, additional solid state drives (SSDs) and energy storage devices to checkpoint-restart jobs interrupted by a power outage are needed.[94] Combined with hardware for free cooling, the total additional cost incurred is $0.175/W per year.

The amortized compute cost and network cost are assumed to be the same under the two scenarios. Workloads migration has the potential to increase software licensing costs, particularly if additional virtual instances are required. I do not model this cost, due to the lack of public information both on software use and licensing. The detailed cost breakdown is summarized in Table S4. Summing up all the cost changes across facility cost, electricity cost and additional cost due to workloads migration, I estimate the total abatement cost for each year. Then by dividing the total abatement cost by the total net GHG emissions reduction, I derive the net abatement cost standardized by one unit of GHG emissions reduction in a certain year. All the computation steps are presented in Equations S1-S21, with nomenclature listed in Table S5.

4. Limitations

There are a few uncertainties and limitations with this study. First, I used a typical data center energy consumption profile to estimate the remaining absorption capacity for excess VRE. In reality, it may not be representative enough as the data centers in CAISO region probably have various energy consumption patterns. I also extrapolated the weekly energy consumption data to the entire year, while in fact the profile may change because of temperature range under different climate conditions. Second, there is no complete and

transparent database available on the current data center capacity in the U.S., and the information of the power consumption of the data centers is particularly scarce, so I had to use limited available data points to estimate the existing capacity of data centers in CAISO region. Third, the DR and PUE values of data centers in real world vary depending on the data center type, scale and location. I simulated the average values as a simplification when geographic-specific and fine-grained data are lacking. I also simplified the analysis by assuming that the migration occurs between data centers of similar scale with typical energy use characteristics, while the electricity consumption to process a same compute task may be different for data centers with contrasting characteristics. Lastly, there is uncertainty with the data center costs. The cost components of data centers fall in a broader spectrum in the real-world, and they may evolve in the future due to a variety of reasons including disruptive technology development. The abatement cost of workloads migration may involve more potential cost categories such as new devices and algorithms that are necessary to enable the load migration and communication between grid operators and data centers.

C. Results

1. Historical curtailment of CAISO

I collected and analyzed the historical curtailment data of CAISO during 2015-2019. The total annual curtailment of CAISO grew from 188 GWh to 965 GWh from 2015 to 2019, at an average annual growth rate of 51%. Curtailment data at CAISO shows wide daily and seasonal variations, with an upward trend over time (Fig. 1a). Solar PV curtailment accounted for 90% of the total cumulative curtailment during this period and wind accounted for 10%. The majority of curtailment occurred in the first and second quarter,

which combined accounted for 69% of the total curtailment in the period. Monthly curtailment peaked in April or May. This results from growing solar radiation strength and extended daytime length during spring, combined with mandatory runoffs from northwest hydro generation imports and cool weather. Both solar and wind curtailment occurred the least in the third quarter with July or August seeing the minimum, which can be explained by higher cooling demands in summer's warmer weather. The surge of solar curtailment during 2015-2019 mirrors the fact that the share of solar power in total CAISO generation had increased from 6.7% to 13.0% in this period. In comparison, the share of wind power in the generation mix increased from 5.3% to 7.2%, representing a milder growth than solar. When disaggregated at hourly resolution (Fig. 1b), curtailment took place rather randomly throughout the 24 hours of a day in 2015 and 2016, but as solar PV capacity grew and

nighttime wind curtailment decreased during 2017-2019, total curtailment became increasingly more conspicuous in the daytime.

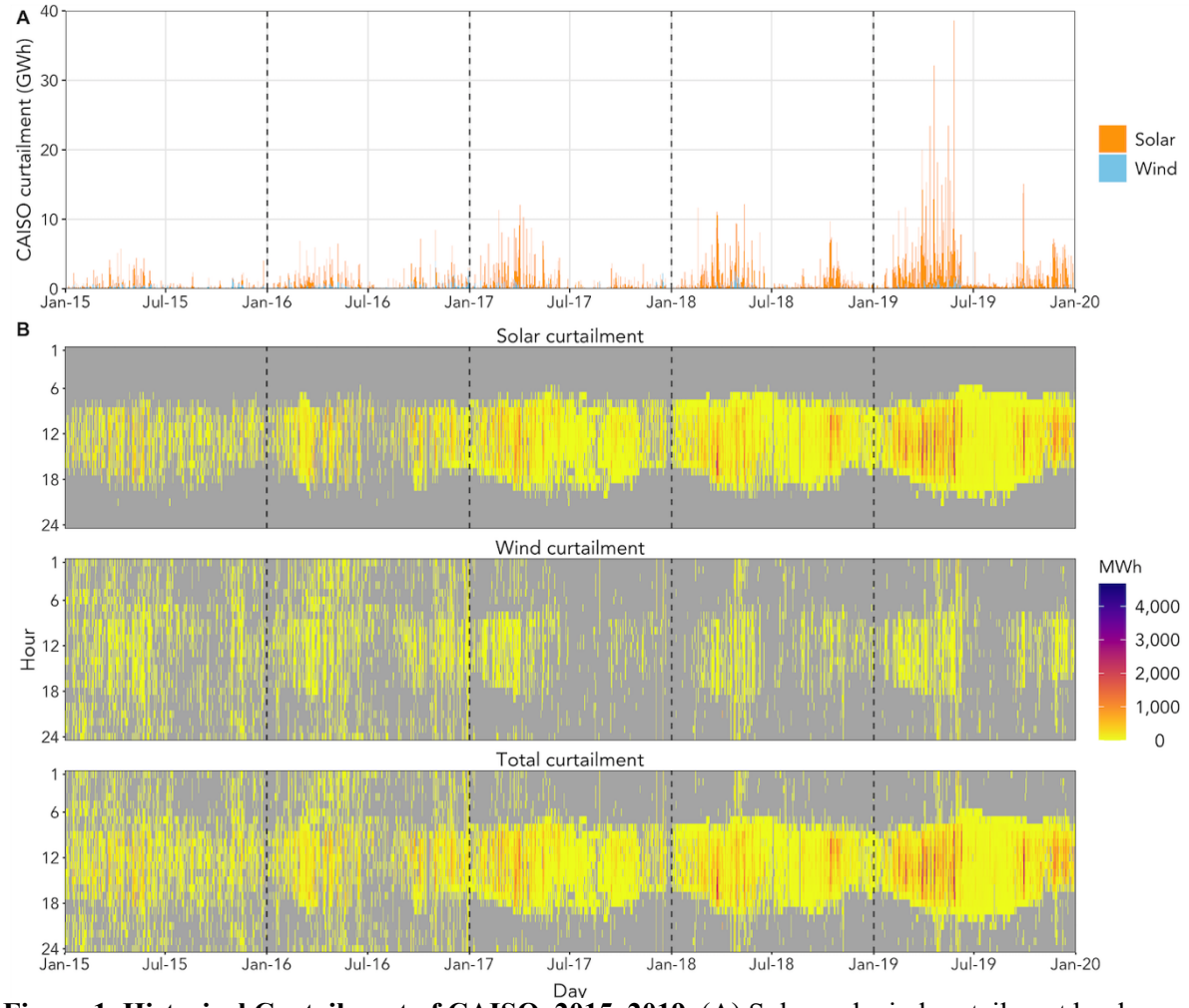

Figure 1. Historical Curtailment of CAISO, 2015–2019. (A) Solar and wind curtailment by day. (B) Solar, wind, and total curtailment by day and hour.

Instead of curtailing, the excess VRE generation in CAISO could be used to process data center workloads migrated from carbon-intensive grid regions. Many data centers operate at less than 50% average server utilization rate,[101,118,126] and the time-zone difference between PJM and CASIO helps avoid peaking load at the same time, allowing the data centers served by CAISO to take on additional data processing jobs migrated from PJM-served data centers

during the off-peak hours. I use the historical curtailment data, which is referred to as "excess VRE" hereafter, to evaluate the potential of migrating workloads between data centers.

2. Hourly GHG intensity of CAISO and PJM

I collected and treated the electricity generation by energy resource data for CAISO and PJM during 2016-2019.[105,111] The life-cycle GHG intensities of the two ISOs during 2016-2019 (Fig. 2) were calculated on an hourly basis based on the historical generation data and U.S.-specific GHG emission factors, which include both combustion emissions and life-cycle emissions embodied in the inputs to power generation (Table S1). Imported electricity is not included in the calculation.

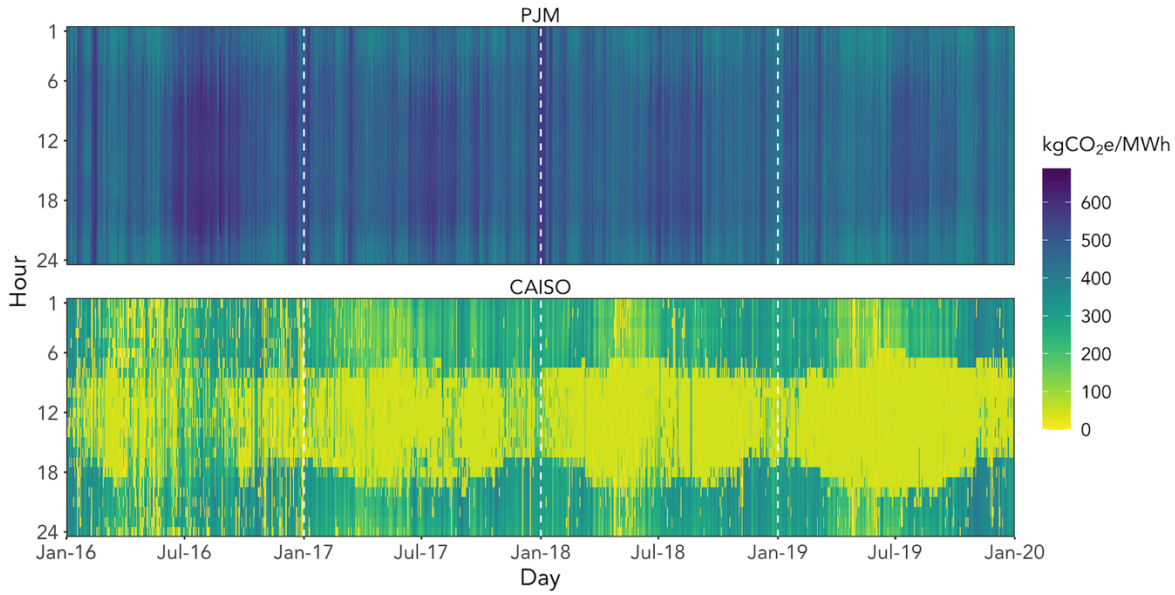

Figure 2. Hourly Life-Cycle GHG Intensity of PJM and CAISO, 2016–2019. During the time when there was curtailment in CAISO, only the intensity of curtailment (assumed proportionally contributed by solar and wind curtailment) is shown. Intensity of imports is not included.

The annual average GHG intensity of PJM decreased from 499 to 452 $kgCO_2e/MWh$ during 2016-2019. The monthly average intensity of PJM peaked in summer (July or August) and reached its lowest around April and October, with a range between 417-557 $kgCO_2e/MWh$. For CAISO, the annual average GHG intensity changed from 262 to 231 $kgCO_2e/MWh$ during the same period. The monthly intensity of CAISO hit the lowest in April or May due to prominent solar and hydro power production.

During the hours when curtailment occurred in CAISO, only the intensity values of the curtailment (i.e., excess VRE) are shown (Fig. 2 - CAISO), which is assumed to be proportionally contributed by curtailed solar and wind power. In other words, the GHG emissions intensity of the excess generation is calculated as the average life-cycle GHG emissions intensity of solar and wind weighted by their shares in the total curtailment during that hour. While the average GHG intensity of CAISO excess generation during 2016-2019 was 41 $kgCO_2e/MWh$, the average GHG intensity of PJM during CAISO's excess generation time was 476 $kgCO_2e/MWh$. The significant differences of the GHG intensities between the two grids during CAISO excess generation time present a great opportunity for GHG emissions mitigation by migrating the data center workloads geographically.

3. The capacity of data centers to absorb excess VRE

I first estimated the existing data center capacity in CAISO region. I collected the available data center location and power consumption data from a colocation data center industry website.[123] By examining the profiles of all the listed data centers in California, I calculated that the average annual total power consumption per colocation site is 9.92 MW, based on 26 data points that provided the information. I also identified that currently there are 288 data centers in CAISO region by the end of 2019.[127] I use a typical data center

energy profile with an IT peak power (or critical power) of 10 MW as a standardized unit[117] in this study to estimate the excess VRE absorption capacity, GHG emissions reduction potential and abatement cost.

I then simulate the Dynamic Range (DR) and Power Usage Effectiveness (PUE) of the data centers served by CAISO. DR is the ratio of a server's idling power to its maximum power,[101] based on which I calculate the energy consumption of servers given the rated power and utilization rate. PUE is defined as the ratio of the data center total energy consumption to IT equipment energy consumption, calculated, measured or assessed across the same period.[128] PUE values vary depending on data center type and geographical location. Here, I model the average PUE of colocation data centers in California. Detailed assumptions of the two parameters can be found in Experimental Procedures and Table S3. I also developed linear model between the hourly server utilization rate and the energy use of non-server components,[117] through which I can calculate the non-server energy consumption given a certain PUE value in a year.

I compare two scenarios for evaluating the excess VRE absorption potential of data center workloads migration: Baseline Scenario and Migration Scenario. In Baseline Scenario, workloads are processed by typical data centers served by PJM without any migration. In Migration Scenario, workloads are first migrated to and processed by the existing typical data centers served by CAISO. I assume that the migration occurs between data centers of similar scale with typical energy use characteristics in our model. Once the existing capacity is exhausted, I assume building additional data center capacity which run solely on the remaining excess VRE. I assume that the data centers all have advanced algorithms and automation mechanisms in place to enable the load migration.

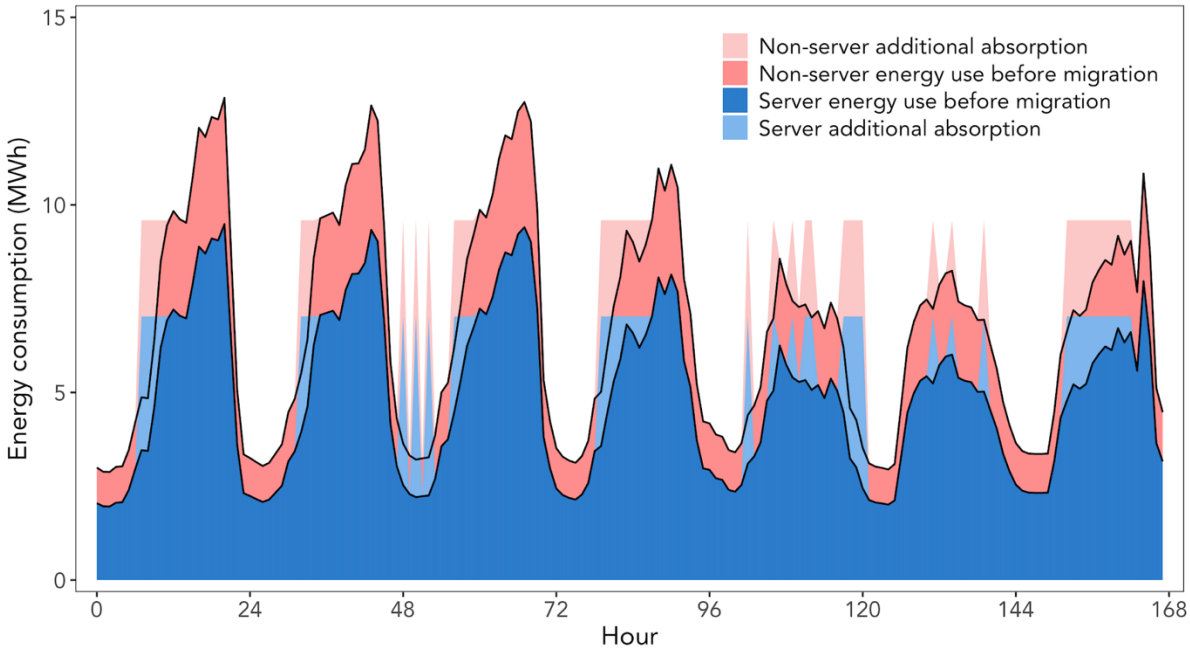

Figure 3. Illustration of the Energy Consumption Profile Change of a Typical Data Center in the Baseline Scenario (No Workloads Migration) and the Migration Scenario (with Workloads Migration) in a Week. A maximum allowed server UR of 65% during underutilized hours is assumed in this graph as an example.

Fig. 3 illustrates the excess VRE absorption potential of a typical data center in a week. The remaining capacity of an existing data center in an underutilized hour is calculated by subtracting the existent load of the data center in that hour from its maximum allowed load. Load migration is only enabled during the hours that the servers in data centers served by CAISO are underutilized. I test different scenarios by varying the assumption of the maximum allowed server utilization rate (UR) between 65% and 90% during underutilized time, representing an improved management and a maximized utilization scenario, respectively. Average utilization rate of large-scale cloud providers is estimated as 65%.[129] Once the remaining capacities of all existing data centers are exhausted, I calculate the respective additional data center capacity needed to absorb different portions of the total

excess VRE. During excess generation hours, the servers in the additional data centers would be activated to process the workloads migrated from PJM region and operate at the maximum allowed UR assumed. The servers are assumed to be shut down at times when there is no available excess VRE.

4. GHG emissions reduction and abatement cost

I calculate the achieved total GHG emissions reduction by summing up the products of the hourly GHG intensity difference between the two scenarios and the amount of excess VRE absorbed for each year between 2016-2019. I then estimate the total abatement cost of the plan by comparing the cost difference between the two scenarios. For the excess VRE that fall within the remaining capacity of existing data centers, workloads migration causes only a change in electricity bills between the two scenarios. When additional data centers are built to absorb extra excess VRE, changes in electricity cost, amortized facility cost and additional cost are all captured.

I use the cost estimates developed specifically for zero-carbon cloud (ZCC) data centers that run on stranded renewable power[94] for the additional data center capacity in Migration Scenario. These intermittent data centers have lower facility cost because they use containers and can be located near renewable generation sites with less power distribution costs.[94] The electricity cost is also significantly lower for ZCC data centers than the traditional ones as the otherwise-curtailed VRE electricity is assumed to have zero cost. Additional cost for installing data and energy storage devices will incur due to the intermittent characteristic of the power supply for ZCC data centers. The cost of applications including software licenses, system and database administration are not considered as they vary greatly and do not constitute part of the infrastructure-related capital or operational

cost. The total abatement cost sums up the difference of facility, electricity and additional costs between the two scenarios on an annual basis. The net abatement cost (in $/metric ton CO_2e) is then calculated by dividing the total abatement cost by the total net GHG emissions reduction achieved.

Fig. 4 summarizes the results of total GHG emissions reduction and net GHG abatement cost using 2019 data. The existing data center capacity alone (i.e., when additional data center capacity is zero) can absorb 29%-62% of the total excess VRE in CAISO in 2019, assuming that the maximum server UR ranges between 65% and 90%. As I increase the maximum server UR and additional data center capacity, the excess VRE absorption level grows. At a given absorption level, a higher maximum server UR means a reduced need for additional data center capacity.

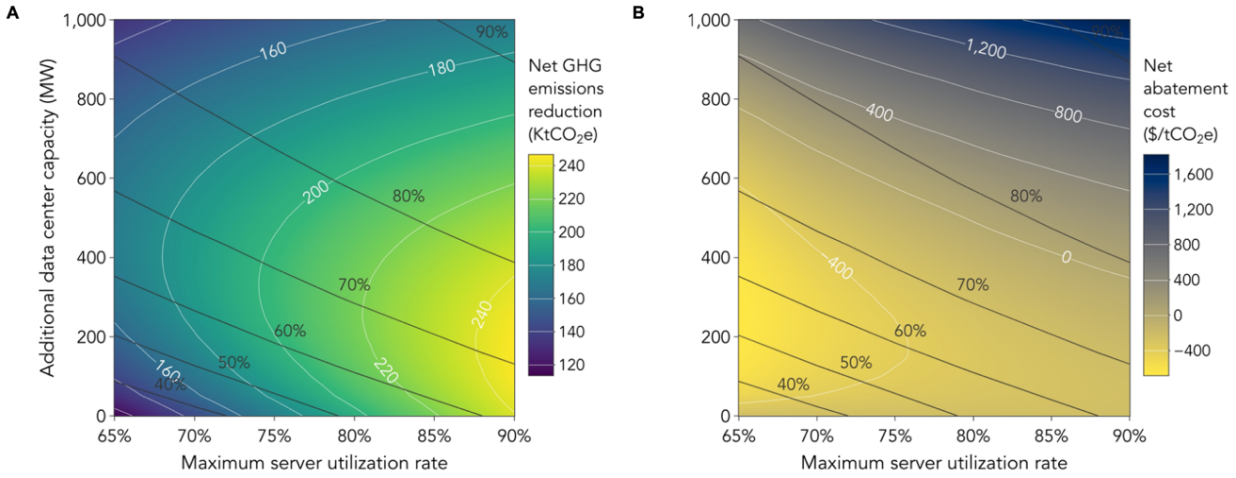

Figure 4. Estimated Net GHG Emissions Reduction and Net Abatement Cost as a Result of Assumed Maximum Server Utilization Rate and Additional Data Center Capacity (2019). (A) GHG emissions reduction in $KtCO_2e$. (B) Net abatement cost in $/ton$CO_2e$ reduction—negative net abatement cost indicates profitable GHG mitigation. The annotated black lines represent the percentages of total excess VRE absorbed.

The resulting GHG emissions reduction is the net reduction after accounting for the embodied GHG emissions of the additional data centers, which are incurred due to the manufacturing of IT equipment and infrastructure materials. The embodied emissions are proportional to the total number of new data centers built and would offset a fair amount of the operational GHG emissions reduction achieved by data center workloads migration. A total net GHG emissions of 113-239 $KtCO_2e$ could have been reduced in 2019 given the maximum server UR range assumed, and additional data center capacity can bring the total reduction further up to 247 $KtCO_2e$ (Fig. 4a). The net GHG emissions reduction peaks at an absorption level between 68%-75% when the maximum server UR exceeds 85%. Absorbing 80% of the total excess VRE or above does not bring more GHG emissions reduction benefits because the embodied emissions from more additional data centers would outweigh the reduction from operational phase.

Fig. 4b shows the estimated net abatement cost of the Migration Scenario. A negative abatement cost means that data centers can generate extra profits by mitigating GHG emissions through load migration. Without building any additional data center capacity, the existing capacity has a net abatement cost of -$242/$tCO_2e$ under any maximum server UR, driven by a decrease in electricity cost. The economic break-even point of additional data center capacity that should be built decreases from 780 MW to 350 MW as the maximum server UR increases from 65% to 90% (Fig 4b, the white line of zero). The lowest abatement costs (up to -$688/$tCO_2e$) can be reached by keeping the maximum server UR below 70% and the additional data center capacity between 150 MW-350 MW, corresponding to an absorption level of 45%-60%. It is possible to absorb up to 77%-79% excess VRE while still manage to keep the net abatement cost negative, but an absorption goal of more than 80%

does not make sense economically under any maximum server UR as the net abatement cost would always stay positive. The results of GHG emissions reduction and abatement costs for years 2016-2018 are shown in Figures S1-S3.

D. Discussion and conclusions

The inherent intermittent nature of VRE poses a major challenge to the stability and profitability of electric grids. Curtailment around the world is likely to grow as the share of VRE continues to rise, unless strong measures are taken to mitigate it[83]. Even with curtailment, over-generation still occurs, in which case, electricity is routinely sold at negative prices. In CAISO, for example, the share of 5-minute intervals with negative prices between 2014 and 2018 ranged 2%-4%.[130]

Our study shows that workloads migration between data centers can potentially absorb excess VRE, reducing both curtailment and GHG emissions at no or negative cost. The existing data center capacity served by CAISO has the potential to absorb up to 62% of the excess VRE and reduce GHG emissions of up to 239 $KtCO_2e$ with a net abatement cost of -\$242/tCO_2e in 2019, provided that server utilization rate is improved (Fig. 4). Additional data centers could further absorb the cumulative excess VRE up to 79% and reduce the GHG emissions up to 247 $KtCO_2e$ while still maintaining negative abatement cost.

Furthermore, the potential for workloads migration among data centers to mitigate curtailment and GHG emissions is likely to grow, as the needs for data processing services and data center infrastructure continue to expand. In order to capture such growing potential for workloads migration, a number of institutional and technological changes are due. In particular, development of the technology, policy, and protocols that enable real-time workloads migration among data centers during the time of excess renewable generation

would be needed. In addition, it is essential to develop the mechanism to incentivize data centers on load migration between grid regions and to facilitate the fluid communication among multiple grid operators and data centers. Technologies should be developed to support highly dynamic data center operation based on instantaneous generation, load and capacity data. Reliable short-term VRE generation forecasting capability for accurate projection of VRE over-generation is indispensable for dynamic load migration during the excess generation hours.[131]

Besides the spatial flexibility of data centers, the temporal flexibility of certain types of workloads also holds great potential for demand response, which is not evaluated in this analysis. Flexibly scheduling delay-tolerant workloads can increase renewable energy usage and accommodate more renewable resources in the grid.[19,43] Some Internet service providers, for example Google, have developed carbon-aware scheduling technology to shift compute tasks across time to maximize renewable energy utilization, noting that their next step is to move the tasks between data centers in different locations.[133] Incentivized deadline deferral can be an effective way to change customers' behaviors and encourage workloads shifting.[134] Energy storage devices in data centers can also play a role at smoothing VRE power by charging during over-generation time and discharging at a later time.[135,136]

There are some challenges facing workloads migration, but potential solutions are available. First, workloads migration incurs additional network delay and thus potential service violations.[96,97] The network latency time from U.S. east to west is currently around 60 milliseconds,[137] which is short but not trivial. Fortunately, delay-tolerant workloads including scientific computation, big data analytics, medical image processing etc. are a major component of data center workloads, accounting for more than 50% of total

workloads,[126] far more than the fraction of workloads I model the migration of. Interactive workloads which are inappropriate to shift because of the user-response latencies required, such as web search and videoconference, are assumed not to be migrated. Network latency has been decreasing thanks to the growing transmission speed and capacity of optic fibers; some companies already achieved speeds of hundreds of terabytes per second. The intermittent nature of excess renewable generation requires the workloads to be easily interruptible as needed, which makes it challenging for some workloads.[136] Nevertheless, this problem can be alleviated through installing more solid state drives and energy storage to checkpoint-restart the jobs.[94] The confidentiality of data center information remains another major concern. Data center owners are usually reluctant to share data about their facilities, including power consumption, to the public.[138] The confidentiality-related concerns can potentially be addressed through data reporting and aggregation protocols, advanced encryption technology and economic incentives.[10]

Our findings are applicable not only in the U.S. but also in other world regions with growing penetration of VRE. Data centers can and should play an important role in global VRE integration and GHG emission mitigation, especially in a future when the capacities of data processing and renewable energy are both rapidly growing.

E. Acknowledgements

J.Z. is, in part, supported by Bren School Graduate Student Fellowship. S.S. and J.Z. are, in part, supported by the National Science Foundation under Grant No.1360445. A.A.C is supported by National Science Foundation under Grant No.1832230. We thank Eric Masanet, Mahnoosh Alizadeh, and Ranjit Deshmukh, all at the University of California, Santa Barbara, for their valuable comments.

F. Appendix

Table S1. Life-cycle GHG emissions of electricity generation technology by energy resource

Energy resource	Life-cycle GHG emissions ($kgCO_2e/MWh$)	Reference
Solar	48	[114]
Wind	11	
Geothermal	38	
Biomass	230	
Hydro	24	
Nuclear	12	
Biogas	253	[139]
Natural Gas	537	[112]
Coal	1,046	[113]
Oil	733	[140]
Unspecified	428	[115]

Table S2. Characteristics of the 10 MW* typical data center used for analysis[117]

Metric	Value
Number of servers	40,000
Idling power per server	120 W
Maximum power per server	250 W
Range of hourly server utilization rate	5.4% - 94.0%
Annual average server utilization rate	40%
Peak total IT load	10 MW
Peak total load	20.7 MW
Estimated annual total energy consumption	114,234 MWh

*IT (or critical) power.

Table S3. Assumptions of annual average Dynamic Range (DR) and Power Usage Effectiveness (PUE) values of data centers served by CAISO[118–120,122]

Year	PUE	DR
2012	1.59	0.25
2013	1.55	0.23
2014	1.51	0.21
2015	1.47	0.19
2016	1.42	0.17
2017	1.38	0.15
2018	1.34	0.13
2019	1.30	0.11

*Only values assumed for the modeled years 2016-2019 are used in the analysis.

Table S4. Estimated amortized cost for Zero-Carbon Cloud (ZCC) data centers and traditional data centers[94]

Category	ZCC data centers powered by CAISO excess VRE generation (Migration Scenario)	Traditional data centers powered by PJM (Baseline Scenario)
Compute cost ($/W*)	5.18	5.18
Physical facility cost ($/W)	0.50	5.25
Network cost ($/W)	0.20	0.20
Electricity cost (cent/kWh)	0	9.09, 9.18, 9.48, 9.68** (2016-2019, respectively)
Total additional cost ($/W)	0.175	-
SSD cost	0.075	-
Battery cost	0.025	-
Hardware for free cooling	0.075	-

*The unit $/W is dollar per watt of IT power (2015 dollars).
**Historical average retail electricity rate of Virginia[141].

Supplemental Figures

In the following Figures S1-S3, I show the GHG emissions reduction and net abatement cost for the year 2016-2018, respectively.

The total curtailment in CAISO was 307 GWh, 379 GWh and 461 GWh in 2016, 2017 and 2018, respectively. Therefore, the absorption level of the excess VRE (which would otherwise be curtailed) achieved by the same combination of maximum server UR and additional data center capacity decreases over time, comparing across Figures S1-S3. Particularly, the existing data centers alone could reduce 38%-73% of the total cumulative curtailment in CAISO during 2016-2019 (53%-89% in 2016, 46%-81% in 2017, 41%-78% in 2018, and 29%-62% in 2019), with the maximum server UR ranging between 65% and 90% during underutilized hours.

During 2016-2018, the net GHG emissions reduction can be up to 120-150 $KtCO_2e$ per year if the maximum server UR falls in higher range, similar to the observation from 2019 results. The most reduction falls in the absorption level of between 75%-90%, and a further absorption beyond 85% would potentially have negative effects as the embodied emissions of additional data centers would offset the mitigation efforts, which is similar with 2019 results. The total cumulative net GHG emissions reduction during 2016-2019 ranges between 342-647 $KtCO_2e$ for the existing data center capacity, depending on the maximum server UR assumed.

The net abatement cost of the existing data centers alone is -\$202/tCO_2e, -\$210/tCO_2e and -\$226/tCO_2e for 2016, 2017 and 2018, respectively. The slight drop in net abatement cost results from higher availability of excess VRE electricity along the years. The maximum additional data center capacity that permits negative

abatement cost is 50-100 MW, 65-120 MW and 90-220 MW for year 2016, 2017 and 2018, respectively, depending on the maximum server UR. It is possible to absorb up to 85% of the excess VRE while still maintain a negative abatement cost for 2017 and 2018, if the maximum server UR can be improved to a range above 85%. Absorption goals beyond the limit would entail net positive abatement costs. For 2016, it is possible to absorb over 80% even 90% of the excess VRE with negative abatement cost when the maximum server UR can reach a level above 75%.

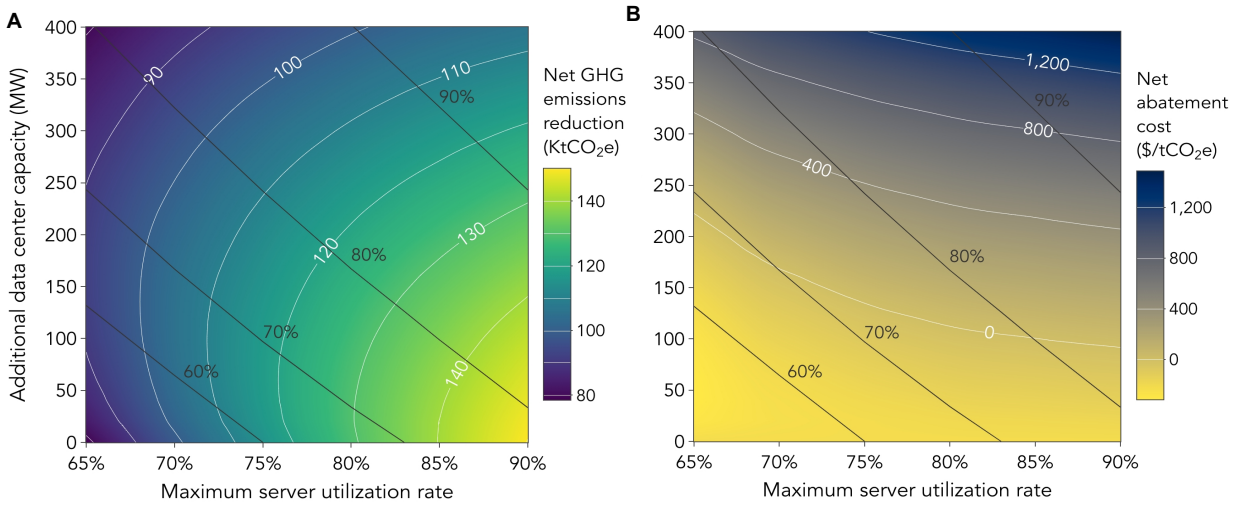

Figure S1. GHG emissions reduction and net abatement cost (2018). Related to Figure 4. (**A**) GHG emissions reduction (in $KtCO_2e$). (**B**) Net abatement cost (in \$/metric ton CO_2e reduction). The annotated black lines represent the percentages of yearly total excess VRE absorbed.

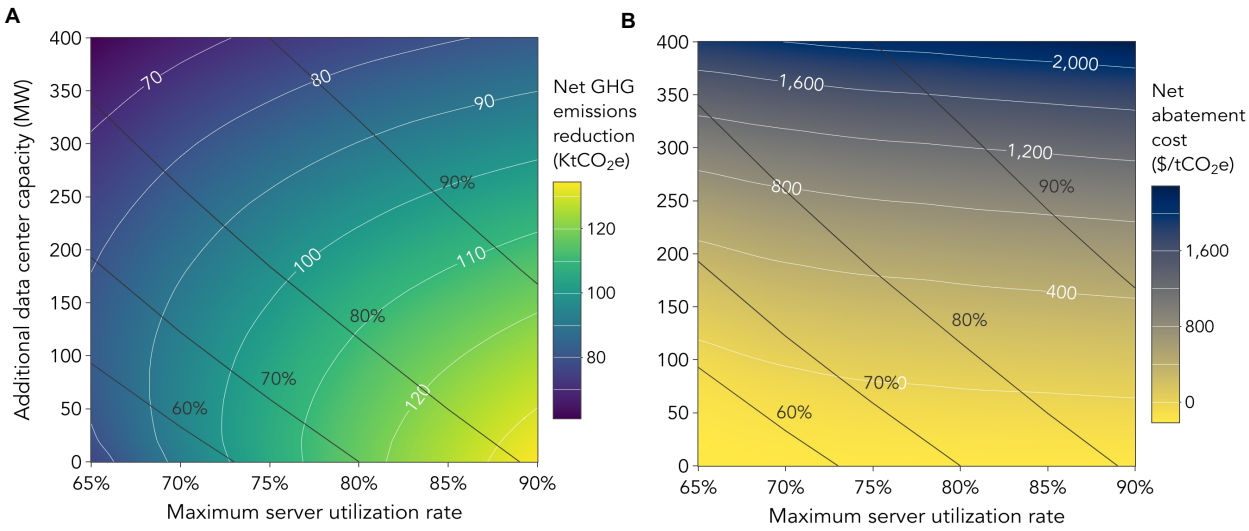

Figure S2. GHG emissions reduction and net abatement cost (2017). Related to Figure 4. (**A**) GHG emissions reduction (in $KtCO_2e$). (**B**) Net abatement cost (in $/metric ton CO_2e reduction). The annotated black lines represent the percentages of yearly total excess VRE absorbed.

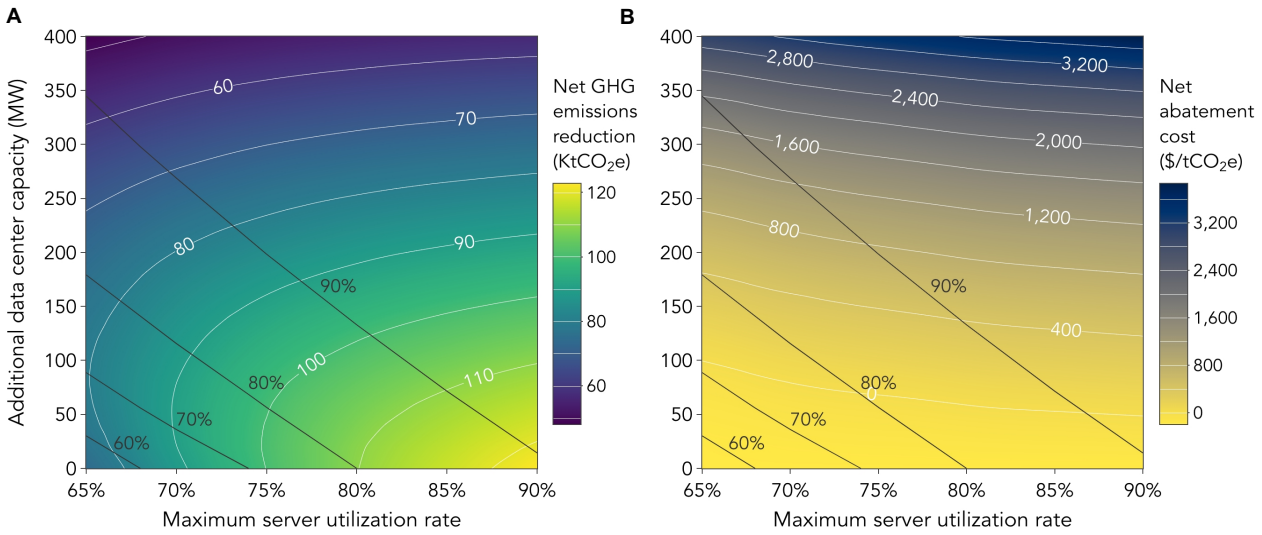

Figure S3. GHG emissions reduction and net abatement cost (2016). Related to Figure 4. (**A**) GHG emissions reduction (in $KtCO_2e$). (**B**) Net abatement cost (in \$/metric ton CO_2e reduction). The annotated black lines represent the percentages of yearly total excess VRE absorbed.

Supplemental Experimental Procedures

As I discussed in detail in Experimental Procedures, I compute the excess VRE in CAISO that can be absorbed by the remaining capacity of existing data centers and additional data center capacity, by varying the maximum server utilization rate in underutilized hours and allowable additional data enter capacity, and then calculate the resulting GHG emissions reduction and net abatement cost.

Below Supplemental Equations illustrate the computation steps of: (A) absorption of excess VRE, (B) GHG emissions reduction, (C) energy consumption by data centers and (D) net abatement cost, with nomenclature listed in Table S5.

Equations S1 – S21

(A) Absorption of excess VRE by existing and additional data center capacities powered by CAISO

$$Rmn\_Cpty_{exstDC_{h,y}} = \left(DCload_{max,y} - DCload_{h,y}\right) * N\_ExstDC \quad \text{(S1)}$$

$$Absp_{exstDC_{h,y}} = \begin{cases} Excess\_VRE_{h,y}, & if\ Excess\_VRE_{h,y} \le Rmn\_Cpty_{exstDCs_h} \\ Rmn\_Cpty_{exstDCs_{h,y}}, & otherwise. \end{cases} \quad \text{(S2)}$$

$$Need\_N_{addDC_{h,y}} = \begin{cases} 0, & if\ Excess\_VRE_{h,y} \le Rmn\_Cpty_{exstDC_h} \\ \frac{Excess\_VRE_{h,y} - Absp_{exstDC_{h,y}}}{DCload_{max,y}}, & otherwise. \end{cases} \quad \text{(S3)}$$

$$Absp_{addDC_{h,y}} = \begin{cases} 0, & if\ Need\_N_{addDC_{h,y}} = 0 \\ Need\_N_{addDC_{h,y}} \times DCload_{max,y}, & if\ 0 < Need\_N_{addDC_{h,y}} \le Thld\_N_{addDC_y} \\ Thld\_N_{addDC_y} \times DCload_{max,y}, & otherwise. \end{cases} \quad \text{(S4)}$$

$$Absp_{exstDC_y} = \sum_{h\in[1,8760]} Absp_{exstDCs_{h,y}} \quad \text{(S5)}$$

$$Absp_{addDC_y} = \sum_{h\in[1,8760]} Absp_{addDCs_{h,y}} \quad \text{(S6)}$$

$$Total\_Absp_y = Absp_{exstDC_y} + Absp_{addDC_y} \quad \text{(S7)}$$

(B) GHG emissions reduction

$$\Delta GHG_{h,y} = (Intst_{PJM_{h,y}} - Intst_{CAISOexcess_{h,y}}) \times (Absp_{exstDCs_{h,y}} + Absp_{addDCs_{h,y}}) \quad \text{(S8)}$$

$$\Delta GHG_y = \sum_{h\in[1,8760]} \Delta GHG_{h,y} \quad \text{(S9)}$$

(C) Energy consumption by data centers

$$PUE_y = \frac{Energy\_Total_y}{Energy\_IT_y} \quad \text{(S10)}$$

$$DR_y = \frac{Power\_Idle_y}{Power\_Max} \quad \text{(S11)}$$

$$Power\_Server_{h,y} = Power\_Idle_y + \left(Power\_Max - Power\_Idle_y\right) \times UR_{h,y} \quad \text{(S12)}$$

$$Energy\_IT_{h,y} = Power\_Server_{h,y} \times N\_Servers \quad \text{(S13)}$$

$$Energy\_nonIT_{h,y} = (m_0 \times UR_{h,y} + b_0) \times m_y \;\; s.t. \; \frac{Energy\_Total_y}{Energy\_IT_y} = PUE_y \quad \text{(S14)}$$

(D) GHG emissions abatement cost

$$\Delta Fac\_Cost_y = Fac\_Cost_{y,MS} - Fac\_Cost_{y,BS} \quad \text{(S15)}$$

$$Fac\_Cost_{y,MS} = Unit\_Fac\_Cost_{MS} \times Total\_Cpty_{addDC\,y} \quad \text{(S16)}$$

$$Fac\_Cost_{y,BS} = \frac{Unit\_Fac\_Cost_{BS} \times IT\_Power_i}{Energy\_Total_{i,y}} \times Absp_{addDC\,y} \quad \text{(S17)}$$

$$\Delta Elec\_Cost_y = 0 - Elec\_Rate_{y,BS} \times Total\_Absp_y \quad \text{(S18)}$$

$$\Delta Other\_Cost_y = Unit\_Add\_Cost_{MS} \times Total\_Cpty_{addDC\,y} - 0 \quad \text{(S19)}$$

$$Total\_Abate\_Cost_y = \Delta Fac\_Cost_y + \Delta Elec\_Cost_y + \Delta Other\_Cost_y \quad \text{(S20)}$$

$$Net\_Abate\_Cost_y = \frac{Total\_Abate\_Cost_y}{\Delta GHG_y} \quad \text{(S21)}$$

Table S5. Nomenclature for supplemental equations

Symbol	Unit	Description
$Rmn\_Cpty_{exstDC_{h,y}}$	MWh	Total remaining capacity of existing data centers powered by CAISO to absorb excess VRE during hour h in year y
$DCload_{max,y}$	MW	Hourly total peak load of a typical 10 MW data center in year y, determined by the assumed maximum server utilization rate which ranges between 65%-90%
$DCload_{h,y}$	MW	Actual existent total load of a typical 10 MW data center at hour h in year y
N_ExstDC	EA	Number of existing 10 MW-equivalent data centers powered by CAISO
$Absp_{exstDC_{h,y}}$	MWh	Absorption of excess VRE by existing data centers powered by CAISO during hour h in year y
$Excess\_VRE_{h,y}$	MWh	CAISO's total excess VRE (i.e., curtailment) at hour h in year y
$Need\_N_{addDC_{h,y}}$	EA	Total number of additional data centers (10 MW IT power) required to absorb all the rest of excess VRE in CAISO that exceeds existing data center capacity during hour h in year y
$Absp_{addDC_{h,y}}$	MWh	Absorption of excess VRE by additional data center capacity powered by CAISO during hour h in year y
$Thld\_N_{addDC_y}$	EA	Threshold number of additional data centers (10 MW critical power) that are allowed to be built in CAISO region in year y
$Absp_{exstDC_y}$	MWh	Annual total absorption of excess VRE by existing data center capacity powered by CAISO in year y
$Absp_{addDC_y}$	MWh	Annual total absorption of excess VRE by additional data center capacity powered by CAISO in year y
$Total\_Absp_y$	MWh	Annual total absorption of excess VRE by both existing and additional data center capacity powered by CAISO in year y
$\Delta GHG_{h,y}$	$kgCO_2e$	GHG emissions reduction at hour h achieved by processing migrated workloads with excess VRE in year y
$Intst_{PJM_{h,y}}$	$kgCO_2e$/MWh	GHG intensity of PJM generation at hour h in year y
$Intst_{CAISOexcess_{h,y}}$	$kgCO_2e$/MWh	GHG intensity of CAISO curtailment at hour h in year y
ΔGHG_y	$KtCO_2e$	Annual total GHG emissions reduction in year y
PUE_y	Unit-less	Annual average Power Usage Effectiveness value assumed for a data center in year y
$Energy\_Total_{i,y}$	MWh	Total energy consumption (IT + non-IT) of a data center in year y

$Energy\_IT_{i,y}$	MWh	Total energy consumption of IT equipment in a data center in year y
DR_y	Unit-less	Dynamic range assumed for servers in year y
$Power\_Server_{h,y}$	W	Power usage of a server at hour h in year y
$Power\_Idle_y$	W	Power usage of a server when they are idling in year y
$Power\_Max_y$	W	Rated power usage of a server in year y
$UR_{h,y}$	%	Utilization rate of the servers at hour h in year y
$N\_Servers$	EA	Number of servers in the data center
$Energy\_nonIT_{h,y}$	MWh	Total energy consumption of non-IT components in a data center at hour h in year y
m_0, b_0, m_y	Unit-less	m_0, b_0 – Slope and intercept of linear model of non-IT vs. server utilization rate, respectively. m_y – Co-efficient of the linear model such that the assumed PUE value is met
$\Delta\, Fac\_Cost_y$	million $	Annual facility cost change due to workloads migration in year y
$Fac\_Cost_{y,MS}$	million $	Amortized facility cost of additional (ZCC) data centers powered by CAISO in year y under Migration Scenario (MS)
$Fac\_Cost_{y,BS}$	million $	Amortized facility cost of traditional data centers powered by PJM in year y under Baseline Scenario (BS)
$Unit\_Fac\_Cost_{MS}$	$/W	Unit cost of amortized facility cost of ZCC data centers under MS
$Total\_Cpty_{addDC_y}$	MW	Total capacity of additional data centers in year y under MS
$Unit\_Fac\_Cost_{BS}$	$/W	Unit cost of amortized facility cost of traditional data centers under BS
IT_Power_i	MW	IT peak load of a typical data center i (i.e., 10 MW)
$\Delta\, Elec\_Cost_y$	million $	Annual electricity cost change due to workloads migration in year y
$Elec\_Rate_{y,BS}$	$/MWh	The average retail electricity rate in year y under BS
$\Delta\, Other\_Cost_y$	million $	Annual other costs change due to workloads migration in year y
$Unit\_Add\_Cost_{MS}$	$/W	Unit annual additional cost of ZCC data centers under MS
$Total\_Abate\_Cost_y$	million $	Total abatement cost in year y under MS
$Net\_Abate\_Cost_y$	$/ton$CO_2$e	Net abatement cost in year y under MS

IV. Life-cycle cost and carbon implications of residential solar-plus-storage in California

Abstract. Capacities of residential photovoltaics (PV) and battery storage are rapidly growing. However, their life-cycle cost and carbon implications under increasingly-decarbonized electric grids and declining costs are not well understood. Here, we integrate PV generation and load data for households in California to assess the current and future life-cycle cost and carbon emissions of installing solar-plus-storage systems. Our results show that installing PV reduces 110-570 $kgCO_2$ and \$180-\$730 per household in 2020. However, adding battery storage to a PV system increases life-cycle costs by 39%-67%, while impact on emissions is mixed (-20% to 24%) depending on tariff structure and marginal emission factors. In 2040, under current decarbonization and cost trajectories, additional life-cycle costs by adding storage decrease (31% to -3%) while additional emissions increase (2%-32%). Tariffs with wider spreads and aligned with marginal emissions, aggressive reduction in capital costs and embodied emissions are essential for residential solar-plus-storage to reduce costs and emissions.

A. Introduction

Variable renewable energy (VRE) such as solar and wind, is experiencing accelerated expansion with decreasing costs. However, the variability of VRE generation poses a major challenge to the low-carbon transition. Energy storage provides various benefits ranging from smoothing renewable generation, reducing curtailment, improving the reliability of

operating transmission and distribution grids, deferring or substituting costly investments in infrastructure, and peak shaving, among others[142,143,144,4].

For households, residential battery storage, typically coupled with rooftop solar photovoltaic (PV), can increase PV self-consumption, save electricity bills, and provide backup power during outages[145]. The capacity of behind-the-meter batteries with rooftop PV is estimated to dramatically increase and match that of utility-scale batteries by 2030 globally[19]. In the U.S., one-quarter of new residential PV systems are expected to be paired with storage by 2025. Among U.S. states, California represents the largest market with 38% of nation-wide residential PV installations during 2016-2020, and is driving the growth of solar-plus-storage systems[146].

Understanding the implications of residential battery storage on greenhouse gas (GHG) emissions is imperative, but existing literature is largely limited to retrospective analyses. Some studies conclude that residential battery storage increases total emissions when performing energy arbitrage (charge when electricity price is low and discharge when it is high), mainly due to energy losses during battery cycling[13,14,147,148]. These analyses often use a set of short-run Marginal Emission Factors (MEFs) derived through regression models based on empirical fossil generation data, which do not take nuclear and renewable generators into account[149,150]. This method is not applicable to regions with large portions of VRE such as California and Mid-West region, where VRE can be often on the margin[147,151]. Extending short-run MEFs to include non-emitting generators in the regression model for a high-wind-penetration area is shown to have about 30% discrepancy compared to the MEFs

based on fossil fuels only[151], and such extended method is frequently employed in later studies[152,153].

While suitable for retrospective analyses, short-run MEFs are unable to inform the impacts of battery storage on GHG emissions as the penetration of VRE in the electric grid increases in the future. Energy storage systems can induce structural changes in grid infrastructure by changing demand profiles[154]. Short-run MEFs evaluate the operational response to a marginal load change, assuming that the underlying grid composition is fixed[155,156]. In comparison, long-run MEFs also account for the structural changes of the electricity system, such as capacity investments of VRE and retirement of fossil-fuel power plants[155,157–159]. We use long-run MEFs in this analysis, which are more appropriate for prospective analysis, as both penetrations of renewable energy and storage increase in the future[155,157,160].

In addition, there is a disconnection between use-phase studies and life-cycle assessment (LCA) studies in existing literature that evaluate the GHG emissions of battery storage. On the one hand, use-phase studies often employ optimization models to quantify operational emissions with little consideration of the embodied impacts from battery production[161,162]. On the other hand, LCA studies generally limit the scope to the production phase or make oversimplified assumptions on battery cycling during the use phase[163,164]. Stationary applications of battery storage, especially in the residential sector, are notably under-evaluated compared with mobile applications such as electric vehicles[165].

Here, we evaluate the life-cycle GHG emissions and costs of installing and operating solar-only and solar-plus-storage systems in 52 representative households across California.

We optimize the operation of residential solar-plus-storage systems with two power modes in three utility areas for the current time (2020) and a highly decarbonized future (2040). By comparing their life-cycle costs and GHG emissions, we explore if adding storage can further reduce cost and emissions and under what conditions would solar-plus-storage outperform solar-only systems. We conclude that marginal emissions-aligned tariff designs, rapid decreases in the capital cost and embodied emissions of batteries are key to reduce the life-cycle GHG emissions of residential solar-plus-storage.

B. Methods

1. Residential load profiles

The residential load profiles in the U.S. are selected from an OpenEI dataset[166]. The dataset has a total of 961 load profiles of households in different cities across the United States. Base Load scenario is selected for our analysis, in which the hourly load profiles for a typical one-story house with three bedrooms are simulated using Typical Meteorological Year 3 (TMY 3) weather data. We use the electricity load profiles of 52 households which fall in the electricity service territory of the three major utility companies, PG&E, SCE, and SDG&E in California. We keep the households' load profiles constant for 2020 and 2040 with a purpose to examine the impacts of electric grid transformation on the life-cycle GHG emissions of solar-only or solar-plus-storage systems, and future changes in climates are not considered.

2. System design

We use the PVWatts simulation tool in System Advisor Model (SAM) model to generate hourly solar PV outputs[167]. We assume that the capacity of the solar PV system is 4 kWdc, which is a reasonable size for a three-bedroom house. The PV panels are assumed to have a tilt angle of 20°, an azimuth of 180° and total system losses of 14.08%, which are common settings according to historical data[168,169]. To generate solar PV outputs for households at different locations, the respective weather files are required in SAM model. We downloaded the TMY 3 weather files[170] from National Solar Radiation Database (NSRDB)[171]. We modified the LK code script provided by SAM model, ran a sequential batch of simulations iterating the weather files of California TMY 3 locations, generated and exported the hourly solar PV outputs for each household. A degradation rate of 0.5% per year and a lifetime of 25 years is assumed for the solar PV system[172].

We use the specifications of Tesla Powerwall II to simulate the battery storage system. We assume that one battery is used in the solar-plus-storage systems, with an usable energy capacity of 13.5 kWh and a power rating of 5 kW[173]. The warranty states that the battery system has no less than 70% energy retention at ten years following the installation date, with an operating limitation of 37.8 MWh of aggregate throughput[174]. Based on this, a degradation rate of 3.89% per year is assumed for the battery system for 10 years of lifetime and a limit of aggregate yearly discharge is set as one constraint.

Two power control configurations are modeled for residential solar-plus-storage systems, ExportOnly (also known as No Grid Charging) mode and ImportOnly (or No

Storage Export) mode that are NEM-eligible, based on a recent rule made by California Public Utilities Commission[175].

3. Emission factors

For emission factors of the grid in 2020 and 2040, we use the Average Emission Rates (AER) and Long-Run Marginal Emission Rates (LRMER) from a mid-case scenario in the Cambium tool developed by National Renewable Energy Laboratory (NREL)[159]. AER is the average CO_2 emission intensity of the grid weighted by the generation amount of each technology during an hour, calculated by dividing the total system emissions by the total system supply. LRMER is the CO_2 emission rate of the mixture of generation that would serve a persistent change in end-use demand, taking into account any structural changes to the grid in response to the change in demand[159]. The emission factors for three balancing areas are used, defined as p9, p10 and p11 in Cambium, which covers PG&E, SCE and SDG&E, respectively. There is a slight misalignment in the borderline of the former two areas, i.e., Santa Barbara weather station lies in p9 but is exposed to the ToU rates of SDG&E while Bakersfield station is located in p10 but exposed to the ToU rates of PG&E. Based on the Cambium model, the portion of electricity generated from variable renewable energy (VRE, i.e., solar and wind) in the total generation for p9, p10 and p11 area is 17%, 36% and 28% in 2020, respectively. The VRE portion is projected to increase to 23%, 64% and 64% in 2040, respectively. Representative hourly AER and LRMER values by season in 2020 and 2040 are shown in Supplementary Fig. 2.

We use AER to calculate the GHG emissions for the baseline scenario, when households have no solar PV or battery system, assuming that they consist part of the existing end-use

demand. When households install new solar PV or solar-plus-storage systems, we apply LRMER to the change in net load and feed-in. As a significant number of households install solar-only or solar-plus-storage systems, the new loads or change in load curves would induce structural change in the electricity supply infrastructure within a balancing area. Specifically, the addition of battery storage can help reduce peak demand of the grid and hence the need for fossil fuel peaker plants, enable the storage of more renewable energy and induce higher electricity consumption due to internal energy loss, which combined can alter both the structure and operation of the grid[155].

4. Capital cost and utility cost

Capital cost is a major component of the life-cycle cost for a household adopting NEM-eligible systems. We assume that the installation cost of residential solar PV systems in California is $3.75/W in 2020, given that the median installed price of such systems before incentives in California was $3.81/W in 2019, and we assume a same price drop (-1.7%) for 2019-2020 with that in 2018-2019 [168]. The unit cost is assumed to decrease to $1.41/W in 2040, excluding subsidy or tax rebates, based on the projected cost decrease in NREL Annual Technology Baseline (ATB) on residential solar PV[176]. For residential battery storage, we use the empirical cost data in 2020 ($670/kWh usable capacity[177]) and the trend projected in ref [178] to estimate the cost in 2040 ($185/kWh). All costs in this analysis are in 2019 U.S. dollars. For a detailed list of assumptions on key technical, cost and unit emissions parameters, see Supplementary Table 1.

Using a life-cycle perspective, we calculate the annualized capital cost of solar PV and battery system based on their lifetimes, shown in equation (1). Salvage value of the system is not considered.

$$Annual\_cap\_cost_i = Cap\_cost_i \times \frac{r}{1-(1+r)^{-Y_i}} \quad (1)$$

In the equation, i indicates the device, i.e., solar panels or battery storage. Cap_cost_i is the total installed cost of the device, r is the assumed discount rate (6.1%)[179] and Y_i is the lifetime of solar PV (25 years) or battery storage system (10 years). Annualized cost would be more if a higher discount rate is used.

The NEM Program 2.0 in California allows households with PV panels to export surplus self-generated electricity to the grid and apply credits equivalent to retail prices to reduce their bills on a monthly-basis[180]. We collected the default ToU tariffs in 2020 for NEM participants from three utility companies. For households served by PG&E, we use E-TOU-D plan[181]. For SCE and SDG&E, we use TOU-D-4-9PM[182] and DR-SES[183], respectively. In a typical ToU rate structure, a high rate is charged during the peak time (4 to 9 p.m. or 5 to 8 p.m.), and lower rates are applied to other hours of the day, which are off-peak or super off-peak times. Detailed tariffs with rates by hour of the day and season are shown in Supplementary Fig. 1. We did not model the households served by other smaller utility entities. Non-bypassable charges and on-time interconnection fees are not included in our cost analysis.

5. Embodied GHG emissions

There are extensive LCA studies of battery or battery systems, with a heavier focus on mobile applications (i.e. electric vehicles) than on stationary applications (grid-scale and residential batteries)[184,165]. Most of the LCA studies have a system boundary of cradle-to-gate, leaving out the use and end-of-life phase due to complexity and lack of data[185]. For example, a recent LCA study on commercialized residential battery systems reported that the cradle-to-gate GHG emissions are around 200 kg CO_2e per kWh of usable storage capacity[165]. In our analysis, we use this data to estimate the total embodied GHG emissions of a battery storage system based on its usable storage capacity.

We calculate the annualized embodied emissions of battery storage based on its lifetime, assuming an equal allocation to each year throughout a 10-year lifetime (equation 2).

$$Annual\_emb\_GHG_i = \frac{Emb\_GHG_i}{Y_i} \quad (2)$$

Emb_GHG_i represents the total embodied emissions of device i (solar PV or battery storage) and Y_i is the lifetime of the device (25 years for solar PV and 10 years for battery storage). For solar PV, the unit life-cycle GHG emissions is 48 gCO_2e per kWh of electricity output[114], and the total life-cycle GHG emissions of a 4-kW solar PV system are calculated by multiplying this unit embodied emissions with the average lifetime total output of the sampled households (in kWh).

We also estimated the embodied emissions of solar PV and battery storage for 2040. The International Energy Agency projects that the global average carbon intensity of power generation would decrease from 440 gCO_2/kWh in 2020 to 282 gCO_2/kWh in 2040[186] in a Stated Policies Scenario (STEPS). In the STEPS scenario, future carbon intensities of the

U.S. grid are aligned with those modelled in Cambium mid-case scenario. Electricity consumption contributes to 53% and 64% to the life-cycle GHG emissions of a battery pack[187] and a solar PV module[188], respectively. Assuming that the GHG emissions from non-electricity contributors stay unchanged, we estimate that the embodied emissions of battery storage would decrease from 200 to 162 $kgCO_2e$ per kWh usable capacity and the embodied emissions of solar PV would decrease from 48 to 37 gCO_2/kWh output from 2020 to 2040.

In Cambium, the emissions rates only account for emissions of electricity generation during the operational phase. So, we calculated the indirect GHG emissions of the grid, i.e., the infrastructure and supply chain emissions for all generation technologies and added them to the model. The indirect emissions factors of the grid by balancing area for 2020 and 2040 are listed in Supplementary Table 1.

6. Optimization model

The optimization model dispatches battery storage under two separate objectives: minimizing annual utility cost (*minCost*) and minimizing annual operational emissions (*minGHG*) of the solar-plus-storage system. In addition, we optimize utility cost considering a carbon price that is equivalent to the social cost of carbon ($51/tonne$CO_2$ for 2020 and $73/tonne$CO_2$ for 2040)[189]. Under the *minCost* objective, since a certain electricity rate spans across a number of hours, the optimization model may have multiple solutions for a minimal total cost, but the resulting GHG emissions would vary slightly. This difference is small (0.3% for ImportOnly scenario and 1.7% for ExportOnly scenario on average in 2020), and we show the upper bounds of the life-cycle emissions in the main text. For solar-

only systems, no optimization is required. We built the optimization model using Pyomo in Python and solved it as a Mixed Integer Problem using Gurobi Optimizer 9.0.3.

We calculate the life-cycle cost and GHG emissions of the systems based on the optimal battery dispatching solution under a *minCost* objective (equation 3). In an alternative scenario where there is a carbon price, we assume that the carbon cost is charged based on the household's net grid consumption and the hourly average emission factor of the grid:

$$minCost = \sum_{h=1}^{8760} ToU_h \times (E_{net\_load,h} - E_{feed-in,h}) + C\_price \times (AEF_h \times E_{net\_load,h}) \quad (3)$$

ToU_h is the Time-of-Use rate in hour h ($/kWh), $E_{net\_load,\,h}$ is the net load of the household in hour h (kWh) and $E_{feed-in,\,h}$ is the surplus electricity fed back to the grid in hour h (kWh), AEF_h is the average emission factor of the grid in hour h (kgCO_2e/kWh) and C_price is the carbon price (0 or social cost of carbon).

We also minimize the annual operational GHG emissions for the solar-plus-storage system, applying MEFs to the change in net load. The objective function is shown in equation 4, where $E_{load,\,h}$ is the original load of the household in the baseline scenario in hour h (kWh) and MEF_h is the long-run marginal emission rates of the grid in hour h (kgCO_2e/kWh):

$$minGHG = \sum_{h=1}^{8760} AEF_h \times E_{load,h} + MEF_h \times (E_{net\_load,h} - E_{load,h} - E_{feed-in,h}) \quad (4)$$

There are a series of constraints in our optimization model. In ExportOnly mode, batteries can charge from solar PV only and export to the grid. In ImportOnly mode, batteries can charge from both solar PV and the grid but can only discharge to serve on-site load. In both modes, the battery system is set to be 50% charged in the first hour of the year. We assume a 90% round-trip efficiency and impose equal amounts of energy loss during

battery charging and discharging. There are other technical constraints for the battery system, for example, the household cannot send surplus PV generation to the grid and pull power from the grid at the same time. There is a yearly discharge limit which allows the battery system to meet the requirement specified in warranty. In addition, the household's load must be met in any hour and the balance of solar PV output must be maintained. For a full list of constraints with notations, see Supplementary Table 2-4.

7. Life-cycle cost and GHG emissions

In the baseline scenario when households have no solar PV or battery storage installed, annual cost only consists of utility cost, and carbon cost if assumed. When households install only solar PV systems, the annual life-cycle cost includes net utility cost, carbon cost (if any) and the annualized capital cost of solar PV. When households install solar-plus-storage systems, the annual life-cycle cost include the aforementioned components plus the annualized capital cost of battery system:

$$Lifecycle\_Cost_{baseline} = \sum_h ToU_h \times E_{load,h,y} + C\_price \times (lcAEF_h \times E_{load,h}) \quad (5)$$

$$Lifecycle\_Cost_{solar-only} = \sum_h ToU_h \times (E_{net\_load,h,y} - E_{feed-in,h,y}) + C\_price \times [(lcAEF_h \times E_{net\_load,h}) + Annual\_emb\_GHG_{PV}] + Annual\_cap\_cost_{PV} \quad (6)$$

$$Lifecycle\_Cost_{solar+storage} = \sum_h ToU_h \times (E_{net\_load,h,y} - E_{feed-in,h,y}) + C\_price \times [(lcAEF_h \times E_{net\_load,h}) + Annual\_emb\_GHG_{PV} + Annual\_emb\_GHG_{storage}] + Annual\_cap\_cost_{PV} + Annual\_cap\_cost_{storage} \quad (7)$$

The life-cycle GHG emissions of households in the baseline scenario are the direct and indirect GHG emissions from grid electricity consumption. $lcAEF_h$ represents the life-cycle

average emission factors in hour h including the embodied emissions of grid infrastructure. The life-cycle GHG emissions in Solar-Only scenario include the GHG emissions from grid electricity use, GHG emissions avoidance due to feed-in and the embodied emissions of solar PV. In solar-pus-storage scenario, besides these components, embodied emissions of battery storage are added.

$$Lifecycle\_GHG_{baseline} = \sum_{h,y} lcAEF_h \times E_{load,h} \quad (8)$$

$$Lifecycle\_GHG_{solar-only} = \sum_{h,y} lcAEF_h \times E_{load,h} + MEF_h \times (E_{net\_load,h} - E_{load,h} - E_{feed-in,h}) + Annual\_emb\_GHG_{PV} \quad (9)$$

$$Lifecycle\_GHG_{solar+storage} = \sum_{h,y} lcAEF_h \times E_{load,h} + MEF_h \times (E_{net\_load,h} - E_{load,h} - E_{feed-in,h}) + Annual\_emb\_GHG_{PV} + Annual\_emb\_GHG_{storage} \quad (10)$$

The annual life-cycle cost and GHG results in three scenarios are therefore calculated and compared, shown in the main text.

8. Limitations

There are limitations with the methodology and data used in this study. First, we use the current ToU rates and NEM policy in California, which is subject to change in the future. The conclusions we draw here may not be applicable to regions with substantially different tariff designs or feed-in policies. Second, there are some limitations on the emission factors used, such as omission of transmission losses and distortion of data in the event of outages in the Cambium tool, as described in the reference[159]. Third, although we used the most recent and best available data, there are uncertainties around the future costs and embodied emissions of solar PV and battery systems, depending on technology development and

policy implementation, etc. Fourth, in our model, we assumed perfect information of the emissions factors of the grid for optimization. However, this information would not be known to the households until advanced technology which can quickly predict marginal generator(s) is in place. Furthermore, our model is limited to optimize individual households with two commonly-used power modes currently and cannot simulate complex grid-level power management with households running systems with various sizes and operation modes. Lastly, the weather data used by Cambium is 2012, while the load data we used is based on TMY 3 dataset, which is a condensation of a number of historical years to represent the weather of a typical year.

C. Results

1. Operation modes

We estimate the life-cycle GHG emissions and cost of households under three power control modes - Solar-Only, ExportOnly, and ImportOnly. These are the most common residential self-generation configurations that are compliant with the current California Net Energy Metering (NEM) policy. Solar-Only refers to the case when households install only rooftop solar PV systems (Fig. 1a). In ExportOnly mode, households install solar-plus-storage systems, in which the battery storage only charges from solar PV and the battery can discharge and export to the grid in addition to meeting the on-site load (Fig. 1b). In ImportOnly mode, households install solar-plus-storage systems where the battery can charge from solar PV or the grid, but the battery can only discharge to meet the on-site load (Fig. 1c). For both ExportOnly and ImportOnly modes, we assume that the households

dispatch batteries in order to minimize their annual electric utility cost (*minCost*). We model the hourly PV generation, grid electricity consumption, and battery dispatch for each sampled household through optimization.

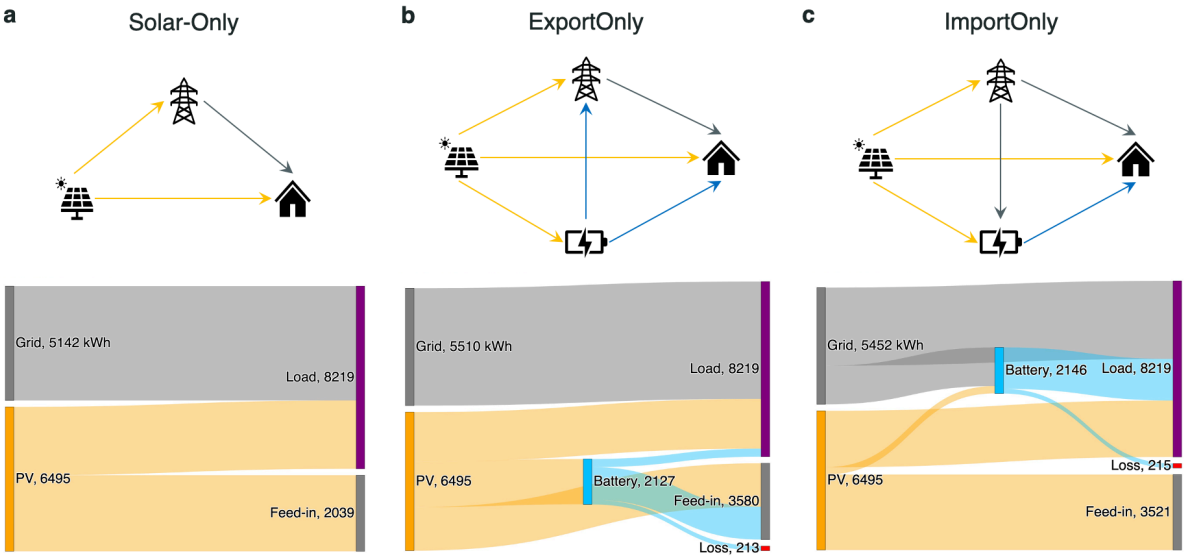

Figure 1. Illustration of different power control modes of solar-only or solar-plus-storage systems and resulting annual electricity flow for an example household. (**a**) Solar-Only mode, (**b**) ExportOnly mode and (**c**) ImportOnly mode. Shown in ExportOnly and ImportOnly modes are optimized electricity flows under an objective of minimizing annual utility cost.

We use representative Time-of-Use (ToU) tariffs in 2020 from three major utility companies in California - Pacific Gas and Electric Company (PG&E), Southern California Edison (SCE), and San Diego Gas and Electric Company (SDG&E) - with hourly rates shown in Supplementary Fig. 1. We collect the hourly electric load for typical three-bedroom houses across California, with the annual load varying by local climate (7,500-13,000 kWh)[166]. We simulate a 4-kilowatt (kW) solar PV system, coupled with lithium-ion battery storage with usable capacity of 13.5 kilowatt hours (kWh) and round-trip efficiency

of 90%[173]. This system size is typical for a three-bedroom house and would ensure that the PV generation does not exceed the on-site load, as required by the NEM policy[180].

Depending on the location of the houses, the solar PV generation ranges between 5,000-7,300 kWh/year.

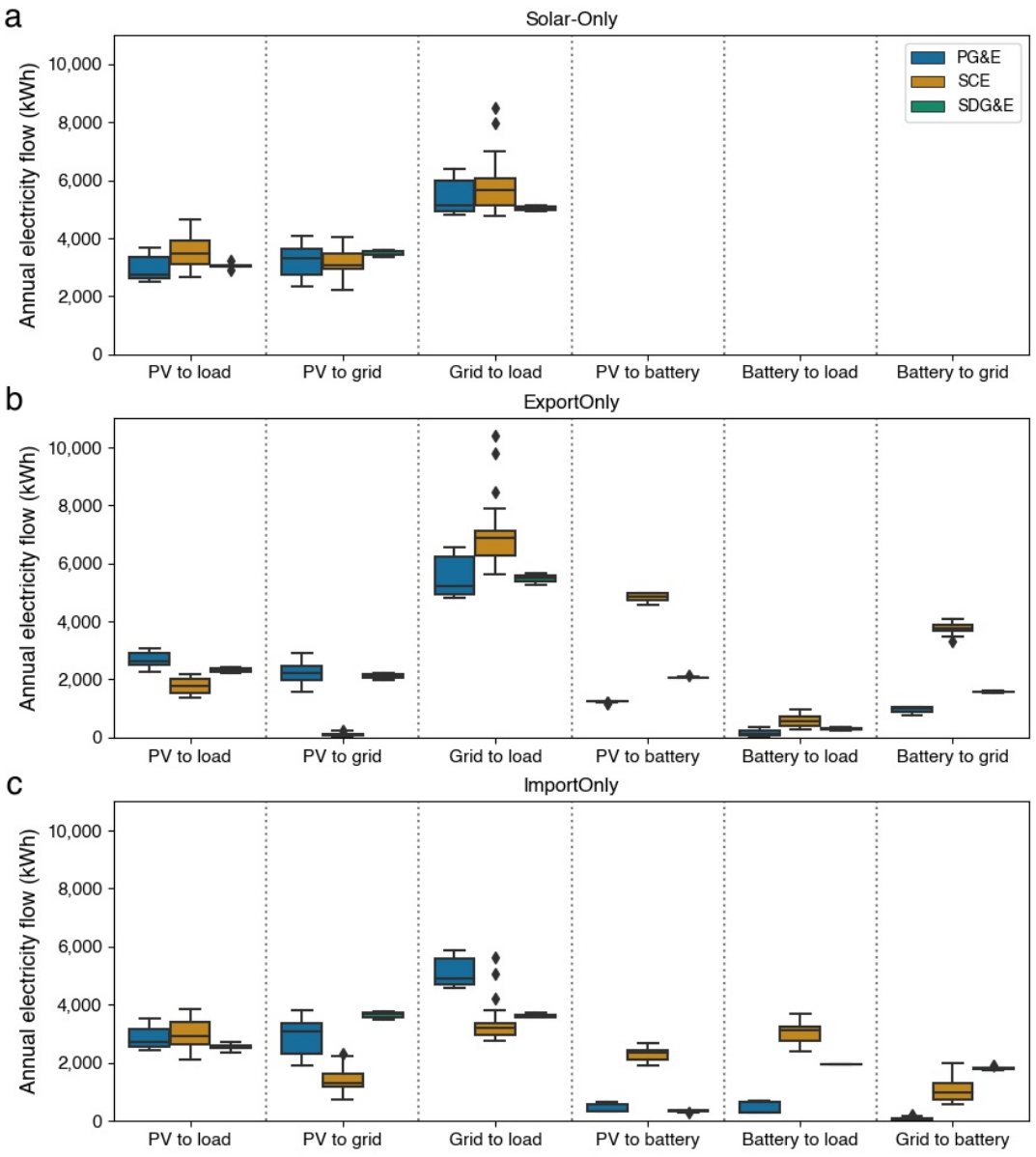

Figure 2. Annual electricity flows of all sampled households in California by utility area in different scenarios. (a) Solar-Only mode, (b) ExportOnly mode and (c) ImportOnly mode. Results for ExportOnly and ImportOnly modes are optimized under an objective of minimizing annual utility cost.

In Solar-Only mode, 33%-40% of the household's on-site load is met by solar PV, with the remaining demand met by the grid. Surplus PV generation is fed back to the grid (33%-60% of annual PV generation, depending on the location and load size) and the household receives financial credits for feed-in. The annual PV-to-load ratio of the sampled households ranges between 53%-90% with a mean value of 75%.

In ExportOnly mode, the electricity flows of households served by SCE show a contrasting pattern with the others (Fig. 2b). Particularly, 72% of PV generation is used to charge batteries in SCE on average, with the rest serving on-site load directly (26%) or feeding back to the grid (2%). In comparison, only 20% of PV generation is stored in households served by PG&E, with a higher percentage used on site (44%) or fed back to the grid (36%). For SDG&E, the average percentage of PV generation used for battery charging, on-site consumption and feed-in is 32%, 36% and 32%, respectively. Across all three areas, the majority of the electricity stored in batteries (61%-86%) is discharged to the grid in exchange for credit, mostly during peak hours when retail rates are high.

In ImportOnly mode, 33%-56% PV generation is used for on-site consumption, greater than in ExportOnly mode. The portion of PV generation stored in batteries is very low for PG&E and SDG&E (7% and 5% on average, respectively) but is much greater for SCE (34%). For households served by SDG&E, batteries charge mostly from the grid at nighttime rather than from solar PV. However, in SCE area, households charge more during the day from both on-site PV and the grid. Across all areas, batteries discharge in late afternoon and early night to displace expensive grid electricity. For detailed battery dispatching and state-of-charge curve, see Supplementary Fig. 4-9.

The differences in battery dispatching patterns can be attributed to the ToU tariff structures. The selected ToU plan of PG&E (E-TOU-D) has a very small price difference between on-peak and off-peak hours in winter and sets a flat rate for weekends (Supplementary Fig. 1). Thus, it provides little opportunity for arbitrage for households to dispatch batteries (except for summer weekdays), given that the energy loss during cycling leads to higher electricity consumption. The ToU rates of SDG&E (DR-SES) have very little variation across the day during wintertime but have a much larger gap between on-peak and off-peak hours during summertime. Further, off-peak rates are lower during nighttime (0-6 a.m.) than daytime (6 a.m.- 4 p.m.), which results in frequent charging from the grid at night and more PV feed-in during the day in the ImportOnly mode. Conversely, the ToU plan of SCE (TOU-D-4-9PM) maintains a significant and consistent gap between on-peak and off-peak times across all seasons. It also sets the lowest rate during off-peak hours (8 a.m.-4 p.m.) in winter, which encourages more PV generation to be stored and later discharged during peak hours. Consequently, the battery storage at our modelled households served by SCE cycle more frequently than those by other utilities.

2. Annual life-cycle cost and GHG emissions

We calculate the resulting life-cycle cost and GHG emissions after optimizing the solar-plus-storage systems for one year under the *minCost* (minimizing utility cost) objective for each household. Annual life-cycle cost consists of annualized capital cost of the device(s), utility cost based on ToU rates, credits from feed-in, and extra cost from imposing a carbon price in addition to ToU charges (when assumed). Under the current Net-Energy Metering (NEM) program in California, residential customers who produce surplus renewable

electricity and feed back into grid receive a financial credit on electricity bills at the same retail rate that they would have paid without the renewable generator[180]. Annual life-cycle GHG emissions include the annualized embodied emissions of the system, life-cycle emissions from grid electricity usage, and avoided emissions from feed-in.

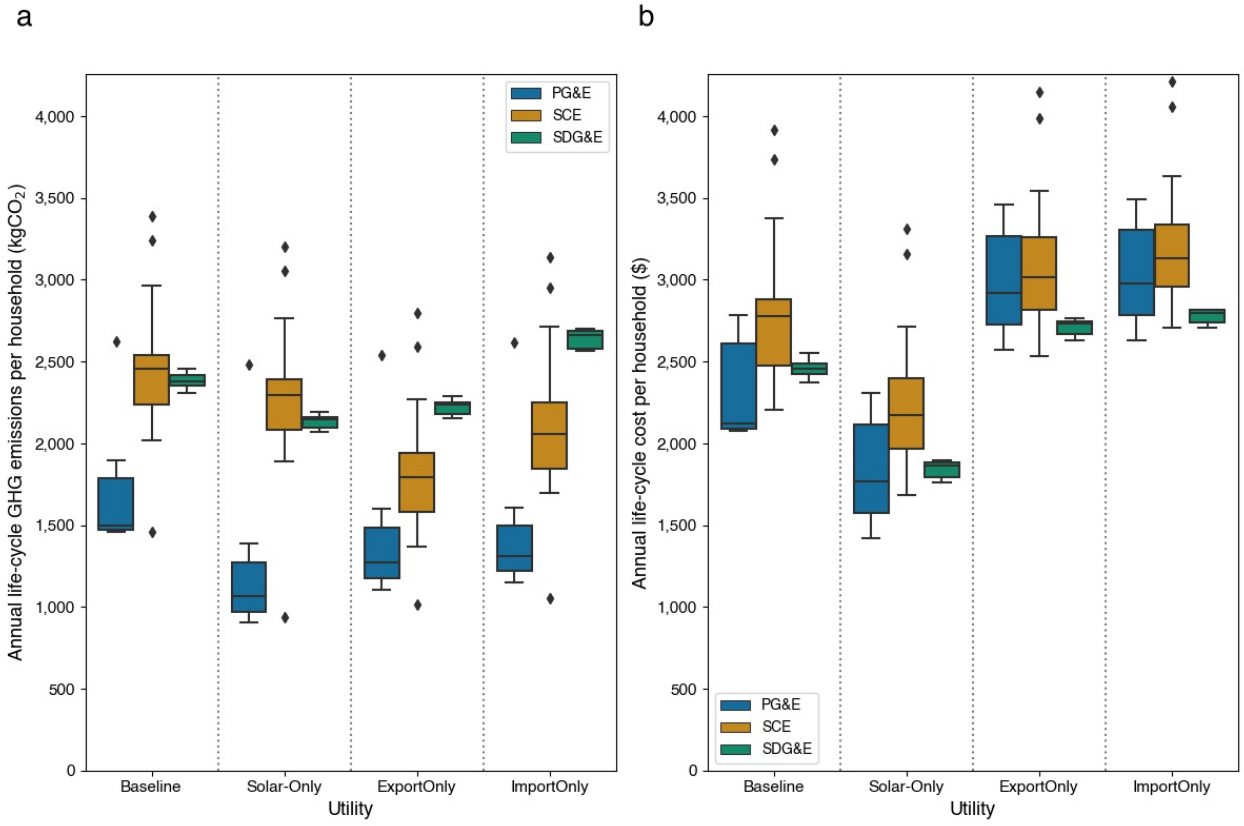

Figure 3. Life-cycle GHG emissions and cost of sampled households in 2020 by utility area in different scenarios. (a) Annual life-cycle GHG emissions and (b) annual life-cycle cost. Baseline – households have no PV or storage. Solar-Only – households install only solar PV systems. ExportOnly – households install solar-plus-storage systems with ExportOnly mode. ImportOnly – households install solar-plus-storage systems with ImportOnly mode. Results for ExportOnly and ImportOnly modes are optimized under an objective of minimizing annual utility cost for the household.

Fig. 3 shows the annual life-cycle GHG emissions and cost of all sampled households in different scenarios. Baseline scenario assumes households have no PV or storage installed. Compared to the baseline scenario, installing Solar-Only systems lead to 110-570 $kgCO_2$ (or 5%-39%) reduction. Across all scenarios, life-cycle GHG emissions of households in PG&E area are lower than those in the other two areas (Fig. 3a), due to fewer cooling degree days (less need for air-conditioning) and a lower-carbon grid. There is a larger variation in emissions among households served by SCE due to a greater variation in climate and load size within the utility area.

For households served by PG&E, installing solar-plus-storage systems results in 2%-27% higher life-cycle GHG emissions in 2020 than the Solar-Only scenario, due to a lack of tariff incentives for battery dispatch and a lower-carbon grid mix. For SCE, installing solar-plus-storage systems can reduce more GHG emissions from the baseline than installing only solar PV. This is because households served by SCE fully utilize batteries by charging from on-site PV and discharge during peak time to replace generation from mostly natural gas peaker plants. Reduction of emissions in ExportOnly mode is greater since more stored electricity can feed back to the grid. For SDG&E, ImportOnly mode leads to a 9%-12% increase in life-cycle GHG emissions from the baseline, owing to nighttime charging from the grid when marginal costs are low while marginal emissions are high from the mostly fossil fuel-based generation.

Although solar-plus-storage systems may reduce life-cycle GHG emissions, they result in 4%-49% more life-cycle cost compared to the baseline in 2020 without subsidy (Fig. 3b), because the annualized capital cost of battery storage exceeds the savings on utility bills

from optimizing the battery operation. Solar-Only mode, however, outperforms both modes of the solar-plus-storage systems by decreasing the life-cycle costs from the baseline scenario by 8%-32% (or $180-$730) across all utility areas in 2020. Breakdown of the life-cycle GHG emissions and cost for representative households with similar annual loads served by each utility is shown in Supplementary Fig. 10-12.

3. Comparing solar-plus-storage with solar-only systems

The cost of battery storage is expected to decrease, making solar-plus-battery systems increasingly competitive compared to solar-only systems. In addition, the grid will be increasingly decarbonized. These dynamics will significantly affect the extent to which residential solar-plus-storage systems reduce life-cycle GHG emissions and costs, especially when compared with solar-only systems. We present results from both 2020 and 2040 scenarios to highlight their differences (Fig. 4). For 2040, we use estimated long-run MEFs of the grid[190] and estimated embodied emissions and capital costs of the systems. For 2040, we keep ToU tariff and load profiles unchanged from 2020, with a goal to illustrate the impacts of electric grid decarbonization on the life-cycle GHG emissions of the systems.

To understand if a carbon price can change dispatch behaviors, we also consider a carbon price of $51/tonne CO_2 in 2020 and $73/tonne CO_2 in 2040[189], charged in addition to the utility bills of households under the *minCost* objective, to account for the social cost of carbon. An additional objective of minimizing operational GHG emissions (*minGHG*) is also evaluated. Results of these two scenarios are shown in Supplementary Fig. 13-14.

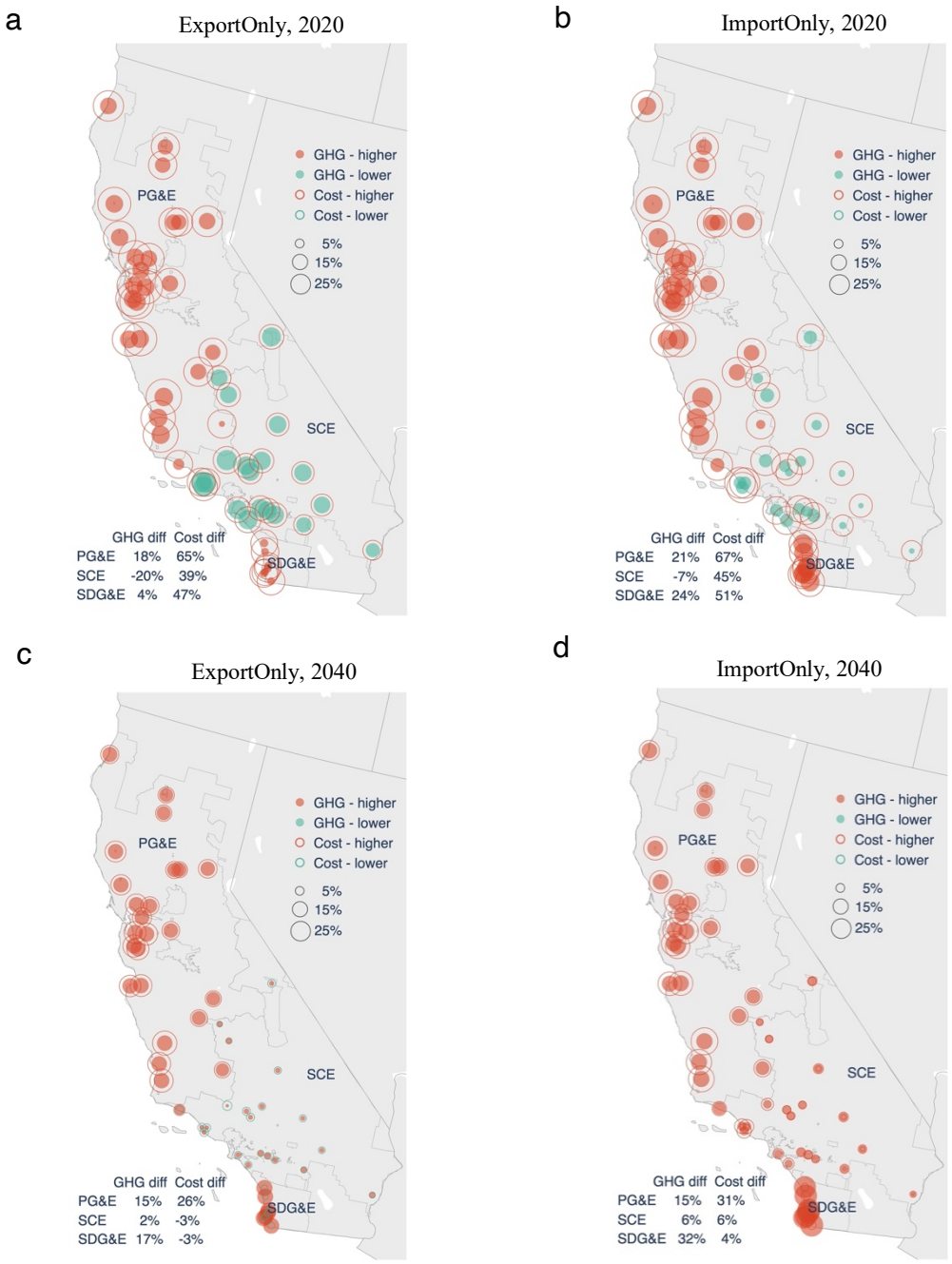

Figure 4. Differences in annual life-cycle GHG emissions and costs between installing solar-plus-storage systems and installing solar-only systems for households in California. (a) ExportOnly mode, 2020 (b) ImportOnly mode, 2020 (c) ExportOnly mode, 2040 and (d) ImportOnly mode, 2040. Results for solar-plus-storage systems are optimized under the objective of minimizing annual utility cost. The tables in lower left summarize average differences for households by utility area. Red color indicates solar-plus-storage systems lead to higher life-cycle emissions or cost and green means the opposite. Solid circles represent differences in life-cycle GHG emissions and hollow circles represent differences in life-cycle costs.

ExportOnly mode leads to lower life-cycle costs and GHG emissions compared to ImportOnly mode across all utilities in both 2020 and 2040. With ExportOnly mode, households served by SCE can have on average 20% lower life-cycle GHG emissions than Solar-Only scenario in 2020, but with 39% higher life-cycle costs (Fig. 4a). For PG&E, there are on average 18% more life-cycle emissions, because the small reduction in operational emissions from low dispatching of batteries cannot offset their embodied emissions (Supplementary Fig. 10a). The life-cycle cost is much higher as the small price difference between peak and off-peak hours and the narrow peak-hour window of the ToU result in little savings in utility cost, in addition to the relatively high cost of battery storage. For SDG&E, the emissions and cost reduction from the operational phase cannot offset the annualized embodied emissions and capital cost either. In ImportOnly mode (Fig. 4b), households served by SCE have lower emissions reduction potential than when ExportOnly mode is adopted. For SDG&E, solar-plus-storage systems with ImportOnly modes lead to an average of 24% higher life-cycle GHG emissions than Solar-Only systems.

The distinct results across utility areas can again be explained by their ToU plans, MEFs, and climates. The representative ToU plan of SCE provides higher incentives for battery dispatch and encourages more charging from on-site solar PV or from the grid during daytime. In comparison, SDG&E's ToU plan incentivizes nighttime charging when MEFs are the highest. In 2020, the variations in MEFs of PG&E area are lower than those of SCE and SDG&E, due to a higher portion of non-solar renewable energy, such as wind, hydro and geothermal as marginal generation mix.

In the future, to meet decarbonization targets, more renewable energy and energy storage capacity will be added to the grid. Fig. 4c-4d show the modeled results for 2040 using the estimated capital cost, embodied emissions, and MEFs in 2040. The differences in life-cycle GHG emissions between solar-plus-storage and Solar-Only systems (2%-32%) are higher than 2020, but the differences in life-cycle cost are lower and could potentially be negative (-3% with ExportOnly mode) due to a lower cost of battery storage. With an increasingly decarbonized grid and growing utility-scale storage, the long-run MEFs in the future are much lower and with less variations than those in 2020 (Supplementary Fig. 2-3). This change leads to smaller or no reduction in operational GHG emissions from dispatching residential battery storage with the evaluated modes, in addition to their lower but non-trivial embodied emissions in 2040 (Supplementary Fig. 10b-12b).

Applying a carbon price can reduce the life-cycle emissions of solar-plus-storage systems, especially with ImportOnly mode (Supplementary Fig. 13). This is because battery charging is discouraged when carbon-intensive fossil fuels are on the margin, which would incur higher cost for the household. Under *minGHG* objective (minimize annual operational GHG emissions), the life-cycle GHG emissions reduction is much higher for solar-plus-storage systems, but with higher life-cycle cost compared to the *minCost* scenario (Supplementary Fig. 14).

D. Discussion and conclusions

Our results show that installing residential solar PV systems in 2020 has the potential to significantly reduce both life-cycle GHG emissions and utility costs of households. But compared to solar PV systems, installing solar-plus-storage systems can drive the life-cycle

GHG emissions up or down depending on the utility area and operation mode, while increasing life-cycle costs for households across all utilities in California. In 2040, the differences in life-cycle GHG emissions increase but the differences in life-cycle cost decrease. We discuss the factors that would enable residential solar-plus-storage systems to reduce life-cycle costs and emissions effectively.

ToU tariff design determines residential battery dispatch patterns as households seek to minimize their utility cost. A larger price gap between on-peak and off-peak hours is needed to provide more cost arbitrage opportunities and motivate households to move towards low-carbon consumption during off-peak hours. To minimize life-cycle GHG emissions, an effective ToU rate structure should also reflect or internalize the marginal emissions of electricity generation in the grid, by enabling storage of low-carbon energy when VRE generation is abundant and avoiding low rates when the MEFs are high. Current NEM policy in California has been driving residential PV adoption, although a re-evaluation is urged as it raises social equity issues[191].

Applying a carbon price can improve the alignment between electricity prices and marginal emission factors of the grid and therefore enhance the GHG emissions mitigation potential of solar-plus-storage systems. It would enable more solar PV generation to be shifted and discourage pulling from the grid when fossil fuel generators are on the margin. Alternatively, Real-Time Pricing (RTP), which is based on the real-time marginal generation cost with a higher temporal resolution than ToU[192], may be more effective in aligning economic and environmental goals as the capacity of low-carbon energy expands.

Assuming current life-cycle costs and rate structures, solar-plus-storage systems do not offer savings for most households in California. The savings in utility bills through battery arbitrage often cannot compensate for the high upfront cost. However, direct financial incentives such as the Self-Generation Incentive Program in California and the federal investment tax credit[193], have been used to ease the financial burdens of households and drive large-scale uptake of solar-plus-storage systems. Furthermore, battery storage is projected to be more affordable in the coming decades due to technology improvement and economies of scale[194,195].

The net GHG emissions from a solar-plus-storage system are determined not only by operational parameters including the marginal electricity generation, ToU rate structure, load profile of the household and operation mode, but also embodied emissions due to materials production and manufacturing of the system, which contributes as a significant portion. For solar-plus-storage systems to mitigate life-cycle GHG emissions, reducing the upstream emissions by advancing energy efficiency and materials efficiency during production, improving round-trip efficiency during operation and increasing end-of-life reuse and recycling are essential.

In the long run, as a growing portion of VRE and utility-scale storage capacities added to the electricity systems, the MEFs of the grid become lower and less variable, leaving smaller opportunities for residential battery storage to reduce emissions with the two operation modes evaluated. However, with the marginal generation cost and marginal emissions of the grid becoming increasingly temporally-aligned due to the growing penetration of VRE in California, residential battery storage has the potential to reduce utility bills and emissions

simultaneously in the future, especially with a full cost arbitrage mode in which the battery can import and export without constraints.

Distributed energy resources can reduce the total cost and emissions of electricity systems by providing stacked benefits[196]. Especially, solar-plus-storage can reduce utility-observed peak, prevent curtailment, defer distribution system upgrades and improve energy resilience. Our study shows that, to maximize the potential of residential solar-plus-storage systems in reducing life-cycle GHG emissions and cost, ToU tariffs that have wider spreads and are more aligned with MEFs, rapid cost reduction of and subsidy for battery storage and adoption of carbon prices are critical. Collaboration among policy-makers, utility companies, and residents is required to ensure that solar-plus-storage systems achieve economic and environmental goals without bringing unintended outcomes.

E. Acknowledgements

J.Z. is supported by Bren School Graduate Student Fellowship. We thank Thomas Dandres at Ecole Polytechnique de Montreal, Pieter Gagnon at National Renewable Energy Laboratory, Mahnoosh Alizadeh and Yang Qiu at UC Santa Barbara for their valuable comments.

F. Appendix

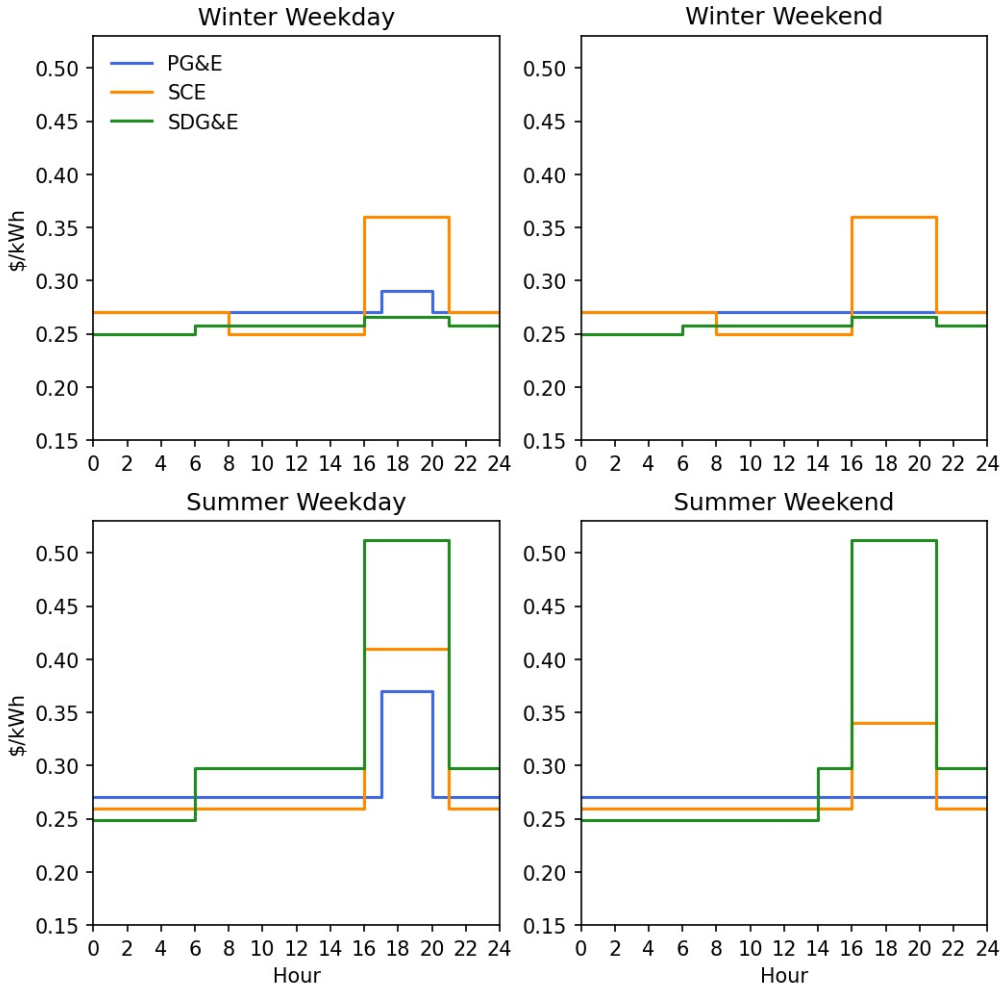

Supplementary Figure 1. Time-of-Use Rates by Utility Company in California (2020). PG&E: E-TOU-D. SCE: TOU-D-4-9PM. SDG&E: DR-SES. Summer is June-September for PG&E and SCE but June-October for SDG&E.

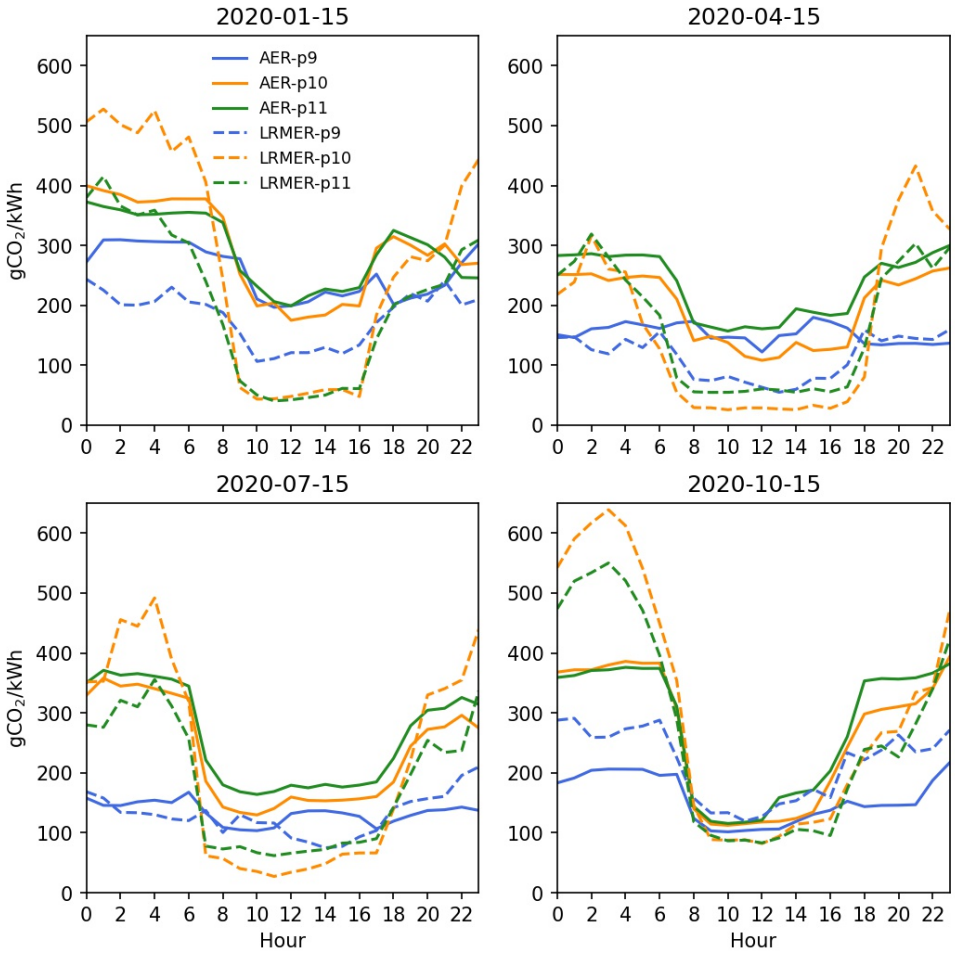

Supplementary Figure 2. Average Emissions Rates (AER) and Long-run Marginal Emission Factors (LRMER) of the electric grid in 2020 by balancing area in Cambium[190]. The balancing area p9, p10 and p11 covers PG&E, SCE and SDG&E service area respectively, with slight misalignment in the borderlines of the first two areas.

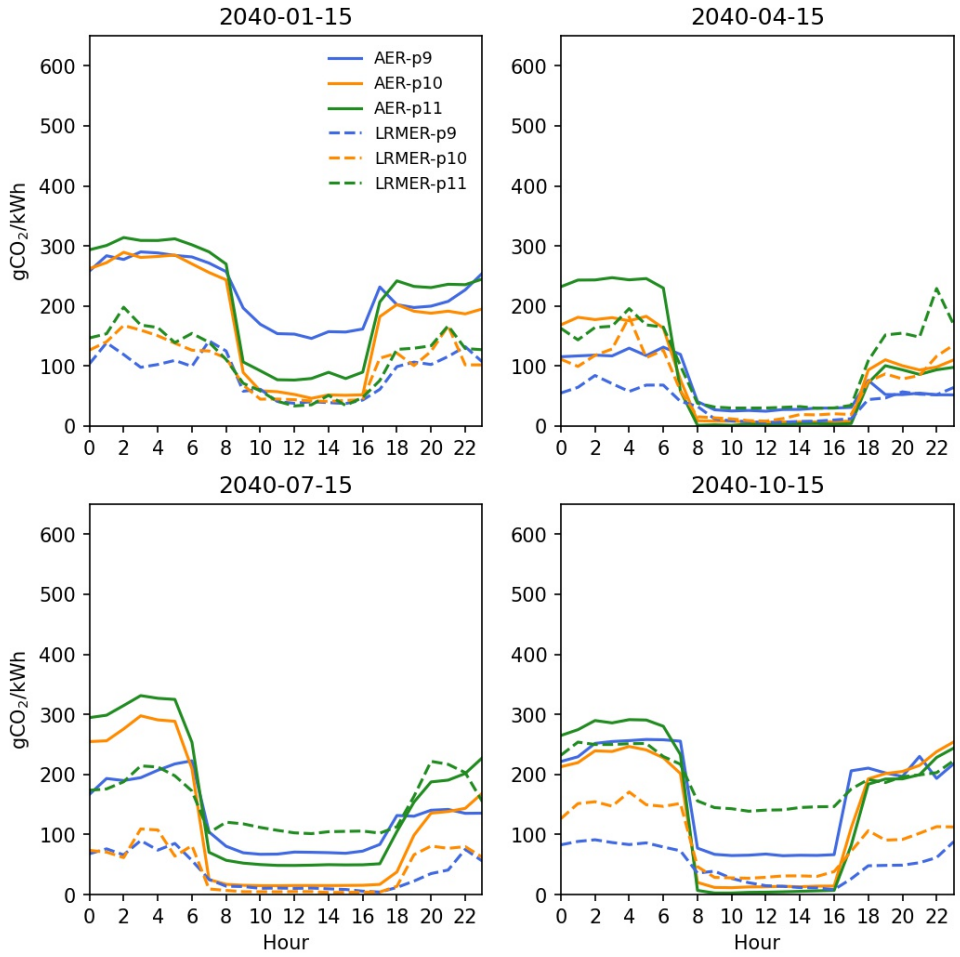

Supplementary Figure 3. Average Emissions Rates (AER) and Long-run Marginal Emission Factors (LRMER) of the electric grid in 2040 by balancing area in Cambium[190]. The balancing area p9, p10 and p11 covers PG&E, SCE and SDG&E service area respectively, with slight misalignment in the borderlines of the first two areas.

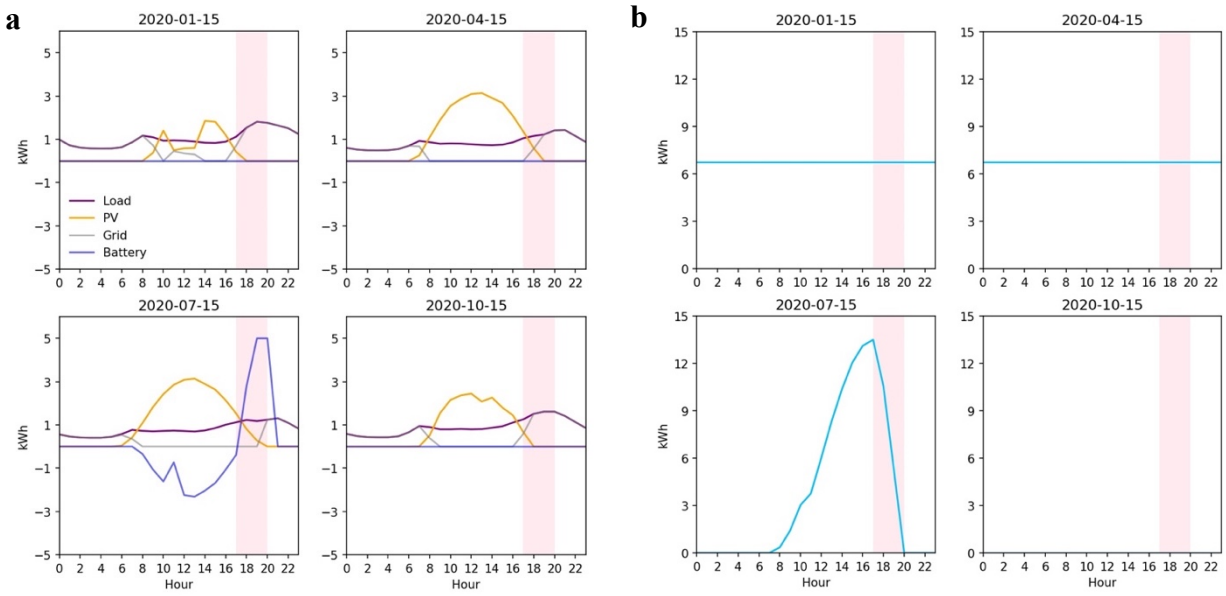

Supplementary Figure 4. (**a**) Electricity supply and demand and (**b**) state of charge level of a representative household served by PG&E by hour of the day and season (ExportOnly mode), optimized under an objective of minimizing annual utility cost (*minCost*).

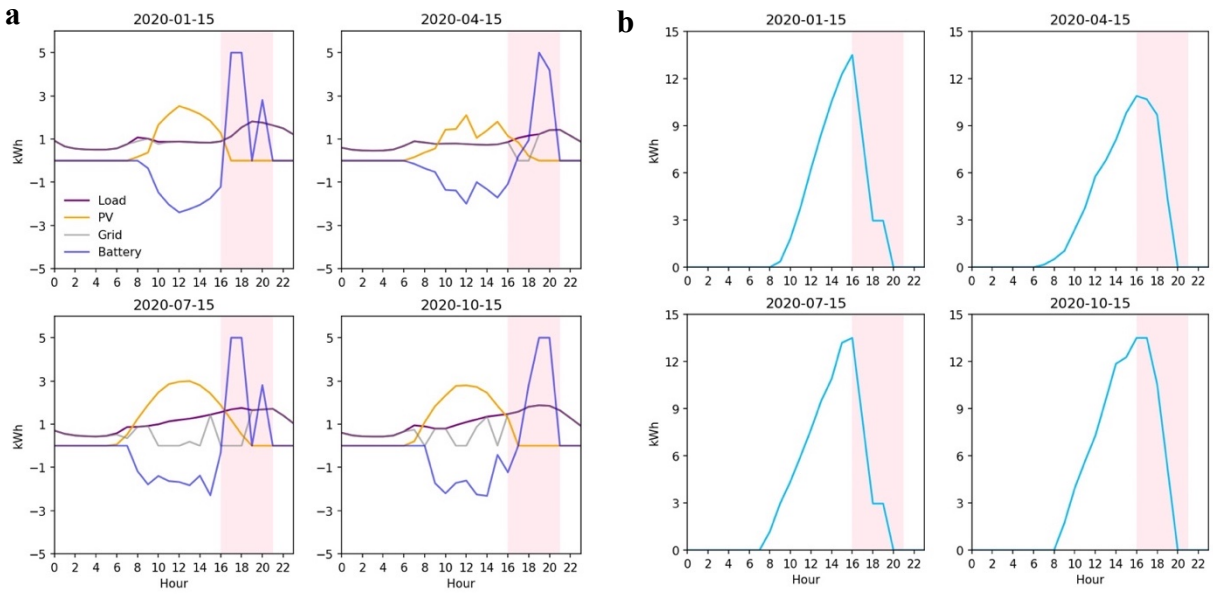

Supplementary Figure 5. (**a**) Electricity supply and demand and (**b**) state of charge level of a representative household served by SCE by hour of the day and season (ExportOnly mode), optimized under an objective of minimizing annual utility cost (*minCost*).

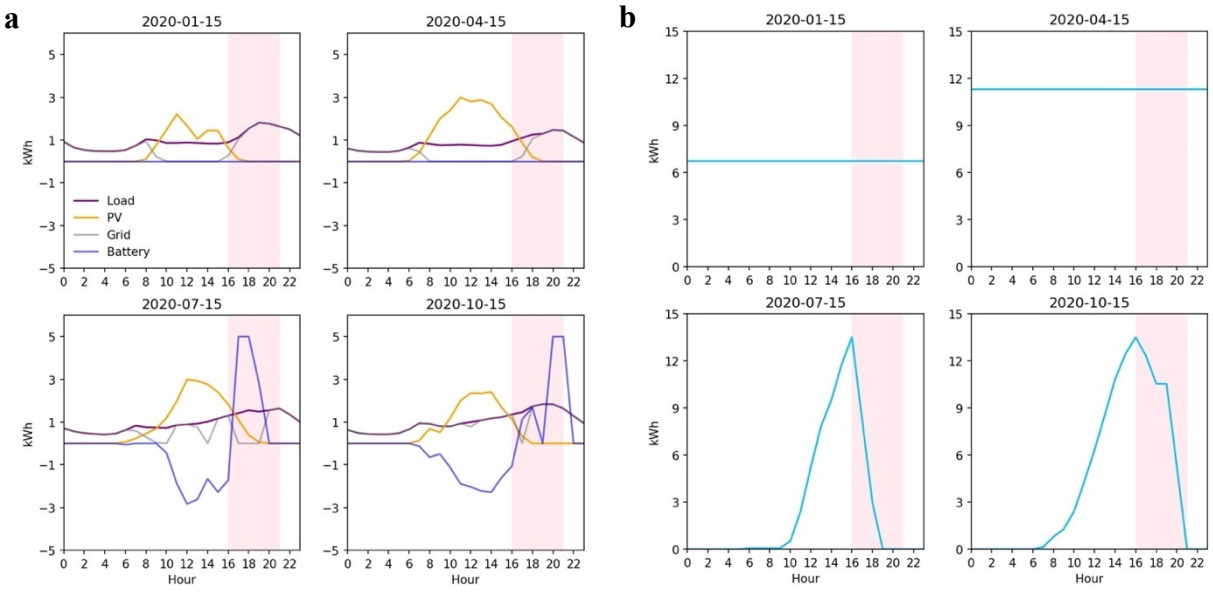

Supplementary Figure 6. (**a**) Electricity supply and demand and (**b**) state of charge level of a representative household served by SDG&E by hour of the day and season (ExportOnly mode), optimized under an objective of minimizing annual utility cost (*minCost*).

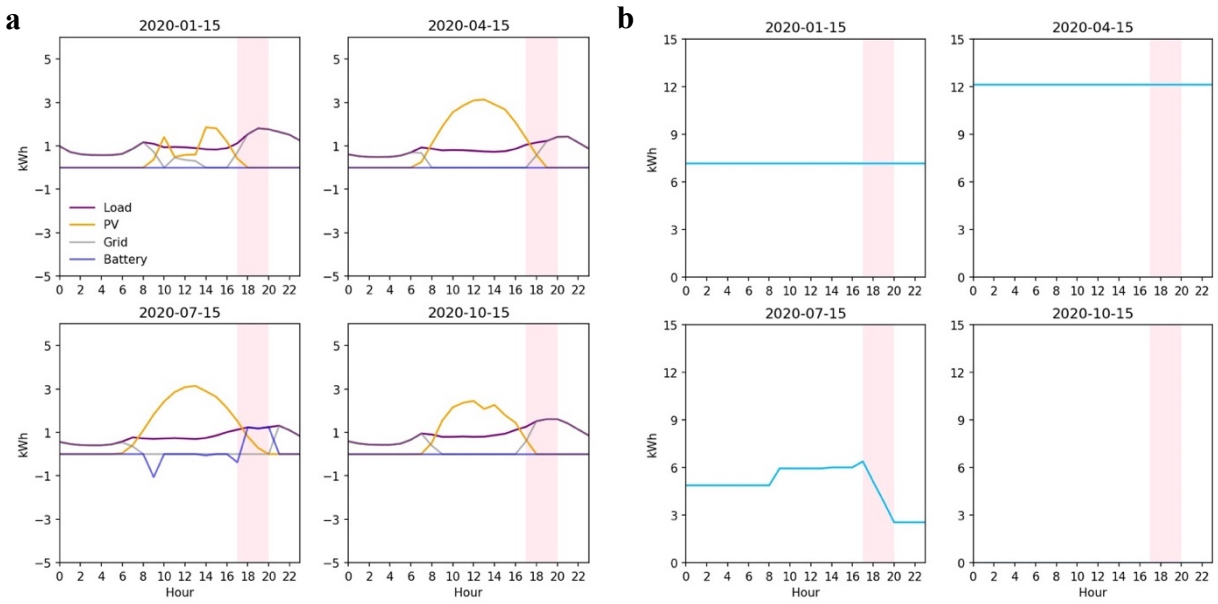

Supplementary Figure 7. (**a**) Electricity supply and demand and (**b**) state of charge level of a representative household served by PG&E by hour of the day and season (ImportOnly mode), optimized under an objective of minimizing annual utility cost (*minCost*).

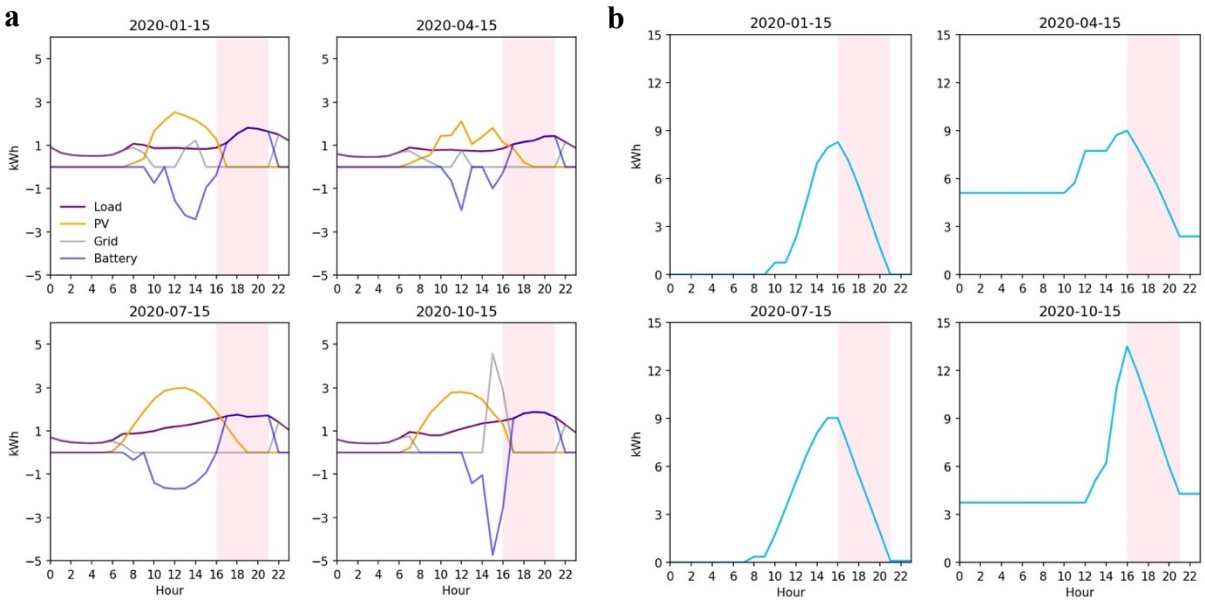

Supplementary Figure 8. (**a**) Electricity supply and demand and (**b**) state of charge level of a representative household served by SCE by hour of the day and season (ImportOnly mode), optimized under an objective of minimizing annual utility cost (*minCost*).

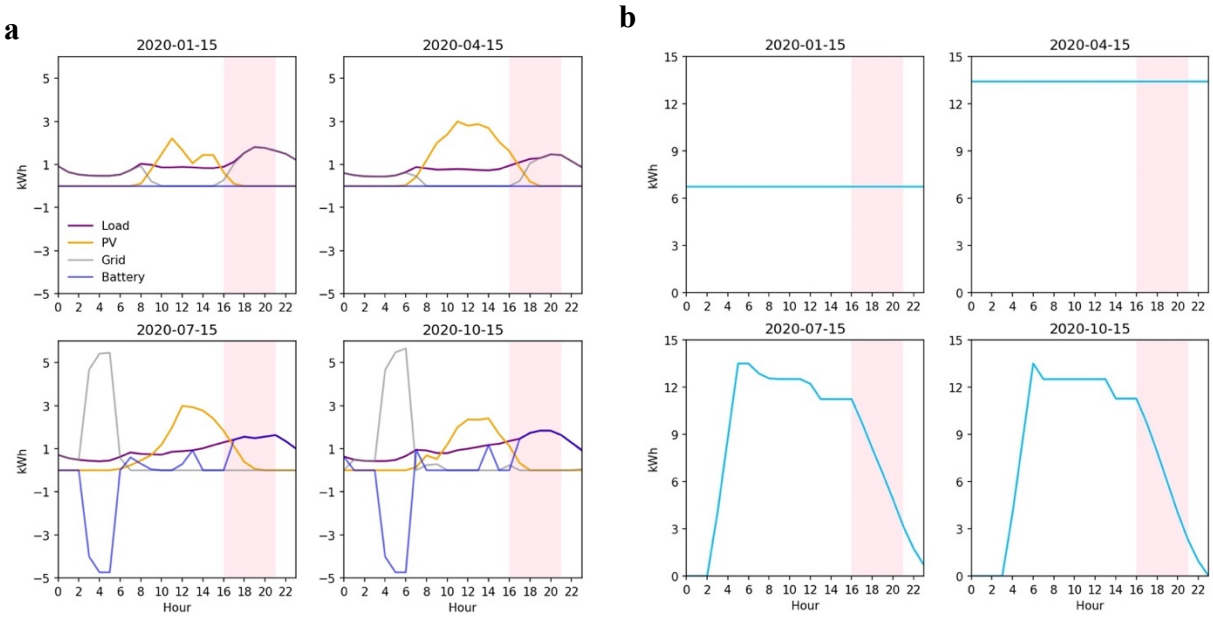

Supplementary Figure 9. (**a**) Electricity supply and demand and (**b**) state of charge level of a representative household served by SDG&E by hour of the day and season (ImportOnly mode), optimized under an objective of minimizing annual utility cost (*minCost*).

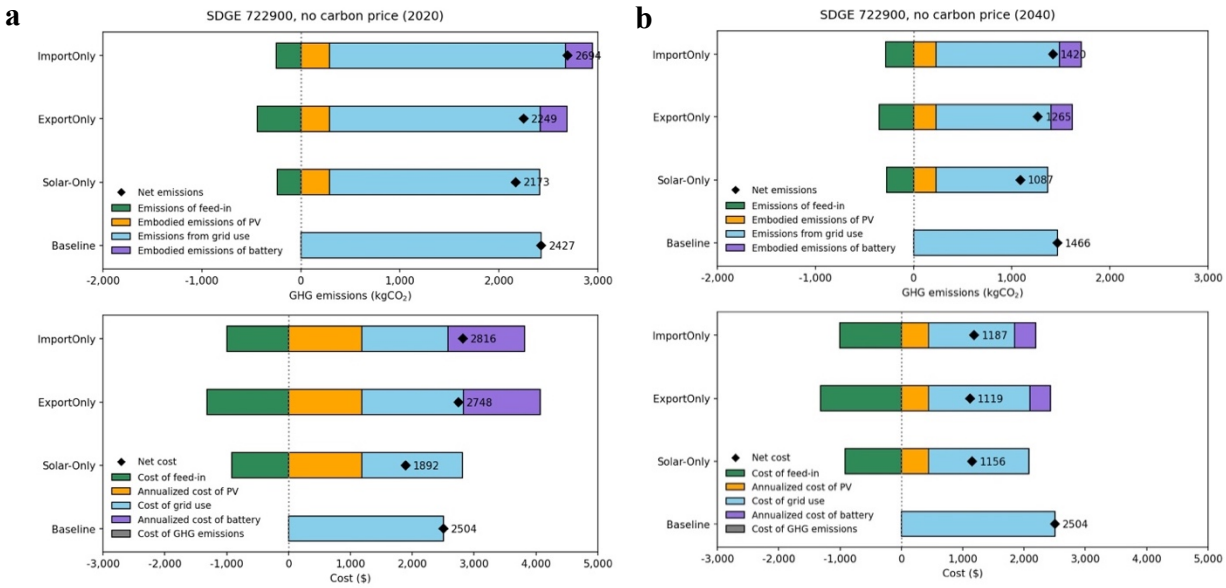

Supplementary Figure 10. Breakdown of life-cycle GHG emissions and life-cycle cost for a representative household (TMY 3 code 724936 – Concord Buchanan Field) served by PG&E. (**a**) 2020 and (**b**) 2040. Results for ExportOnly and ImportOnly modes are based on optimized battery scheduling under an objective of minimizing annual utility cost (*minCost*). No carbon price assumed.

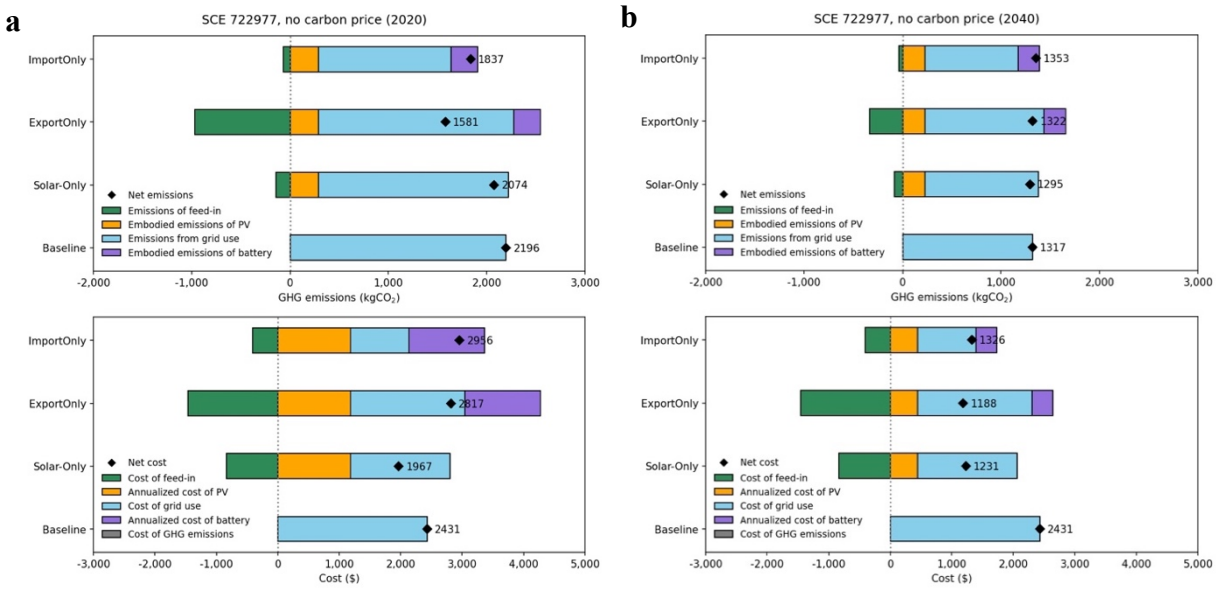

Supplementary Figure 11. Breakdown of life-cycle GHG emissions and life-cycle cost for a representative household (TMY 3 code 722977 – Santa Ana John Wayne) served by SCE. (**a**) 2020 and (**b**) 2040. Results for ExportOnly and ImportOnly modes are based on optimized battery scheduling under an objective of minimizing annual utility cost (*minCost*). No carbon price assumed.

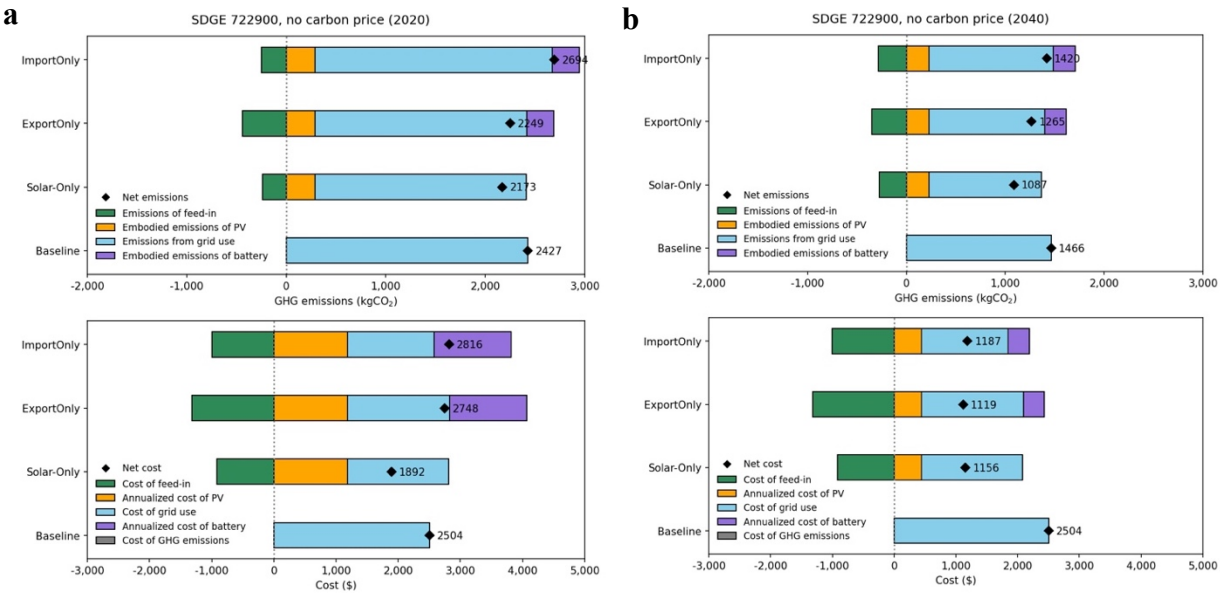

Supplementary Figure 12. Breakdown of life-cycle GHG emissions and life-cycle cost for a representative household (TMY 3 code 722900 – San Diego Lindbergh Field) served by SDG&E. (**a**) 2020 and (**b**) 2040. Results for ExportOnly and ImportOnly modes are based on optimized battery scheduling under an objective of minimizing annual utility cost (*minCost*). No carbon price assumed.

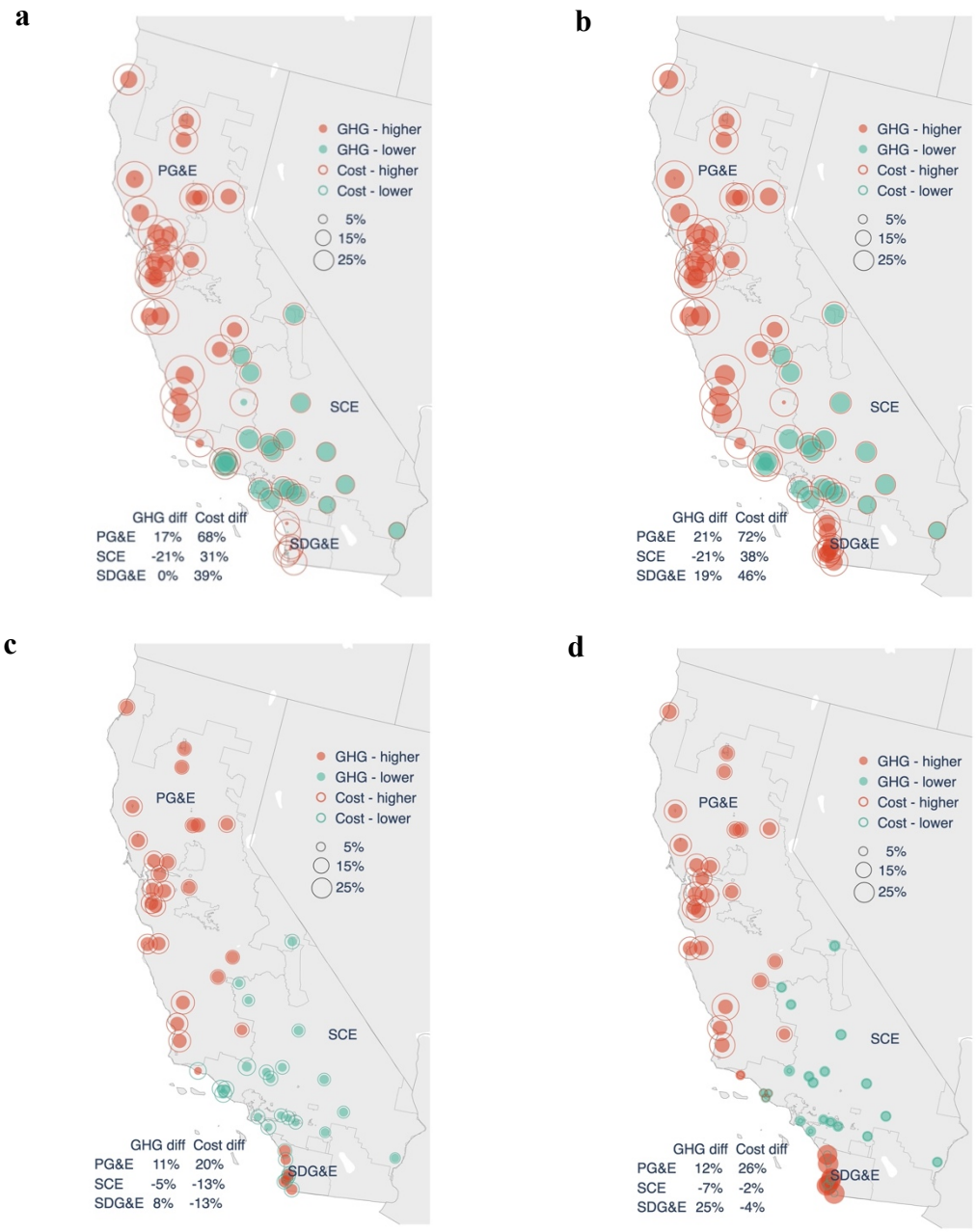

Supplementary Figure 13. Differences in annual life-cycle GHG emissions and costs between installing solar-plus-storage systems with objective to minimize annual utility cost considering a carbon price ($51/tonne$CO_2$ in 2020 and $73/tonne$CO_2$ in 2040) and and installing solar-only systems for households in California. (**a**) ExportOnly mode, 2020; (**b**) ImportOnly mode, 2020; (**c**) ExportOnly mode, 2040 and (**d**) ImportOnly mode, 2040. The tables summarize average values for households in each utility area. Red color indicates solar-plus-storage systems lead to higher life-cycle emissions or cost and green means the opposite. Solid circles represent differences in life-cycle GHG emissions and hollow circles represent differences in life-cycle costs.

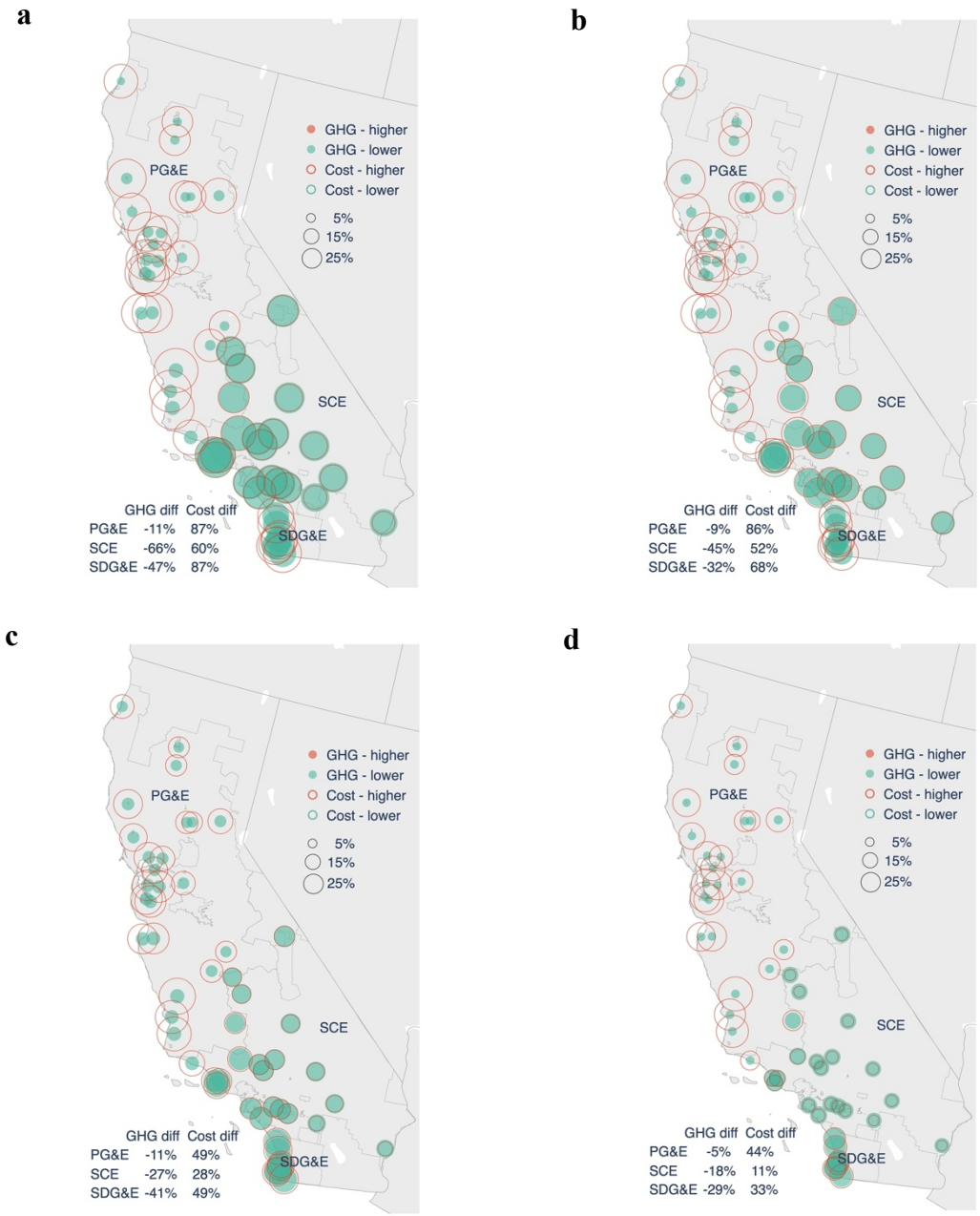

Supplementary Figure 14. Differences in annual life-cycle GHG emissions and costs between installing solar-plus-storage systems with objective to minimize annual GHG emissions and installing solar-only systems for households in California. (**a**) ExportOnly mode, 2020; (**b**) ImportOnly mode, 2020; (**c**) ExportOnly mode, 2040 and (**d**) ImportOnly mode, 2040. The tables summarize average values for households in each utility area. Red color indicates solar-plus-storage systems lead to higher life-cycle emissions or cost and green means the opposite. Solid circles represent differences in life-cycle GHG emissions and hollow circles represent differences in life-cycle costs.

Supplementary Table 1. Parameters in 2020 and 2040

Parameters	2020	2040	Unit	Reference
Time step	1		Hour	-
Solar PV size	4		kW	168,197
Battery round-trip efficiency	90%		-	173
Rated peak power of the battery system	5		kW	
Usable storage capacity of the battery system	13.5		kWh	
Lifetime aggregate discharge limit of the battery system	37,800		kWh	174
Lifetime of the solar PV system	25		years	198
Solar output degradation rate	0.5%		per year	172,198
Initial cost to purchase the battery system	$670	$185	per kWh usable capacity	177,178
Initial cost to purchase the solar PV system	$3.75	$1.41	per watt capacity	168,176
Embodied emissions of residential battery system	200.5	162	$kgCO_2$ per kWh usable capacity	165,186,187
Embodied emissions of solar PV system	48	37	gCO_2 per kWh electricity produced	114,186,188
Indirect emissions of the grid (balancing area p9)	23	10	gCO_2 per kWh electricity generated	114,190
Indirect emissions of the grid (balancing area p10)	27	23		
Indirect emissions of the grid (balancing area p11)	19	17		

Supplementary Table 2. Nomenclature for constraints

Notation	Variable/Parameter	Unit
$P_{char,\,h}$	Power charge in hour h, before loss, non-positive	kW
$P_{disc,\,h}$	Power discharge in hour h, after loss, non-negative	kW
$Load_h$	Load of the household in hour h	kWh
dt	Time interval	1 hour
$E_{batt,\,h}$	Stored energy in the battery system in hour h	kWh
$E_{batt,\,max}$	Maximum storage capacity of the battery system	kWh
$Loss_{char,\,h}$	Energy loss during charging in hour h	kWh
$Loss_{disc,\,h}$	Energy loss during discharging in hour h	kWh
eff_{rt}	Round-trip efficiency of the battery in hour h	-
$E_{PV\_to\_load,h}$	Energy flow from PV to meet on-site load in hour h	kWh
$E_{grid\_to\_load,\,h}$	Energy flow from the grid to meet on-site load in hour h	kWh
$E_{PV\_to\_batt,\,h}$	Energy flow from PV to charge battery in hour h	kWh
$E_{grid\_to\_batt,\,h}$	Energy flow from the grid to charge battery in hour h	kWh
$E_{PV\_to\_grid,h}$	Energy flow from PV to feed back to grid in hour h	kWh
$E_{batt\_to\_grid,h}$	Energy flow from battery to feed back to grid in hour h	kWh
PV_gen_h	Solar PV generation in hour h	kWh
E_limit_{batt}	Yearly total discharge limit of the battery system	kWh

Supplementary Table 3. Constraints in the optimization model (ExportOnly mode)

Constraint	Equation
Battery cannot charge and discharge at the same time	$P_{char,h} \times P_{disc,h} = 0$
Battery does not charge nor discharge in the first hour of the year	$P_{char,0} + P_{disc,0} = 0$
Battery is 50% charged in the first hour of the year	$E_{batt,0} = 0.5 \times E_{batt,max}$
Electricity discharged to serve load cannot exceed load in any hour	$E_{batt\_to\_load,h} \leq Load_h$
Energy loss of battery (charging)	$Loss_{char,h} = -P_{char,h} \times dt \times (1 - \sqrt{eff_{rt}})$
Energy loss of battery (discharging)	$Loss_{disc,h} = (P_{disc,h} \times dt + Loss_{disc,h}) \times (1 - \sqrt{eff_{rt}})$
Stored energy in the battery	$E_{batt,h} = E_{batt,h-1} - (P_{char,h} + P_{disc,h}) \times dt - Loss_{char,h} - Loss_{disc,h}$
The household cannot send excess PV to grid while using grid power or vice versa	$E_{PV\_to\_grid,h} \times E_{grid\_to\_load,h} = 0$
Battery can only charge from solar PV	$P_{char,h} \times dt + E_{PV\_to\_batt,h} = 0$
Battery discharge balance	$P_{disc,h} \times dt = E_{batt\_to\_load,h} + E_{batt\_to\_grid,h}$
Load balance	$Load_h = E_{grid\_to\_load,h} + E_{PV\_to\_load,h} + E_{batt\_to\_load,h}$
PV balance	$PV\_gen_h = E_{PV\_to\_load,h} + E_{PV\_to\_battery,h} + E_{PV\_to\_grid,h}$
Yearly battery discharge limit	$\sum_{h=1}^{8760} P_{disc,h} \times dt \leq E\_limit_{batt}$

Supplementary Table 4. Constraints in the optimization model (ImportOnly mode)

Constraint	Equation
Battery cannot charge and discharge at the same time	$P_{char,h} \times P_{disc,h} = 0$
Battery does not charge nor discharge in the first hour of the year	$P_{char,0} + P_{disc,0} = 0$
Battery is 50% charged in the first hour of the year	$E_{batt,0} = 0.5 \times E_{batt,max}$
Electricity discharged to serve load cannot exceed load in any hour	$P_{disc,h} \times dt \leq Load_h$
Energy loss of battery (charging)	$Loss_{char,h} = -P_{char,h} \times dt \times (1 - \sqrt{eff_{rt}})$
Energy loss of battery (discharging)	$Loss_{disc,h} = (P_{disc,h} \times dt + Loss_{disc,h}) \times (1 - \sqrt{eff_{rt}})$
Stored energy in the battery	$E_{batt,h} = E_{batt,h-1} - (P_{char,h} + P_{disc,h}) \times dt - Loss_{char,h} - Loss_{disc,h}$
The household cannot send excess PV to grid while using grid power or vice versa	$E_{PV\_to\_grid,h} \times (E_{grid\_to\_load,h} + E_{grid\_to\_batt,h}) = 0$
Battery can charge from both solar PV and the grid	$P_{char,h} \times dt + (E_{PV\_to\_batt,h} + E_{grid\_to\_batt,h}) = 0$
Battery discharge balance	$P_{disc,h} \times dt = E_{batt\_to\_load,h}$
Load balance	$Load_h = E_{grid\_to\_load,h} + E_{PV\_to\_load,h} + E_{batt\_to\_load,h}$
PV balance	$PV\_gen_h = E_{PV\_to\_load,h} + E_{PV\_to\_battery,h} + E_{PV\_to\_grid,h}$
Yearly battery discharge limit	$\sum_{h=1}^{8760} P_{disc,h} \times dt \leq E\_limit_{batt}$

V. Summary

To sum up, this dissertation evaluates the opportunities to reduce the life-cycle GHG emissions of rapidly-growing technologies including plastics, data centers and residential solar-plus-storage systems. I combine life-cycle GHG emissions accounting, scenario analysis, life-cycle cost and optimization modeling to achieve the research objectives.

In Chapter II, I quantified the global life-cycle GHG emissions of plastics and evaluated the mitigation potential of demand reduction, renewable energy, bio-based plastics and recycling. In 2015, the global carbon footprint of plastics was 1.7 $GtCO_2e$, or 3.5% of global total GHG emissions in that year. Resin production contributed the most to the total footprint (61%), followed by conversion (30%) and end-of-life treatment (9%). Among the strategies, adoption of renewable energy and demand reduction have the most reduction potential, followed by use of bio-based plastics and recycling. Only by combining the four mitigation strategies can we keep the future life-cycle GHG emissions of plastics below the 2015 level. This chapter calls for urgent needs to rapidly decarbonize our energy systems, reduce our reliance on plastics, switch to renewable feedstocks and increase plastic recycling capability across the globe.

In Chapter III, I assessed the potential of using workloads migration between data centers in different locations to absorb excess renewable electricity and reduce GHG emissions. By using underutilized server capacities, existing data centers in the CAISO grid region could have absorbed up to 62% of the yearly curtailment in that region and reduced up to 239 $KtCO_2e$ emissions with negative abatement cost. Building additional data centers that run intermittently based on the availability of excess renewable electricity could reduce

curtailment and GHG emissions further while keeping the net abatement cost negative, with the embodied emissions of data centers considered. This chapter underscores the potential of flexible demand such as workloads in data centers in mitigating the problem of renewable over-generation and thereby reducing GHG emissions. With data processing needs and renewable energy production both growing rapidly, this technology should be more widely adopted. Collaborations between the grid operators and data center owners and technological advancement in reducing data transmission latency should take place.

In Chapter IV, I examined the life-cycle cost and GHG emissions of residential solar-plus-storage systems in California. Installing PV reduces 110-570 $kgCO_2$ and \$180-\$730 per household in 2020. However, adding battery storage to a PV system increases life-cycle costs by 39%-67%, while impact on emissions is mixed (-20% to 24%) depending on tariff structure and marginal emission factors. In 2040, under current decarbonization and cost trajectories, additional life-cycle costs by adding storage decrease (31% to -3%) while additional emissions increase (2%-32%). This Chapter concludes that ToU tariff, operation mode, capital cost and embodied emissions of the systems jointly determine the life-cycle cost and GHG emissions. It highlights the importance of marginal emissions-aligned tariff design, rapid decreases in battery cost and embodied emissions and use of carbon price to maximize the potential of residential solar-plus-storage systems.

This dissertation advances the research agenda of assessing the decarbonization opportunities of rapidly-growing technologies. The data, methods, models and results from this dissertation address multiple research gaps and can be used in further research to accelerate the low-carbon transition of energy and technological systems.

VI. References

1. *Climate change 2014: synthesis report*. (Intergovernmental Panel on Climate Change, 2015).
2. Rogelj, J., Forster, P. M., Kriegler, E., Smith, C. J. & Séférian, R. Estimating and tracking the remaining carbon budget for stringent climate targets. *Nature* **571**, 335–342 (2019).
3. Höhne, N. *et al.* Emissions: world has four times the work or one-third of the time. *Nature* **579**, 25–28 (2020).
4. Franklin Associates. Impact of Plastics Packaging on Life Cycle Energy Consumption & Greenhouse Gas Emissions in the United States and Canada. https://plastics.americanchemistry.com/Education-Resources/Publications/Impact-of-Plastics-Packaging.pdf (2014).
5. Inderwildi, O., Zhang, C., Wang, X. & Kraft, M. The impact of intelligent cyber-physical systems on the decarbonization of energy. *Energy Environ. Sci.* (2020) doi:10.1039/C9EE01919G.
6. Vinuesa, R. *et al.* The role of artificial intelligence in achieving the Sustainable Development Goals. *Nat Commun* **11**, 1–10 (2020).
7. Braff, W. A., Mueller, J. M. & Trancik, J. E. Value of storage technologies for wind and solar energy. *Nature Climate Change* **6**, 964–969 (2016).
8. Kittner, N., Lill, F. & Kammen, D. M. Energy storage deployment and innovation for the clean energy transition. *Nature Energy* **2**, 17125 (2017).
9. Geyer, R., Jambeck, J. R. & Law, K. L. Production, use, and fate of all plastics ever made. *Sci. Adv.* **3**, e1700782 (2017).
10. Masanet, E., Shehabi, A., Lei, N., Smith, S. & Koomey, J. Recalibrating global data center energy-use estimates. *Science* **367**, 984–986 (2020).
11. World Economic Forum, Ellen MacArthur Foundation & McKinsey & Company. *The New Plastics Economy - Rethinking the future of plastics*. https://www.ellenmacarthurfoundation.org/assets/downloads/EllenMacArthurFoundation_TheNewPlasticsEconomy_Pages.pdf (2016).
12. Jones, N. How to stop data centres from gobbling up the world's electricity. *Nature* **561**, 163 (2018).
13. Babacan, O., Abdulla, A., Hanna, R., Kleissl, J. & Victor, D. G. Unintended Effects of Residential Energy Storage on Emissions from the Electric Power System. *Environ. Sci. Technol.* **52**, 13600–13608 (2018).
14. Fares, R. L. & Webber, M. E. The impacts of storing solar energy in the home to reduce reliance on the utility. *Nature Energy* **2**, 1–10 (2017).

15. Intergovernmental Panel on Climate Change. *Introductory Chapter. In: Climate Change 2014: Mitigation of Climate Change. Contribution of Working Group III to the Fifth Assessment Report of the Intergovernmental Panel on Climate Change*. https://www.ipcc.ch/site/assets/uploads/2018/02/ipcc_wg3_ar5_chapter1.pdf (2014).

16. Standardization, I. O. for. *Environmental Management: Life Cycle Assessment: Principles and Framework*. vol. 14040 (ISO, 2006).

17. Arvidsson, R. *et al.* Environmental Assessment of Emerging Technologies: Recommendations for Prospective LCA. *Journal of Industrial Ecology* **22**, 1286–1294 (2018).

18. Moni, S. M., Mahmud, R., High, K. & Carbajales-Dale, M. Life cycle assessment of emerging technologies: A review. *Journal of Industrial Ecology* **24**, 52–63 (2020).

19. International Renewable Energy Agency. *Behind-The-Meter Batteries – Innovation Landscape Brief*. 24 (2019).

20. Jambeck, J. R. *et al.* Plastic waste inputs from land into the ocean. *Science* **347**, 768–771 (2015).

21. Law, K. L. Plastics in the Marine Environment. *Annual Review of Marine Science* **9**, 205–229 (2017).

22. Law, K. L. & Thompson, R. C. Microplastics in the seas. *Science* **345**, 144–145 (2014).

23. Rochman, C. M. *et al.* Policy: Classify plastic waste as hazardous. *Nature* https://www.nature.com/articles/494169a (2013) doi:10.1038/494169a.

24. Lithner, D., Larsson, Å. & Dave, G. Environmental and health hazard ranking and assessment of plastic polymers based on chemical composition. *Science of The Total Environment* **409**, 3309–3324 (2011).

25. Fischedick, M. *et al. Climate Change 2014: Mitigation of Climate Change Ch. 10 - Industry.* https://www.ipcc.ch/pdf/assessment-report/ar5/wg3/ipcc_wg3_ar5_chapter10.pdf (2014).

26. Hillmyer, M. A. The promise of plastics from plants. *Science* **358**, 868–870 (2017).

27. Weiss, M. *et al.* A Review of the Environmental Impacts of Biobased Materials. *Journal of Industrial Ecology* **16**, S169–S181 (2012).

28. Yates, M. R. & Barlow, C. Y. Life cycle assessments of biodegradable, commercial biopolymers—A critical review. *Resources, Conservation and Recycling* **78**, 54–66 (2013).

29. Chen, G.-Q. & Patel, M. K. Plastics Derived from Biological Sources: Present and Future: A Technical and Environmental Review. *Chem. Rev.* **112**, 2082–2099 (2012).

30. Spierling, S. *et al.* Bio-based plastics - A review of environmental, social and economic impact assessments. *Journal of Cleaner Production* **185**, 476–491 (2018).

31. Albertsson, A.-C. & Hakkarainen, M. Designed to degrade. *Science* **358**, 872–873 (2017).

32. OECD. *Policies for Bioplastics in the Context of a Bioeconomy*. https://www.oecd-ilibrary.org/science-and-technology/policies-for-bioplastics-in-the-context-of-a-bioeconomy_5k3xpf9rrw6d-en (2013) doi:10.1787/5k3xpf9rrw6d-en.

33. European Commission. *A European strategy for plastics in a circular economy*. http://ec.europa.eu/environment/circular-economy/pdf/plastics-strategy-brochure.pdf (2018).

34. European Bioplastics. *Bioplastics market data 2017*. http://docs.european-bioplastics.org/publications/market_data/2017/Report_Bioplastics_Market_Data_2017.pdf (2017).

35. Posen, I. D., Jaramillo, P., Landis, A. E. & Griffin, W. M. Greenhouse gas mitigation for U.S. plastics production: energy first, feedstocks later. *Environ. Res. Lett.* **12**, 034024 (2017).

36. Hopewell, J., Dvorak, R. & Kosior, E. Plastics recycling: challenges and opportunities. *Philos Trans R Soc Lond B Biol Sci* **364**, 2115–2126 (2009).

37. Lazarevic, D., Aoustin, E., Buclet, N. & Brandt, N. Plastic waste management in the context of a European recycling society: Comparing results and uncertainties in a life cycle perspective. *Resources, Conservation and Recycling* **55**, 246–259 (2010).

38. Hottle, T. A., Bilec, M. M. & Landis, A. E. Sustainability assessments of bio-based polymers. *Polymer Degradation and Stability* **98**, 1898–1907 (2013).

39. Wernet, G. *et al.* The ecoinvent database version 3 (part I): overview and methodology. *Int J Life Cycle Assess* **21**, 1218–1230 (2016).

40. European Life Cycle Database (ELCD). http://eplca.jrc.ec.europa.eu/ELCD3/index.xhtml?stock=default.

41. Voet, E. van der, Oers, L. van, Rydberg, T., Westerdahl, J. & Larsen, H. F. Life Cycle Assessment of Additives: Methodology and Data. in *Global Risk-Based Management of Chemical Additives II* 7–23 (Springer, Berlin, Heidelberg, 2012). doi:10.1007/698_2012_185.

42. European Council for Plasticisers and Intermediates. *Eco-profiles and Environmental Product Declarations of the European Plastics Manufacturers: Di-isononyl phthalate (DINP)*. http://www.ecpi.org/wp-content/uploads/2015/10/21872-ecpi-eco-profile-dinp-2015-02-05.pdf (2015).

43. Keoleian, G., Miller, S., De Kleine, R., Fang, A. & Mosley, J. *Life cycle material data update for GREET model*. (2012).

44. Franklin Associates. *Life Cycle Inventory of Plastic Fabrication Processes: Injection Molding and Thermoforming*. 63 (2011).

45. Madival, S., Auras, R., Singh, S. P. & Narayan, R. Assessment of the environmental profile of PLA, PET and PS clamshell containers using LCA methodology. *Journal of Cleaner Production* **17**, 1183–1194 (2009).

46. Thomas, B. *A Carbon Footprint for UK Clothing and Opportunities for Savings*. http://www.wrap.org.uk/sites/files/wrap/Appendix%20IV%20-%20Carbon%20footprint%20report.pdf (2012).

47. Franklin Associates. *Life Cycle Inventory of 100% Postconsumer HDPE and PET Recycled Resin from Postconsumer containers and packaging*. https://www.plasticsrecycling.org/images/pdf/PE_PP_Resins/Life-Cycle-Inventory-Study/Life_Cycle_Inventory.pdf (2010).

48. Lovett, J. Sustainable Sourcing of Feedstocks for Bioplastics. 17 (2016).

49. Posen, I. D., Jaramillo, P. & Griffin, W. M. SM - Uncertainty in the Life Cycle Greenhouse Gas Emissions from U.S. Production of Three Biobased Polymer Families. *Environmental Science & Technology* **50**, 2846–2858 (2016).

50. Rossi, V. *et al.* Life cycle assessment of end-of-life options for two biodegradable packaging materials: sound application of the European waste hierarchy. *Journal of Cleaner Production* **86**, 132–145 (2015).

51. Liptow, C. & Tillman, A.-M. A Comparative Life Cycle Assessment Study of Polyethylene Based on Sugarcane and Crude Oil. *Journal of Industrial Ecology* **16**, 420–435 (2012).

52. Tsiropoulos, I. *et al.* Life cycle impact assessment of bio-based plastics from sugarcane ethanol. *Journal of Cleaner Production* **90**, 114–127 (2015).

53. Shen, L. & Patel, M. K. Life Cycle Assessment of Polysaccharide Materials: A Review. *J Polym Environ* **16**, 154 (2008).

54. Groot, W. J. & Borén, T. Life cycle assessment of the manufacture of lactide and PLA biopolymers from sugarcane in Thailand. *Int J Life Cycle Assess* **15**, 970–984 (2010).

55. Harding, K. G., Dennis, J. S., von Blottnitz, H. & Harrison, S. T. L. Environmental analysis of plastic production processes: Comparing petroleum-based polypropylene and polyethylene with biologically-based poly-β-hydroxybutyric acid using life cycle analysis. *Journal of Biotechnology* **130**, 57–66 (2007).

56. Tsiropoulos, I. *et al.* Life cycle assessment of sugarcane ethanol production in India in comparison to Brazil. *Int J Life Cycle Assess* **19**, 1049–1067 (2014).

57. Castro-Aguirre, E., Iñiguez-Franco, F., Samsudin, H., Fang, X. & Auras, R. Poly(lactic acid)—Mass production, processing, industrial applications, and end of life. *Advanced Drug Delivery Reviews* **107**, 333–366 (2016).

58. Lim, L.-T., Auras, R. & Rubino, M. Processing technologies for poly(lactic acid). *Progress in Polymer Science* **33**, 820–852 (2008).

59. Hermann, B. G., Debeer, L., De Wilde, B., Blok, K. & Patel, M. K. To compost or not to compost: Carbon and energy footprints of biodegradable materials' waste treatment. *Polymer Degradation and Stability* **96**, 1159–1171 (2011).

60. Shen, L., Haufe, J. & Patel, M. K. *Product Overview and Market Projection of Emerging Bio-based Plastics*. 243 (2009).

61. Ashter, S. A. Commercial Applications of Bioplastics. in *Introduction to Bioplastics Engineering* 227–249 (Elsevier, 2016). doi:10.1016/B978-0-323-39396-6.00009-9.

62. Luckachan, G. E. & Pillai, C. K. S. Biodegradable Polymers- A Review on Recent Trends and Emerging Perspectives. *J Polym Environ* **19**, 637–676 (2011).

63. Babu, R. P., O'Connor, K. & Seeram, R. Current progress on bio-based polymers and their future trends. *Prog Biomater* **2**, (2013).

64. Chanprateep, S. Current trends in biodegradable polyhydroxyalkanoates. *Journal of Bioscience and Bioengineering* **110**, 621–632 (2010).

65. Wang, X.-L., Yang, K.-K. & Wang, Y.-Z. Properties of Starch Blends with Biodegradable Polymers. *Journal of Macromolecular Science, Part C* **43**, 385–409 (2003).

66. Broeren, M. L. M., Kuling, L., Worrell, E. & Shen, L. Environmental impact assessment of six starch plastics focusing on wastewater-derived starch and additives. *Resources, Conservation and Recycling* **127**, 246–255 (2017).

67. Olivier, J. G. J., Schure, K. M. & Peters, J. A. H. W. *Trends in global CO2 and total greenhouse gas emissions - 2017 Report*. 69 (2017).

68. Zhu, J.-B., Watson, E. M., Tang, J. & Chen, E. Y.-X. A synthetic polymer system with repeatable chemical recyclability. *Science* **360**, 398–403 (2018).

69. Bing, X., Bloemhof-Ruwaard, J., Chaabane, A. & van der Vorst, J. Global reverse supply chain redesign for household plastic waste under the emission trading scheme. *Journal of Cleaner Production* **103**, 28–39 (2015).

70. Soroudi, A. & Jakubowicz, I. Recycling of bioplastics, their blends and biocomposites: A review. *European Polymer Journal* **49**, 2839–2858 (2013).

71. Reddy, R. L., Reddy, V. S. & Gupta, G. A. *Study of Bio-plastics As Green & Sustainable Alternative to Plastics*. (2013).

72. Hottle, T. A., Bilec, M. M. & Landis, A. E. Biopolymer production and end of life comparisons using life cycle assessment. *Resources, Conservation and Recycling* **122**, 295–306 (2017).

73. Sovacool, B. K. Valuing the greenhouse gas emissions from nuclear power: A critical survey. *Energy Policy* **36**, 2950–2963 (2008).

74. International Energy Agency. Electricity Statistics. https://www.iea.org/statistics/electricity/.

75. Geyer, R., Jambeck, J. R. & Law, K. L. Production, use, and fate of all plastics ever made. *Science Advances* **3**, e1700782 (2017).

76. EPA. *Advancing Sustainable Materials Management: 2014 Fact Sheet*. 22 (2016).

77. PlasticEurope. *Plastics – the Facts 2016*. https://www.plasticseurope.org/application/files/4315/1310/4805/plastic-the-fact-2016.pdf (2016).

78. Eurostats. Municipal waste 2016 - tables and figures. https://ec.europa.eu/eurostat/statistics-explained/index.php/Municipal_waste_statistics#Municipal_waste_treatment.

79. European Union. 2030 climate & energy framework. *Climate Action - European Commission* https://ec.europa.eu/clima/policies/strategies/2030_en (2016).

80. State of California. California Renewables Portfolio Standard (RPS) Program. https://www.cpuc.ca.gov/rps/.

81. Jenkins, J. D., Luke, M. & Thernstrom, S. Getting to Zero Carbon Emissions in the Electric Power Sector. *Joule* **2**, 2498–2510 (2018).

82. Frew, B. *et al.* Sunny with a chance of curtailment: Operating the U.S. grid with very high levels of solar photovoltaics. *iScience* S2589004219303967 (2019) doi:10.1016/j.isci.2019.10.017.

83. Wiser, R. H., Mills, A., Seel, J., Levin, T. & Botterud, A. *Impacts of Variable Renewable Energy on Bulk Power System Assets, Pricing, and Costs*. 1411668 http://www.osti.gov/servlets/purl/1411668/ (2017) doi:10.2172/1411668.

84. Bird, L. *et al.* Wind and solar energy curtailment: A review of international experience. *Renewable and Sustainable Energy Reviews* **65**, 577–586 (2016).

85. Denholm, P., O'Connell, M., Brinkman, G. & Jorgenson, J. *Overgeneration from Solar Energy in California. A Field Guide to the Duck Chart*. http://www.osti.gov/servlets/purl/1226167/ (2015) doi:10.2172/1226167.

86. Fu, R., Remo, T. & Magolis, R. 2018 U.S. Utility-Scale Photovoltaics-Plus-Energy Storage System Costs Benchmark. (2018).

87. Wood Mackenzie Power & Renewable. *Global energy storage outlook 2019*. https://www.woodmac.com/reports/power-markets-global-energy-storage-outlook-2019-295618 (2019).

88. Enerdata. Global Energy Statistic Yearbook 2019. https://yearbook.enerdata.net/electricity/electricity-domestic-consumption-data.html (2019).

89. Bird, S. *et al.* Distributed (green) data centers: A new concept for energy, computing, and telecommunications. *Energy for Sustainable Development* **19**, 83–91 (2014).

90. Rehman, S., Al-Hadhrami, L. M. & Alam, Md. M. Pumped hydro energy storage system: A technological review. *Renewable and Sustainable Energy Reviews* **44**, 586–598 (2015).

91. Gahleitner, G. Hydrogen from renewable electricity: An international review of power-to-gas pilot plants for stationary applications. *International Journal of Hydrogen Energy* **38**, 2039–2061 (2013).

92. Barton, J. P. & Infield, D. G. Energy storage and its use with intermittent renewable energy. *IEEE Transactions on Energy Conversion* **19**, 441–448 (2004).

93. Klerke, A., Christensen, C. H., Nørskov, J. K. & Vegge, T. Ammonia for hydrogen storage: challenges and opportunities. *J. Mater. Chem.* **18**, 2304–2310 (2008).

94. Yang, F. & Chien, A. A. Large-Scale and Extreme-Scale Computing with Stranded Green Power: Opportunities and Costs. *IEEE Transactions on Parallel and Distributed Systems* **29**, 1103–1116 (2018).

95. Chien, A. A., Wolski, R. & Yang, F. The Zero-Carbon Cloud: High-Value, Dispatchable Demand for Renewable Power Generators. in *The Electricity Journal* vol. 28 110–118 (2015).

96. Liu, Z., Lin, M., Wierman, A., Low, S. H. & Andrew, L. L. H. Geographical Load Balancing with Renewables. *SIGMETRICS Perform. Eval. Rev.* **39**, 62–66 (2011).

97. Kong, F. & Liu, X. A Survey on Green-Energy-Aware Power Management for Datacenters. *ACM Comput. Surv.* **47**, 30:1-30:38 (2014).

98. Goiri, Í. *et al.* Matching renewable energy supply and demand in green datacenters. *Ad Hoc Networks* **25**, 520–534 (2015).

99. Jin, X., Zhang, F., Vasilakos, A. V. & Liu, Z. Green Data Centers: A Survey, Perspectives, and Future Directions. *arXiv:1608.00687 [cs]* (2016).

100. Liu, Z., Wierman, A., Chen, Y., Razon, B. & Chen, N. Data center demand response: Avoiding the coincident peak via workload shifting and local generation. *Performance Evaluation* **70**, 770–791 (2013).

101. Shehabi, A. *et al. United States Data Center Energy Usage Report*. http://www.osti.gov/servlets/purl/1372902/ (2016) doi:10.2172/1372902.

102. Reinsel, D., Gantz, J. & Rydning, J. *The Digitization of the World from Edge to Core*. 28 (2018).

103. Masanet, E., Shehabi, A. & Koomey, J. Characteristics of low-carbon data centres. *Nature Climate Change* **3**, 627–630 (2013).

104. PJM. PJM At a Glance. https://www.pjm.com/~/media/about-pjm/newsroom/fact-sheets/pjm-at-a-glance.ashx (2019).

105. PJM. PJM Data Miner 2 - Generation by Fuel Type. https://dataminer2.pjm.com/feed/gen_by_fuel.

106. Sverdlik, Y. The Cloud Data Center Construction Boom, in Two Charts. *Data Center Knowledge* https://www.datacenterknowledge.com/cloud/cloud-data-center-construction-boom-two-charts (2019).

107. Ghatikar, G., Ganti, V., Matson, N. & Piette, M. A. *Demand Response Opportunities and Enabling Technologies for Data Centers: Findings From Field Studies*. http://www.osti.gov/servlets/purl/1174175/ (2012) doi:10.2172/1174175.

108. DatacenterMap.com. Colocation USA - Data Centers. https://www.datacentermap.com/usa/.

109. Curran, J. *IBISWorld Industry Report OD5899 - Colocation Facilities in the US*. https://clients1.ibisworld.com/reports/us/industry/default.aspx?entid=5899 (2018).

110. CAISO. California ISO - Managing Oversupply. http://www.caiso.com/informed/Pages/ManagingOversupply.aspx (2019).

111. CAISO. California ISO - Renewables and emissions reports. http://www.caiso.com/market/Pages/ReportsBulletins/RenewablesReporting.aspx.

112. Littlefield, J., Roman-White, S., Augustine, D., Pegallapati, A. & Zaimes, G. *Life Cycle Analysis of Natural Gas Extraction and Power Generation*. https://www.netl.doe.gov/energy-analysis/details?id=3198 (2019).

113. Gilbert, A. Q. & Sovacool, B. K. Benchmarking natural gas and coal-fired electricity generation in the United States. *Energy* **134**, 622–628 (2017).

114. Intergovernmental Panel on Climate Change. *Annex III: Technology-specific cost and performance parameters. In: Climate Change 2014: Mitigation of Climate Change. Contribution of Working Group III to the Fifth Assessment Report of the Intergovernmental Panel on Climate Change*. (Cambridge University Press, 2014). doi:10.1017/CBO9781107415416.

115. Hundiwale, A. CAISO Greenhouse Gas Emission Tracking Methodology. https://www.caiso.com/Documents/GreenhouseGasEmissionsTracking-Methodology.pdf (2016).

116. PJM. PJM Data Miner 2 - Actual/Schedule Summary Report. https://dataminer2.pjm.com/feed/act_sch_interchange/definition.

117. Rahmani, R., Moser, I. & Seyedmahmoudian, M. A Complete Model for Modular Simulation of Data Centre Power Load. (2018).

118. Barroso, L. A., Hölzle, U. & Ranganathan, P. *The Datacenter as a Computer: Designing Warehouse-Scale Machines*. (Morgan & Claypool, 2019).

119. Jiang, C., Wang, Y., Ou, D., Luo, B. & Shi, W. Energy Proportional Servers: Where Are We in 2016? in *2017 IEEE 37th International Conference on Distributed Computing Systems (ICDCS)* 1649–1660 (2017). doi:10.1109/ICDCS.2017.285.

120. Malla, S. & Christensen, K. The effect of server energy proportionality on data center power oversubscription. *Future Generation Computer Systems* **104**, 119–130 (2020).

121. Uptime Institute. 2013 Data Center Industry Survey. https://uptimeinstitute.com/resources/asset/2013-data-center-industry-survey (2013).

122. Lawrence, A. Is PUE actually going UP? *Uptime Institute Blog* https://journal.uptimeinstitute.com/is-pue-actually-going-up/ (2019).

123. CloudandColocation.com. California Data Center Location Map. *Cloud and Colocation* https://cloudandcolocation.com/state/california/.

124. Whitehead, B., Andrews, D. & Shah, A. The life cycle assessment of a UK data centre. *Int J Life Cycle Assess* **20**, 332–349 (2015).

125. Shah, A. J., Chen, Y. & Bash, C. E. Sources of variability in data center lifecycle assessment. in *2012 IEEE International Symposium on Sustainable Systems and Technology (ISSST)* 1–6 (2012). doi:10.1109/ISSST.2012.6227975.

126. Cortez, E. *et al.* Resource Central: Understanding and Predicting Workloads for Improved Resource Management in Large Cloud Platforms. in *Proceedings of the 26th Symposium on Operating Systems Principles - SOSP '17* 153–167 (ACM Press, 2017). doi:10.1145/3132747.3132772.

127. Cloudscene. Data Centers Market in United States of America. *Cloudscene* https://cloudscene.com/market/data-centers-in-united-states/all.

128. International Organization for Standardization. ISO/IEC 30134-2:2016(en), Information technology — Data centres — Key performance indicators — Part 2: Power usage effectiveness (PUE). https://www.iso.org/obp/ui/#iso:std:iso-iec:30134:-2:ed-1:v1:en (2016).

129. AWS News Blog. Cloud Computing, Server Utilization, & the Environment. *Amazon Web Services* https://aws.amazon.com/blogs/aws/cloud-computing-server-utilization-the-environment/ (2015).

130. CAISO. *2018 Annual Report on Market Issues & Performance*. http://www.caiso.com/Documents/2018AnnualReportonMarketIssuesandPerformance.pdf (2019).

131. Sun, Y., Szűcs, G. & R. Brandt, A. Solar PV output prediction from video streams using convolutional neural networks. *Energy & Environmental Science* **11**, 1811–1818 (2018).

132. Alstone, P. *et al. 2025 California Demand Response Potential Study - Charting California's Demand Response Future: Final Report on Phase 2 Results*. (2017).

133. Radovanovic, A. Our data centers now work harder when the sun shines and wind blows. *Google* https://blog.google/inside-google/infrastructure/data-centers-work-harder-sun-shines-wind-blows/ (2020).

134. Paul, D., Zhong, W. & Bose, S. K. Demand Response in Data Centers Through Energy-Efficient Scheduling and Simple Incentivization. *IEEE Systems Journal* **11**, 613–624 (2017).

135. Goiri, Í., Katsak, W., Le, K., Nguyen, T. D. & Bianchini, R. Parasol and GreenSwitch: Managing Datacenters Powered by Renewable Energy. in *Proceedings of the Eighteenth International Conference on Architectural Support for Programming Languages and Operating Systems* 51–64 (ACM, 2013). doi:10.1145/2451116.2451123.

136. Kong, F. & Liu, X. GreenPlanning: Optimal Energy Source Selection and Capacity Planning for Green Datacenters. in *2016 ACM/IEEE 7th International Conference on Cyber-Physical Systems (ICCPS)* 1–10 (2016). doi:10.1109/ICCPS.2016.7479104.

137. AT&T. Global IP Network Latency. http://ipnetwork.bgtmo.ip.att.net/pws/network_delay.html (2020).

138. Avgerinou, M., Bertoldi, P. & Castellazzi, L. Trends in Data Centre Energy Consumption under the European Code of Conduct for Data Centre Energy Efficiency. *Energies* 1470 (2017).

139. Meyer-Aurich, A. *et al.* Impact of uncertainties on greenhouse gas mitigation potential of biogas production from agricultural resources. *Renewable Energy* **37**, 277–284 (2012).

140. World Nuclear Association. Comparison of Lifecycle Greenhouse Gas Emissions of Various Electricity Generation Sources. https://www.world-nuclear.org/uploadedFiles/org/WNA/Publications/Working_Group_Reports/comparison_of_lifecycle.pdf (2011).

141. EIA - State Electricity Profiles. https://www.eia.gov/electricity/state/virginia/.

142. Arbabzadeh, M., Sioshansi, R., Johnson, J. X. & Keoleian, G. A. The role of energy storage in deep decarbonization of electricity production. *Nature Communications* **10**, 3413 (2019).

143. Craig, M. T., Jaramillo, P. & Hodge, B.-M. Carbon dioxide emissions effects of grid-scale electricity storage in a decarbonizing power system. *Environ. Res. Lett.* **13**, 014004 (2018).

144. California Independent System Operator. *Energy Storage - Perspectives from California and Europe*. http://www.caiso.com/Documents/EnergyStorage-PerspectivesFromCalifornia-Europe.pdf (2019).

145. O'Shaughnessy, E., Cutler, D., Ardani, K. & Margolis, R. Solar plus: Optimization of distributed solar PV through battery storage and dispatchable load in residential buildings. *Applied Energy* **213**, 11–21 (2018).

146. Solar Energy Industries Association. Solar Industry Research Data. *SEIA* https://www.seia.org/solar-industry-research-data (2021).

147. Fisher, M. J. & Apt, J. Emissions and Economics of Behind-the-Meter Electricity Storage. *Environ. Sci. Technol.* **51**, 1094–1101 (2017).

148. Hittinger, E. & Ciez, R. E. Modeling Costs and Benefits of Energy Storage Systems. *Annual Review of Environment and Resources* **45**, 445–469 (2020).

149. Siler-Evans, K., Azevedo, I. L. & Morgan, M. G. Marginal Emissions Factors for the U.S. Electricity System. *Environ. Sci. Technol.* **46**, 4742–4748 (2012).

150. Center For Climate and Energy Decision Making. Electricity Marginal Factor Estimates. https://cedm.shinyapps.io/MarginalFactors/ (2019).

151. Li, M., Smith, T. M., Yang, Y. & Wilson, E. J. Marginal Emission Factors Considering Renewables: A Case Study of the U.S. Midcontinent Independent System Operator (MISO) System. *Environ. Sci. Technol.* **51**, 11215–11223 (2017).

152. Gai, Y., Wang, A., Pereira, L., Hatzopoulou, M. & Posen, I. D. Marginal Greenhouse Gas Emissions of Ontario's Electricity System and the Implications of Electric Vehicle Charging. *Environ. Sci. Technol.* **53**, 7903–7912 (2019).

153. Thind, M. P. S., Wilson, E. J., Azevedo, I. L. & Marshall, J. D. Marginal Emissions Factors for Electricity Generation in the Midcontinent ISO. *Environ. Sci. Technol.* **51**, 14445–14452 (2017).

154. Bistline, J. E. T. & Young, D. T. Emissions impacts of future battery storage deployment on regional power systems. *Applied Energy* **264**, 114678 (2020).

155. Yang, C. A framework for allocating greenhouse gas emissions from electricity generation to plug-in electric vehicle charging. *Energy Policy* **60**, 722–732 (2013).

156. Hawkes, A. D. Estimating marginal CO2 emissions rates for national electricity systems. *Energy Policy* **38**, 5977–5987 (2010).

157. Hawkes, A. D. Long-run marginal CO2 emissions factors in national electricity systems. *Applied Energy* **125**, 197–205 (2014).

158. Chalendar, J. A. de & Benson, S. M. Why 100% Renewable Energy Is Not Enough. *Joule* **3**, 1389–1393 (2019).

159. Gagnon, P., Frazier, W., Hale, E. & Cole, W. *Cambium Documentation: Version 2020*. 63 (2020).

160. Soimakallio, S., Kiviluoma, J. & Saikku, L. The complexity and challenges of determining GHG (greenhouse gas) emissions from grid electricity consumption and conservation in LCA (life cycle assessment) – A methodological review. *Energy* **36**, 6705–6713 (2011).

161. Elzein, H., Dandres, T., Levasseur, A. & Samson, R. How can an optimized life cycle assessment method help evaluate the use phase of energy storage systems? *Journal of Cleaner Production* **209**, 1624–1636 (2019).

162. Ren, M., Mitchell, C. R. & Mo, W. Dynamic life cycle economic and environmental assessment of residential solar photovoltaic systems. *Science of The Total Environment* **722**, 137932 (2020).

163. Mayer, M. J., Szilágyi, A. & Gróf, G. Environmental and economic multi-objective optimization of a household level hybrid renewable energy system by genetic algorithm. *Applied Energy* **269**, 115058 (2020).

164. Petrelli, M. & Melià, P. V. A. A literature review of the integration of optimization algorithms and LCA for microgrid design: a replicable model for off-grid systems in developing countries. in 8 (2019).

165. Le Varlet, T., Schmidt, O., Gambhir, A., Few, S. & Staffell, I. Comparative life cycle assessment of lithium-ion battery chemistries for residential storage. *Journal of Energy Storage* **28**, 101230 (2020).

166. Office of Energy Efficiency & Renewable Energy (EERE). Commercial and Residential Hourly Load Profiles for all TMY3 Locations in the United States - OpenEI Datasets. https://openei.org/datasets/dataset/commercial-and-residential-hourly-load-profiles-for-all-tmy3-locations-in-the-united-states (2013).

167. Freeman, J. M. *et al. System Advisor Model (SAM) General Description (Version 2017.9.5)*. http://www.osti.gov/servlets/purl/1440404/ (2018) doi:10.2172/1440404.

168. Barbose, G., Darghouth, N., O'Shaughnessy, E. & Forrester, S. *Distributed Solar 2020 Data Update*. None, 1735556, ark:/13030/qt2dt8q8vz https://www.osti.gov/servlets/purl/1735556/ (2020) doi:10.2172/1735556.

169. Gagnon, P., Margolis, R., Melius, J., Phillips, C. & Elmore, R. *Rooftop Solar Photovoltaic Technical Potential in the United States. A Detailed Assessment*. http://www.osti.gov/servlets/purl/1236153/ (2016) doi:10.2172/1236153.

170. Wilcox, S. & Marion, W. *Users Manual for TMY3 Data Sets*. 58 (2008).

171. Archives - NSRDB. https://nsrdb.nrel.gov/data-sets/archives.html.

172. Jordan, D. C. & Kurtz, S. R. Photovoltaic Degradation Rates—an Analytical Review. *Progress in Photovoltaics: Research and Applications* **21**, 12–29 (2013).

173. Tesla. Powerwall 2 AC Datasheet (North America). https://www.tesla.com/sites/default/files/pdfs/powerwall/Powerwall%202_AC_Datasheet_en_northamerica.pdf (2019).

174. Tesla Powerwall Limited Warranty (USA). https://www.tesla.com/sites/default/files/pdfs/powerwall/powerwall_2_ac_warranty_us_1-4.pdf (2017).

175. California Public Uitlities Commission. Decision 19-01-030 - Decision granting petition for modification of Decision 14-05-033 regarding storage devices paired with Net Energy Metering generating facilities. (2019).

176. National Renewable Energy Laboratory. Electricity Annual Technology Baseline (ATB) Data Download. https://atb.nrel.gov/electricity/2020/data.php (2020).

177. Powerwall | Tesla. https://www.tesla.com/powerwall.

178. Schmidt, O., Hawkes, A., Gambhir, A. & Staffell, I. The future cost of electrical energy storage based on experience rates. *Nature Energy* **2**, 17110 (2017).

179. Feldman, D. *et al. U.S. Solar Photovoltaic System and Energy Storage Cost Benchmark: Q1 2020*. 120 (2021).

180. California Public Uitlities Commission. Net Energy Metering. https://www.cpuc.ca.gov/NEM/.

181. Pacific Gas & Electricity. Residential rate plan pricing. https://www.pge.com/pge_global/common/pdfs/rate-plans/how-rates-work/Residential-Rates-Plan-Pricing-2020.pdf (2020).

182. Southern California Edison. *Schedule TOU-D Rates*. https://library.sce.com/content/dam/sce-doclib/public/regulatory/historical/electric/2020/schedules/residential-rates/ELECTRIC_SCHEDULES_TOU-D_2020.pdf (2020).

183. San Diego Gas & Electric Company. Schedule DR-SES: Domestic Time-of-Use for Households with A Solar Energy System. http://regarchive.sdge.com/tm2/pdf/ELEC_ELEC-SCHEDS_DR-SES.pdf (2020).

184. Pellow, M. A., Ambrose, H., Mulvaney, D., Betita, R. & Shaw, S. Research gaps in environmental life cycle assessments of lithium ion batteries for grid-scale stationary energy storage systems: End-of-life options and other issues. *Sustainable Materials and Technologies* **23**, e00120 (2020).

185. Peters, J. F., Baumann, M., Zimmermann, B., Braun, J. & Weil, M. The environmental impact of Li-Ion batteries and the role of key parameters – A review. *Renewable and Sustainable Energy Reviews* **67**, 491–506 (2017).

186. International Energy Agency. *World Energy Outlook 2020*. https://www.iea.org/reports/world-energy-outlook-2020 (2020).

187. Ellingsen, L. A.-W. *et al.* Life Cycle Assessment of a Lithium-Ion Battery Vehicle Pack. *Journal of Industrial Ecology* **18**, 113–124 (2014).

188. Yao, Y., Chang, Y. & Masanet, E. A hybrid life-cycle inventory for multi-crystalline silicon PV module manufacturing in China. *Environ. Res. Lett.* **9**, 114001 (2014).

189. Interagency Working Group on Social Cost of Greenhouse Gases, United States Government. Technical Support Document: Social Cost of Carbon, Methane, and Nitrous Oxide: Interim Estimates under Executive Order 13990. (2021).

190. National Renewable Energy Laboratory. Cambium. https://cambium.nrel.gov/ (2020).

191. Lukanov, B. R. & Krieger, E. M. Distributed solar and environmental justice: Exploring the demographic and socio-economic trends of residential PV adoption in California. *Energy Policy* **134**, 110935 (2019).

192. Matisoff, D. C., Beppler, R., Chan, G. & Carley, S. A review of barriers in implementing dynamic electricity pricing to achieve cost-causality. *Environ. Res. Lett.* **15**, 093006 (2020).

193. Zinaman, O. R., Bowen, T. & Aznar, A. Y. *An Overview of Behind-the-Meter Solar-Plus-Storage Regulatory Design: Approaches and Case Studies to Inform International Applications*. http://www.osti.gov/servlets/purl/1606152/ (2020) doi:10.2172/1606152.

194. Schmidt, O., Melchior, S., Hawkes, A. & Staffell, I. Projecting the Future Levelized Cost of Electricity Storage Technologies. *Joule* **3**, 81–100 (2019).

195. International Renewable Energy Agency. *Electricity storage and renewables: Costs and markets to 2030*. 132 (2017).

196. Christopher T M Clack, Aditya Choukulkar, Brianna Coté, & Sarah A McKee. *Why Local Solar For All Costs Less: A New Roadmap for the Lowest Cost Grid*. https://www.vibrantcleanenergy.com/wp-content/uploads/2020/12/WhyDERs_TR_Final.pdf (2020).

197. Darghouth, N., McCall, J., Keyser, D., Aznar, A. & Gokhale-Welch, C. *Distributed Photovoltaic Economic Impact Analysis in Indonesia*. NREL/TP--7A40-75281, 1602706, MainId:19621 https://www.osti.gov/servlets/purl/1602706/ (2020) doi:10.2172/1602706.

198. Gilman, P. *et al. SAM Photovoltaic Model Technical Reference Update*. NREL/TP--6A20-67399, 1429291 http://www.osti.gov/servlets/purl/1429291/ (2018) doi:10.2172/1429291.